PB87-175519

Analysis and Evaluation of Statistical Coastal Fumigation Models

North Carolina State Univ. at Raleigh

Prepared for

Environmental Protection Agency
Research Triangle Park, NC

Feb 87

U.S. Department of Commerce
National Technical Information Service
NTIS

PB87-175519

United States
Environmental Protection
Agency

Office of Air Quality
Planning and Standards
Research Triangle Park NC 27711

EPA-450/4-87-002
February 1987

Air

EPA

Analysis and Evaluation of Statistical Coastal Fumigation Models

REPRODUCED BY
U.S. DEPARTMENT OF COMMERCE
NATIONAL TECHNICAL
INFORMATION SERVICE
SPRINGFIELD, VA 22161

214p

EPA-450/4-87-002

Analysis and Evaluation of Statistical Coastal Fumigation Models

By

S. SethuRaman

Department of Marine, Earth and Atmospheric Sciences
North Carolina State University
Raleigh, NC 27695-8208

EPA Project Officer
Jawad S. Touma

U.S. ENVIRONMENTAL PROTECTION AGENCY
Office of Air and Radiation
Office Of Air Quality Planning and Standards
Research Triangle Park, NC 27711

February 1987

ia

DISCLAIMER

This report has been reviewed by the Office of Air Quality Planning And Standards, U.S. Environmental Protection Agency, and approved for publication as received from the contractor. Approval does not signify that the contents necessarily reflect the views and policies of the Agency, neither does mention of trade names or commercial products constitute endorsement or recommendation for use.

Table of Contents

LIST OF TABLES v

LIST OF FIGURES vii

LIST OF SYMBOLS xi

SUMMARY 1

1.0 INTRODUCTION 1-1

2.0 THE THERMAL INTERNAL BOUNDARY LAYER 2-1

- 2.1 TIBL Dynamics 2-1
- 2.2 Review of the TIBL Height Prediction Equations 2-6
- 2.3 Impact of TIBL Variation on Coastal Dispersion 2-17

3.0 COASTAL DISPERSION MODELING 3-1

- 3.1 The Mechanics of Fumigation 3-1
- 3.2 The Lyons and Cole (1973) Model 3-4
- 3.3 The CRSTER Shoreline Fumigation Model (CSFM) 3-8
- 3.4 The Misra Shoreline Fumigation Model (MSFM) 3-14
- 3.5 Empirical Modification to MSFM 3-18
- 3.6 Downdraft Modification of the MSFM Model 3-22

4.0 BRIEF REVIEW OF COASTAL DISPERSION STUDIES 4-1

- 4.1 Nanticoke (NEMP) Study -- General Description 4-3
- 4.2 Nanticoke Plant Characteristics 4-3
- 4.3 NEMP Instrument Deployment - Boundary Layer Measurements 4-4
- 4.4 NEMP Instrument Deployment - Plume Characteristics and Air Quality Measurements 4-8
- 4.5 Data Requirements for Running the Models 4-10

5.0 COASTAL DISPERSION MODEL EVALUATION PROTOCOL 5-1

- 5.1 Brief Overview of Model Evaluation Techniques 5-1
- 5.2 Statistical Evaluation Protocol 5-4

6.0 THERMAL INTERNAL BOUNDARY LAYER EQUATION EVALUATION 6-1

- 6.1 The Brookhaven Coastal Meteorology Experiments 6-3

6.2 The Kashimaura Coastal Meteorology Experiments 6-4
6.3 The Stable Upwind Overwater Case 6-8
6.4 The Unstable Upwind Overwater Case 6-11
6.5 Evaluation of TIBL Equations 6-18
6.6 Analysis by Wind Category 6-22
6.7 Analysis by Stability Category 6-26

7.0 COASTAL DISPERSION MODEL EVALUATION 7-1

7.1 Overall Evaluation 7-1
7.1.1 Results 7-1
7.1.2 Discussion of Results 7-9
7.2 The June 1, 1978 Case 7-18
7.3 The June 6, 1978 Case 7-31
7.4 The June 13, 1979 Case 7-45
7.5 The June 14, 1979 Case 7-48
7.6 Sensitivity Analysis 7-50

8.0 CONCLUSIONS 8-1

9.0 RECOMMENDATIONS 9-1

10.0 REFERENCES 10-1

11.0 APPENDIX 11-1

LIST OF TABLES

4.1 Input factors for the CSFM and MSFM base models 4-13

5.1 Test cases used for model comparison 5-11

6.1 Listing of TIBL data bases 6-2

6.2 TIBL parameters used for BNL data base ... 6-6

6.3 TIBL parameters used for Kashimaura data base 6-9

6.4 BNL #13 meteorological data 6-10

6.5 BNL #6 meteorological data 6-14

6.6 Comparison of h vs h + h_o TIBL values 6-16

6.7 Statistical results of non-categorized TIBL predictions 6-19

6.8a Statistical results of wind categorized TIBL predictions (U1) 6-24

6.8b Statistical results of wind categorized TIBL predictions (U2) 6-25

6.9a Statistical results of stability categorized TIBL predictions (S1) 6-28

6.9b Statistical results of stability categorized TIBL predictions (S2) 6-30

6.9c Statistical results of stability categorized TIBL predictions (S3) 6-31

6.9d Statistical results of stability categorized TIBL predictions (S4) 6-33

7.1 Statistical results of overall model performances 7-7

7.2 Statistical results of model performances for June 1, 1978 7-30

7.3 Location of maximum downwind concentration for June 6, 1978 7-44

7.4 Statistical results of model performances for June 6, 1979 7-46

7.5 Statistical results of model performances for June 13, 1979 7-49

7.6 Statistical results of model performances for June 14, 1979 7-52

LIST OF FIGURES

2.1a Category I TIBL case with stable overwater stability 2-4

2.1b Category II TIBL case with neutral overwater stability 2-4

2.2 Historical flowchart of TIBL prediction equation development 2-8

2.3 Impact of TIBL variation upon location of downwind maximum concentration 2-19

3.1 Vertical plume geometry of Lyons and Cole (1973) model 3-6

3.2 Plume geometry of CSFM model 3-10

3.3 Flowchart of CSFM model 3-15

3.4 Flowchart of MSFM model 3-19

4.1 Deployment map of the various measuring systems of the NEMP study 4-5

4.2 Cross-sectional deployment diagram of the NEMP boundary layer sensing systems 4-6

4.3 Cross-sectional deployment diagram of the NEMP air quality measuring systems 4-11

5.1 Hypothetical model output graph showing deceptively perfect correlation 5-5

6.1 Map of Long Island showing flight tracks for TIBL experiments 6-5

6.2 Map of Kashimaura-Kujukurihama, Japan TIBL experiment area 6-7

6.3 Graph of observed vs predicted TIBL height for BL #13 6-12

6.4 Sounding for BL #6 6-15

6.5 Graph of observed vs predicted TIBL height for BL #6 6-17

7.1a Scatterplots for the MSFM model 7-2

7.1b Scatterplots for the CSFM model 7-3

7.1c Scatterplots for the empirical model 7-4

7.1d Scatterplots for the downdraft model 7-5

7.2 Plume-TIBL relationship for June 1, 1978 7-20

7.3a Concentration isopleths for June 1, 1978 (0900-1000 EDT) 7-21

7.3b Concentration isopleths for June 1, 1978 (1000-1100 EDT) 7-22

7.3c Concentration isopleths for June 1, 1978 (1130-1200 EDT) 7-23

7.3d Concentration isopleths for June 1, 1978 (1230-1300 EDT) 7-24

7.3e Concentration isopleths for June 1, 1978 (1330-1400 EDT) 7-25

7.3f Concentration isopleths for June 1, 1978 (1430-1500 EDT) 7-26

7.3g Concentration isopleths for June 1, 1978 (1530-1600 EDT) 7-27

7.3h Concentration isopleths for June 1, 1978 (1630-1700 EDT) 7-28

7.4 Plume-TIBL relationship for June 6, 1978 7-33

7.5a Concentration isopleths for June 6, 1978 (0900-1000 EDT) 7-35

7.5b Concentration isopleths for June 6, 1978 (1000-1100 EDT) 7-36

7.5c Concentration isopleths for June 6, 1978 (1300-1400 EDT) 7-37

7.5d Concentration isopleths for June 6, 1978 (1400-1430 EDT) 7-38

7.5e Concentration isopleths for June 6, 1978 (1500-1530 EDT) 7-39

7.5f Concentration isopleths for June 6, 1978 (1530-1600 EDT) 7-40

7.5g Concentration isopleths for June 6, 1978 (1600-1630 EDT) 7-41

7.5h Concentration isopleths for June 6, 1978 (1630-1700 EDT) 7-42

7.6 Graph of model results for 1200 EDT June 6, 1978 7-43

7.7 Plume-TIBL relationship for June 13, 1979 7-47

7.8 Plume-TIBL relationship for June 14, 1979 7-51

7.9 w_*/U sensitivity analysis with normalized concentration 7-55

7.10 "A" sensitivity analysis with normalized concentration 7-56

7.11 F_o sensitivity analysis with normalized concentration 7-58

7.12 Brunt-Vaisalla frequency (N) sensitivity analysis with normalized concentration ... 7-60

LIST OF SYMBOLS

a = temperature gradient upwind ($K\ m^{-1}$)

A = TIBL factor containing physics needed for TIBL parameterization (generally ranges from 2 to 6)

$A(t)$ = fraction of fumigant entrained into TIBL with respect to time (MSFM/empirical variation)

C = concentration (PPB, PPM, $\mu g\ m^{-3}$)

C^* = non-dimensional concentration

C_p = specific heat at constant pressure ($0.24\ cal\ g^{-1}K^{-1}$)

C_s = concentration in stable air (PPB, PPM, $\mu g\ m^{-3}$)

C_u = frictional coefficient (dimensionless)

C_θ = heat coefficient (dimensionless)

D_L = length of day

d = index of agreement value, also stack diameter (m)

E = heat emission rate

E_v = gas volume emission rate (m^3s^{-1})

F = entrainment fraction

F_e = entrainment flux

F_o = buoyancy parameter (m^4s^{-3})

f_1 = function used in describing TIBL turbulence

g_1 = function used in describing TIBL turbulence

H_c = 20% of the solar constant ($W\ m^{-2}$)

H_e = effective stack height (m)

H_o = heat flux ($W\ m^{-2}$)

H_s = stack height (m)

h = TIBL interface height (m)

Preceding page blank

$\bar{h}_i$ = mean TIBL height (m)

h_o = initial TIBL interface height under neutral or unstable overwater conditions

$K_{x,y}$ = eddy diffusivity

k = von Karman's constant

N = Brunt-Vaisalla frequency (s^{-1})

O = observed value

P = predicted value

p = a function used in Lyons and Cole model

P_1 = stack height atmospheric pressure (mb)

Q = source strength ($g\ s^{-1}$)

Q_i = mass of plume segment in CRSTER Shoreline Fumigation Model ($g\ s^{-1}$)

r = correlation coefficient

r^2 = coefficient of determination

S = $\partial\theta/\partial z$ potential temperature gradient overwater (K/100m)

S_o = standard deviation of observed values

S_p = standard deviation of predicted values

S_o^2 = variance of observed values

S_p^2 = variance of predicted values

T = air temperature (K)

T_A = average temperature in TIBL (K)

T_L, θ_L = temperature at 2 m above land surface (K)

T_s = stack gas temperature (K)

T_w, θ_w = temperature at water surface (K)

T_1 = air temperature at stack height (K)

t = time (s)

t_s = time since sunrise (s)

t^* = non-dimensional time

t_f^* = non-dimensional time at final fumigation point

U_m = mean wind speed in TIBL (m s^{-1})

U_s = mean wind speed at stack height in stable air (m s^{-1})

U_{10} = mean wind speed at 10m (m s^{-1})

u_* = friction velocity (m s^{-1})

V_f = gas exit velocity (m s^{-1})

V_s = stack gas velocity (m s^{-1})

w_d = downdraft velocity (m s^{-1})

w_e = entrainment velocity (m s^{-1})

w_* = convective velocity scale (m s^{-1})

$(\overline{w'\theta'})_i$ = heat flux at TIBL height (W m^{-2})

$(\overline{w'\theta'})_o$ = heat flux at surface (W m^{-2})

x,X = downwind distance from shoreline (km)

X_B = downwind distance where fumigation begins (m) (Lyons and Cole)

X_E,X_f = end of fumigation downwind (Lyons and Cole, MSFM)

X_o = location of where pollutants begin entraining into the TIBL (MSFM model)

x_o = location of TIBL perturbation [Lyons et al. (1983) TIBL model]

x_o' = virtual point source location (Lyons and Cole model)

X^* = non-dimensional distance

Y = lateral distance (m)

z = height (m)

Z_s = stack height (m)

Z' = Z/h

α = constant (Equation 2.13)

Δh_s = plume rise (m)

$\Delta\theta$ = change in potential temperature overwater from 10 m above the water to base of the inversion (K)

$\Delta\theta_o$ = inversion (K)

γ = lapse rate ($\partial T/\partial z$) overwater (K/100m)

ψ = solar insolation factor

ρ = density of air (1.2×10^{-3} g m^{-3})

σ_y = lateral dispersion coefficient (generic) (m)

$\sigma_{yf}(x,s)$ = lateral dispersion coefficient in fumigation zone (m)

$\sigma_{yf_{ij}}$ = same as $\sigma_{yf}(x,s)$ but represents individual dispersion coefficient for the plume segment

σ_{yh} = dispersion coefficient in TIBL (MSFM model)

σ_z = vertical dispersion coefficient (generic) (m)

σ_{ys} = horizontal dispersion coefficient in stable air (m)

σ_{zs} = vertical dispersion coefficient in stable air (m)

σ_w = standard deviation of vertical velocity (m)

θ_L = temperature at 10 m (K)

θ_m = TIBL mean temperature (K)

θ_o = temperature at coastline (K)

Acknowledgements

The author would like thank R. Lee and J. Dicke of OAQPS/EPA for the helpful discussions and their support for this project.

This report is based on material used to fulfill the requirements for a Master of Science degree at the North Carolina State University for Mr. M.J. Stunder. His dedication and enthusiasm for this study were a major factor in its successful completion. Finally appreciation is extended to Suzanne Viessman who performed much of the technical editing and organization of this report.

Summary

Fumigation caused by elevated sources in coastal areas has been simulated by two base models: the CRSTER Shoreline Fumigation Model (CSFM) and the Misra Shoreline Fumigation Model (MSFM). These two models, along with variations of the MSFM model, are evaluated in this study.

Plume dispersion in the CSFM model is treated as a point source upon intersecting the Thermal Internal Boundary Layer (TIBL). Dispersion coefficents are determined using the Pasquill-Gifford approach. In comparison, the MSFM model treats the plume as an areal-type source upon intersecting the TIBL and utilizes the convective velocity type equations to account for updrafts and downdrafts in the convective boundary layer occurring under the TIBL. Both of the base models assume uniform, instantaneous mixing downward of the plume upon TIBL intersection. Variations of the MSFM model, however, assume that the plume is not uniformly, instantaneously mixed downward and instead use either weighting factors, based on laboratory results, to displace the plume downwind, or use probability estimates of downdrafts to influence the maximum concentration location downwind.

The statistical evaluation procedures incorporated in this study involve the use of scatterplots, variances and total and systematic root-mean-square errors. In addition,

an index of agreement value (d) is used in place of the standard statistical correlation coefficient (r).

The two-year, comprehensive Nanticoke, Canada power plant study is used for evaluation purposes. The 13 test cases taken from this data base met the criteria of daytime onshore flow and sufficient land-water temperature difference.

Initial evaluation indicates that the MSFM base model performed better than the CSFM base model. This decision was based on (among other factors) the comparatively high index of agreement values (0.76 vs. 0.46) for the MSFM model. Reasons for the comparatively poor performance of the CSFM model can be viewed in terms of the Gaussian diffusion formulation (using the Pasquill-Gifford stability classification) versus the convective velocity scaling approach of the MSFM model and of the point source versus areal-type dispersion approach.

Subsequently, attention was given to evaluating two variations of the MSFM model. This evaluation indicates that the MSFM/downdraft model outperformed the MSFM/empirical model, but did not outperform the base MSFM model. Reasons for the better performance of the base MSFM model are given in terms of the near-instantaneous assumption not being critical in highly convective TIBLs.

Sensitivity analysis of the various model input parameters (i.e., convective velocity scaling, buoyancy flux, Brunt-Vaisalla frequency and TIBL parameterizations) revealed that TIBL parameterization was the most sensitive variable. This supports the contention that proper TIBL parameterization is the key to coastal dispersion modeling.

Evaluation of the TIBL height equations is undertaken separately. Six TIBL models are identified from the literature and compared using two TIBL experimental data bases from Long Island and Japan. The statistical evaluation methods are the same as those used in the dispersion model evaluation. The data are also classified according to wind speed and overwater stability. The evaluation indicates that the Weisman (1976) formulation, which includes heat flux and wind speed along with overwater lapse rate all raised to the half power, performed the best. Classifications according to wind speed and stability also showed that the heat flux type of equation worked reasonably well.

1.0 INTRODUCTION

The diffusion and transport of gaseous pollutants released into the atmosphere in coastal areas have been of great concern to those involved in air quality impact analyses. The growth of industrial facilities in coastal areas has created a need for accurate point source air dispersion models that can handle the unique meteorological conditions where a land-water surface discontinuity plays a major role. One such phenomenon is the development of a convective boundary layer generally known as the Thermal Internal Boundary Layer (TIBL), which develops over the land for onshore flows when the air temperature over land is warmer than the water surface temperature. Above the TIBL the air mass is generally stable, while below the TIBL air is unstable due to convective heating from below. A tall stack situated at the shoreline emits pollutants into the stable layer first. The plume travels with relatively little diffusion in this layer, but upon intersecting the TIBL, fumigation occurs leading to high ground level concentrations.

Several methods are available to model the prediction of the ground level concentration in the coastal fumigation zone (Lyons and Cole, 1973; Misra, 1980a; Cole and Fowler, 1982; Van Dop et al., 1979, etc.). The purpose of this study is to evaluate several Gaussian dispersion models using the best available air quality and meteorological data bases, to identify the assumptions, uncertainties and applicability of these models and to identify the model components (e.g., TIBL formulation) that are most valid. Finally, some recommendations are provided regarding the meteorological and stack parameters needed to utilize a selected coastal fumigation model.

2.0 THE THERMAL INTERNAL BOUNDARY LAYER

A reasonably thorough treatment of the unique atmospheric processes present in a coastal area can be included in a numerical model, but such models are rarely used for operational or regulatory purposes because of their complexities. There are several statistical models (Lyons and Cole, 1973; Misra, 1980a; Cole and Fowler, 1982) in use which compute ground-level concentrations based on the assumptions of a Gaussian distribution or a mixed layer hypothesis. An important component of these coastal fumigation models is the Thermal Internal Boundary Layer (commonly called TIBL) that usually originates at the land-water interface and increases in height downwind. Interaction between the TIBL and a plume from an elevated coastal source influences the distribution of the ground-level concentration and the location of its maximum value. The concept of the TIBL is crucial in understanding shoreline dispersion processes. In this chapter the physics of TIBL formation, the characteristics of the TIBL prediction equations and the general impact of the TIBL on coastal plume dispersion are presented.

2.1 TIBL DYNAMICS

Internal boundary layers ("internal" because they are within the higher planetary boundary layer) develop near a coastline because of the two basic physical differences between land and water: roughness and temperature.

Roughness over the water is generally less than roughness over the land. Frictional effects on air moving over a water surface are minimal and mechanical turbulence produced by varying wave heights is generally low. The mechanical turbulence produced by roughness elements over land may be quite high. Thus, with onshore flow a mechanically-forced internal boundary layer develops from the change in shear stress because of the roughness discontinuity present at the shoreline. The roughness internal boundary layer is generally dominated, however, by thermal effects of the surface discontinuity (Raynor et al., 1979). Other definitions of coastal internal boundary layers pertain to discontinuities in specific humidity and momentum (Gamo et al., 1982), however, these internal boundary layers are also dominated by thermal affects.

A convective internal boundary layer forms because of differences between land and water temperatures (hence the name "Thermal Internal Boundary Layer"). The formation of the TIBL based on flow adjustment theory has been given by various authors (Kerman et al., 1982; Lyons, 1975). An airmass advected over a cool lake or ocean surface is not destabilized by convective elements as would be an overland airmass. Instead, the marine air mass cools from below via conduction from the water's surface and thus becomes stable. As the stable marine air crosses the shoreline (i.e., onshore flow) it must adjust itself, first in the lowest levels, then in the higher levels, to the resulting discontinuity in temperature. This adjustment is accomplished by the generation of turbulence which acts as a transport mechanism for surface heat from the land surface. The TIBL interface generally slopes upward from the coastline until at some point downwind (X) it assumes an "equilibrium height" which is the height of the inland mixed layer. The adjustment of the once stable onshore flow is complete at this equilibrium height. TIBLs tend to grow faster with marginally stable, overwater conditions than with intensely stable, overwater conditions (Lyons et al., 1983; Raynor et al., 1979). This is because the overland thermals have less resistance to rise with a weaker capping marine stable layer than with a stronger capping layer.

The TIBL can be classified by stability into two broad categories for descriptive purposes, as shown in Figure 2.1a. Category I TIBLs are characterized by overwater stable lapse rates. In this case TIBL growth begins at the shoreline (X=0) and continues until an equilibrium point is reached downwind. Category II TIBLs are characterized by overwater stabilities that are near-neutral or unstable. In this case the TIBL does not begin at the coastline, but instead grows out of the marine neutral layer with some initial height h_o, as shown in Figure 2.1b.

Several definitions of the height of the TIBL

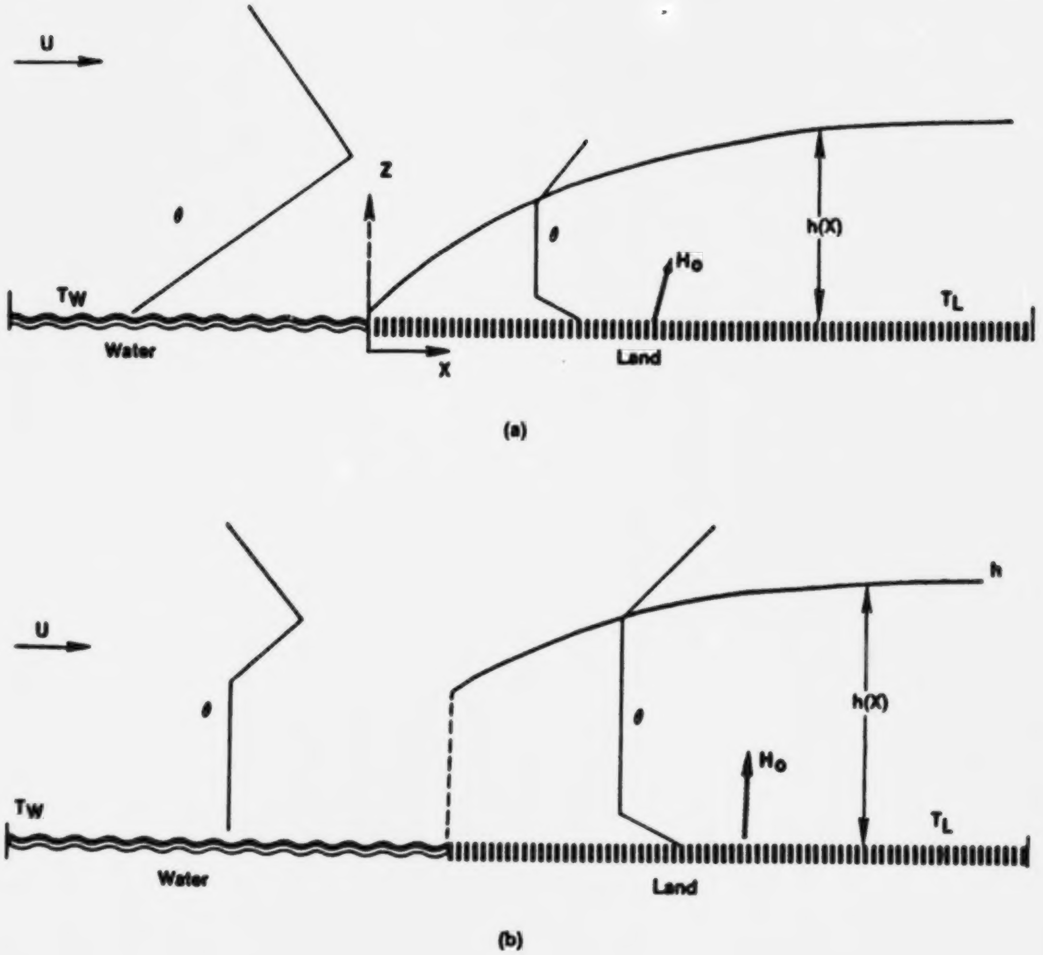
U
θ
Z
θ
h(X)
Tw
Ho
TL
Water
X
Land
(a)
U
θ
h
h(X)
θ
Ho
Tw
TL
Water
Land
(b)

Figures 2.1a and 2.1b: Category I and Category II TIBL cases with stable and unstable/neutral overwater stability, respectively.

interface (h) are given in the literature. Venkatram (1977) defines the TIBL interface as being the point where a temperature profile jump occurs (i.e., a change in stability from neutral to stable). Anthes (1978) in his numerical sea breeze model defines the TIBL height as being the first level greater than 180 meters above ground at which the potential temperature gradient exceeds 1 C km^{-1}.

Lyons (1975) defined the TIBL height as being the average maximum height to which turbulent penetrative convective elements are reaching at a given place and time. Lyons (1975) presented turbulence data to illustrate the sharp turbulence variation across the TIBL interface. An analysis of the variation of the standard deviation of vertical velocity (σ_w) with height for several coastal cases (SethuRaman et al., 1982) shows turbulence variations of a factor of 5 across the TIBL interface. Other investigators (Raynor et al., 1979; Gamo et al., 1983) have also found sharp turbulence changes across the TIBL interface.

Gamo et al. (1982) have investigated the variation in TIBL height (h) based on the two definitions and have concluded that the interface defined by turbulence is higher than the interface defined by temperature. A similar result was obtained by Raynor et al. (1979). In this study the more common turbulence definition of TIBL height is adopted.

It is important to note that the TIBL can develop in either sea breeze or gradient type flows. TIBLs can begin a few kilometers offshore, in response to warm water pockets creating the necessary atmospheric thermal discontinuity. Finally, TIBLs can also form during offshore flow if there is a sufficient land-water temperature contrast. In this case the TIBL develops over warmer water. The structure of the TIBL in terms of its height and the vertical variation of wind and temperature within it will be governed by the mesoscale phenomena both upwind and downwind of the coast.

It has been shown in this section that a distinct change in the air mass can occur at the land-water interface because of two reasons. One is the change in roughness and another is the change in surface heating due to the difference in surface temperature between land and water. During daytime conditions, with warmer land surface temperatures, the latter process usually dominates the air mass modification. This modified layer generally grows in height downwind of the coastline over land with onshore flow and is called the TIBL. A knowledge of the height of the TIBL at various downwind distances will be useful for developing appropriate diffusion models for elevated sources.

2.2 REVIEW OF THE TIBL HEIGHT PREDICTION EQUATIONS

A review of the literature indicates several approaches to determining the TIBL height. A historical flow chart of TIBL equation development is presented in Figure 2.2. Early efforts in specifying the TIBL height are given by Van der Hoven (1967) based on work done by Prophet (1961). The general equation is:

$$h = 8.8 \left(\frac{X}{U_m \Delta \theta} \right)^{0.5} \qquad (2.1)$$

where:

h = TIBL height (m)

X = distance downwind from the land-water interface (m)

U_m = mean wind speed in TIBL (m s^{-1})

$\Delta\theta$ = temperature difference between the top and bottom of the overwater inversion layer (C m^{-1})

The relationship was empirically derived to fit observational data and is not dimensionally homogeneous. The importance of the upwind stability, generally characterized by the $\Delta\theta$ term and the parabolic dependence on downwind distance were first recognized in this formulation.

The first of two recent approaches involves the work of Raynor et al. (1975) and Venkatram (1977). Raynor et al. (1975) derived an equation of the following form based on physical and dimensional considerations:

$$h = \frac{u_*}{U} \left(\frac{X|T_L - T_W|}{|\gamma|} \right)^{0.5} \qquad (2.2)$$

where:

u_* = downwind surface frictional velocity (m s^{-1})

T_L = downwind surface land temperature at a height of 2 m (K)

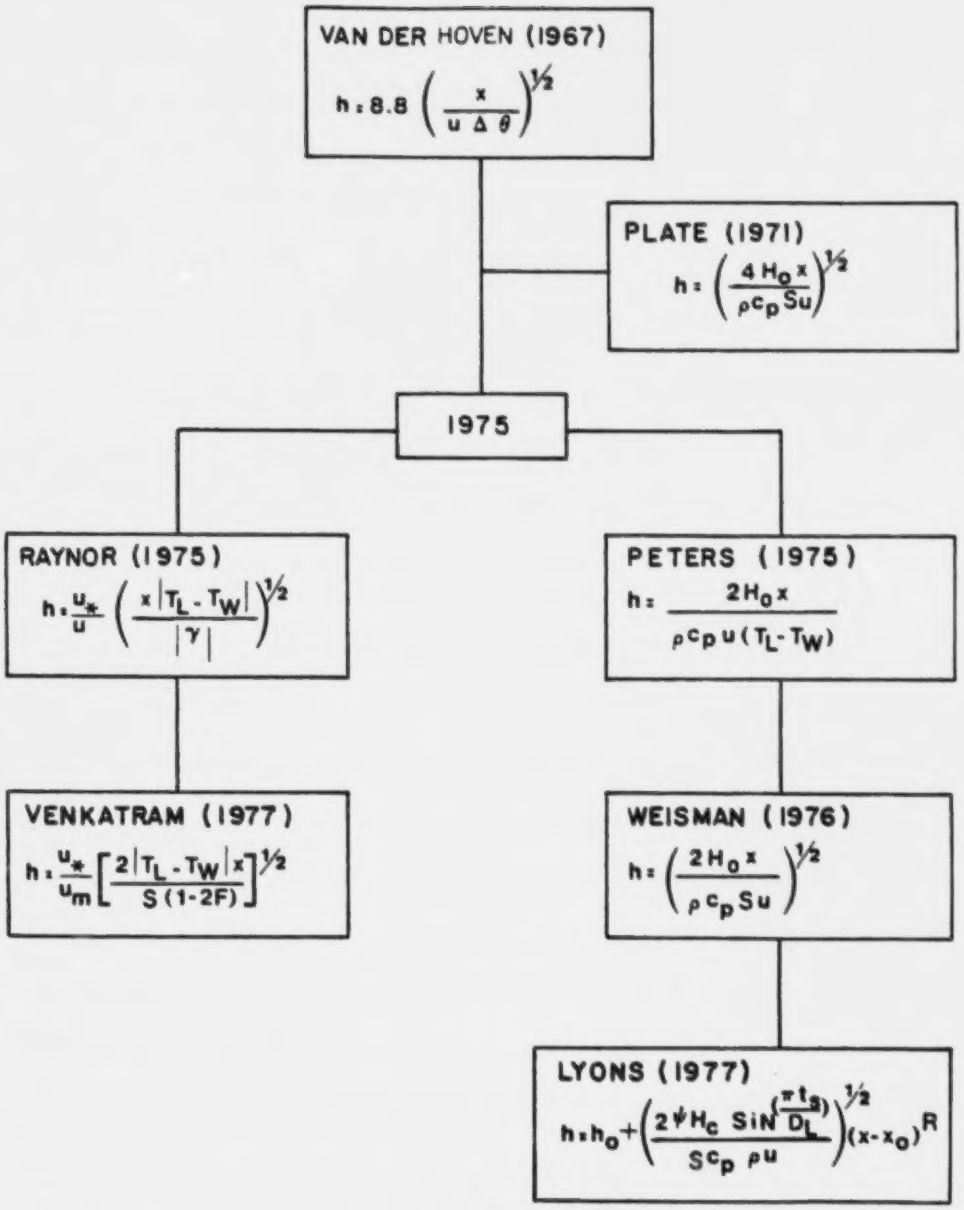
VAN DER HOVEN (1967)
$h = 8.8\left(\frac{x}{u\,\Delta\theta}\right)^{1/2}$
PLATE (1971)
$h = \left(\frac{4H_o x}{\rho c_p S u}\right)^{1/2}$
1975
RAYNOR (1975)
$h = \frac{u_*}{u}\left(\frac{x\left|T_L - T_W\right|}{\left|\gamma\right|}\right)^{1/2}$
PETERS (1975)
$h = \frac{2H_o x}{\rho c_p u(T_L - T_W)}$
VENKATRAM (1977)
$h = \frac{u_*}{u_m}\left[\frac{2\left|T_L - T_W\right|x}{S(1-2F)}\right]^{1/2}$
WEISMAN (1976)
$h = \left(\frac{2H_o x}{\rho c_p S u}\right)^{1/2}$
LYONS (1977)
$h = h_o + \left(\frac{2\psi H_c \sin\left(\frac{\pi t_s}{D_L}\right)}{S c_p \rho u}\right)^{1/2}(x - x_o)^R$

Figure 2.2: Historical flowchart showing development of the TIBL prediction equations (symbols defined in text).

T_W = upwind surface water temperature (K)

γ = absolute lapse rate upwind (K m^{-1})

U = downwind mean wind speed at a height of 10 m

The equation is dimensionally homogeneous and incorporates use of the land-water temperature difference. The vertical structure of TIBL turbulence (and therefore the TIBL height) has been shown to depend significantly on the land-water temperature differential (SethuRaman et al., 1982). A drag coefficient type parameterization (u_*/U), was incorporated into Equation 2.2 to account for the change in surface roughness.

Equation 2.2 does not directly take into account the surface heat flux over land, which is important in the convective growth of the TIBL. Another problem is with singularity as γ approaches 0 in the near-isothermal over-water condition.

The TIBL has been treated analytically by several authors as a horizontally inhomogeneous mixed layer in a steady-state condition (Venkatram, 1977; Gamo et al., 1983). By considering the TIBL as being two-dimensional, the mixed layer energy equation can be written following Venkatram's (1977) notation as:

$$hU_m \frac{\partial \theta_m}{\partial X} = (\overline{w'\theta'})_o - (\overline{w'\theta'})_i \qquad (2.3)$$

where:

θ_m = mixed layer mean potential temperature (K) and

$(\overline{w'\theta'})_{o,i}$ = heat flux at the surface and at the TIBL height, respectively

Venkatram (1977) assumed that vertical motion is small compared to entrainment velocity. A simplified entrainment hypothesis was used which assumed that the temperature jump at the inversion, $\Delta\theta_o$, is proportional to the TIBL depth and the temperature gradient above the TIBL, such that:

$$\Delta\theta_o = F_R \gamma h \tag{2.4}$$

where F_R is an entrainment fraction and $\Delta\theta$ is the temperature jump across the TIBL. The ratio of heat flux at the TIBL interface to that at the surface has been shown to equal a constant (c) (Betts, 1973), where c is also equal to $F(1-2F)^{-1}$. Surface heat flux $(\overline{w'\theta'})_o$ is given by $C_\theta u_*(\theta_1-\theta_m)$ where C_θ is the heat coefficient. This yields a relation for the heat flux at the TIBL top as:

$$(\overline{w'\theta'})_i = -\frac{(F_R C_\theta C_u U_m)}{(1-2F)}(\theta_1-\theta_m) \tag{2.5}$$

where C_u is the frictional coefficient. Substituting Equation 2.5 into Equation 2.4 yields:

$$hdh = \frac{C_\theta C_u U_m}{\gamma}\frac{(\theta_1-\theta_m)}{(1-2F)}dt \tag{2.6}$$

Integrating Equation 2.6, substituting $U_m dt = dX$ and assuming $C_\theta = u_*/U_m$ and $\theta_m = \theta_w$, one obtains the TIBL equation of Venkatram (1977):

$$h = \frac{u_*}{U_m}\left(\frac{2X|T_L-T_W|}{S(1-2F)}\right)^{0.5} \tag{2.7}$$

where S = the potential temperature gradient over water.

Equation 2.7 assumes that the TIBL is dominated by buoyancy. In addition, Equation 2.7 assumes that the layer is well-mixed and therefore produces uniform vertical potential temperature profiles and velocity gradients. The well-mixed assumption may not hold true under all conditions, as shown by SethuRaman (1982). For strongly stable, upwind conditions with a surface-based inversion, a low-level supergeostrophic jet is usually found over the ocean. This layer retains its characteristics for appreciable downwind distances in the TIBL. Supergeostrophic wind velocities are observed over land in the coastal region in spite of convective conditions. Equations 2.2 and 2.3, derived analytically, are essentially similar except for the entrainment variable F (~ 0.2) which increases the estimates of h by a factor of about two.

Peters (1975) developed a scheme of determining TIBL height with the assumption that the upward turbulent transport of energy in the boundary layer causes a temperature gradient which corresponds to a constant, near-ground vertical heat flux. The average overland TIBL temperature may be written as:

$$T_A = 0.5(T_w + ah + T_L) \qquad (2.8)$$

where:

T_A = average temperature of the TIBL layer and

a = temperature gradient upwind (K m^{-1})

Peters (1975) defines (T_w + ah) as being representative of the temperature profile over both land and water. Equation 2.8 therefore relates the TIBL layer temperature obtained over a given width of land. An energy balance performed on the area under h yields the following:

$$H_oX = \rho c_p U_{10}[0.5(T_w + ah + T_L) - 0.5(2T_w + ah)]\ h \qquad (2.9)$$

where:

H_o = surface heat flux over land (W m^{-2})

c_p = specific heat at constant pressure (0.24 cal $g^{-1}K^{-1}$) and

ρ = density of air (1.2 X 10^3 g m^{-3})

The first term in Equation 2.9 is the average overland TIBL temperature as given in Equation 2.8 and the second term represents the average overwater temperature.

Solving for h, Peters (1975) obtained:

$$h = \frac{2\ H_oX}{\rho\ c_pU\ (T_L - T_w)} \qquad (2.10)$$

The linear nature of Equation 2.10 implies that Peters' (1975) scheme should predict a fast growing TIBL. In addition, this model cannot be used for large downwind distances because of the linear growth predicted by the model. Observations indicate a parabolic growth.

Plate (1971), using earlier work by Ball (1960), derived an equation for the height of the free convective boundary layer capped by a stable layer. He assumed that the heat flux at the top of the convective boundary layer is equal to the surface heat flux, so that:

$$\left(\overline{w'\theta'}\right)_i = \left(\overline{w'\theta'}\right)_o \tag{2.11}$$

If a constant surface heat flux and sharp temperature discontinuity at the TIBL interface are assumed, then using the geometry of the assumed thermal structure (see Plate, 1971) total heat input can be written as:

$$h \frac{dT}{dt} + (T_L + Sh - T) \frac{dh}{dt} = \frac{2H_o}{\rho c_p} \tag{2.12}$$

where T is the temperature at height h. Assuming that the temperature change and TIBL thickness are proportional,

$$\alpha \frac{dh}{dt} = \frac{dT}{dt} \tag{2.13}$$

and

$$\alpha h = T - T_L \tag{2.14}$$

where α is an arbitrary constant approximately equal to S. By combining Equations 2.12, 2.13 and 2.14 and solving algebraically for h, Plate (1971) obtained the following:

$$Sh^2 = \frac{4H_o t}{\rho c_p} \tag{2.15}$$

which yields,

$$h = \left(\frac{4H_o X}{\rho c_p SU} \right)^{0.5} \tag{2.16}$$

In Equation 2.16 t was replaced by X/U, where U was taken to be representative of the mean TIBL wind. Weisman (1976) suggested using an equation similar to Equation 2.16 as an extension to Peters' (1975) Equation 2.10, but with a parabolic variation of TIBL height. It is not clear how Weisman (1976) derived his equation, which appears as:

$$h = \left(\frac{2H_o X}{\rho\, c_p SU} \right)^{0.5} \qquad (2.17)$$

Alternatively, Gamo et al. (1983) have derived Equation 2.17 from a mixed layer theory basis. Gamo et al. (1983) assumed that the TIBL is heated uniformly and that the heat flux decreases linearly with height such that:

$$U \frac{\partial \theta(X)}{\partial X} = \frac{-1}{\rho\, c_p} \frac{\partial H(X,Z)}{\partial z} \qquad (2.18)$$

Ignoring the temporal variation of θ and horizontal variation of heat flux, Gamo et al. (1983) integrated Equation 2.18 with the boundary conditions $H = h_o$ at $z = 0$ and $H = 0$ at $z = h$ and obtained:

$$\frac{\partial \theta(X)}{\partial X} = \frac{H_o(X)}{\rho\, c_p Uh(X)} \qquad (2.19)$$

The change in temperature with respect to change in TIBL height may be defined as:

$$\frac{\partial \theta}{\partial h} = S \qquad (2.20)$$

Combining Equations 2.19 and 2.20, Gamo et al. (1983) obtained:

$$\frac{\partial h(X)}{\partial X} = \frac{H_o(X)}{\rho c_p SUh(X)} \qquad (2.21)$$

Integration of Equation 2.20 yields:

$$\theta = \theta_o + S(h - h_o) \qquad (2.22)$$

Integration of Equation 2.21 yields:

$$h = (\rho c_p SU)^{-0.5} \left(2\int_{X_o}^{X} H_o(X)dX + h_o^2\right)^{0.5} + h_o \qquad (2.23)$$

Here the subscript "o" refers to the initial value at the shoreline $(X = X_o)$. At the shoreline $(h_o = 0, X = 0)$, Equation 2.23 becomes:

$$h = (\rho c_p S U)^{-0.5} \left(2\int_0^X H_o(X)\,dX + h_o^2\right)^{0.5} \qquad (2.24)$$

and Equation 2.22 can be conveniently rewritten as:

$$\theta = S\ h \qquad (2.25)$$

Assuming that the surface heat flux does not change with respect to inland distance then Equation 2.25 becomes:

$$h = \left(\frac{2H_oX}{\rho c_p SU}\right)^{0.5} \qquad (2.26)$$

Equation 2.26 is in reality the Weisman (1976) formulation (Equation 2.17). Gamo et al. (1982, 1983) give a more detailed explanation of the above condensed derivation.

There are two practical problems in using the Weisman (1976) approach. To begin, the determination of heat flux is difficult in most meteorological applications. Secondly, the singularity question may arise as S approaches 0 in the near-neutral case. In addition, for operational use Weisman (1976) selected 100 cal m^{-2} to fit the measured TIBL data to the predictive equation, yet it is commonly known that heat flux varies with time of day, latitude and cloud cover.

Lyons et al. (1983) have modified Equation 2.17 to account for the time dependence of heat flux by introducing various parameters such as a solar insolation factor and elapsed time since sunrise. The use of this heat flux parameterization closely follows the heat flux scheme used in a numerical sea breeze model by Anthes (1978).

The modified Equation 2.17 given by Lyons et al. (1983) is:

$$h = h_o + \left(\frac{2 \psi H_c \sin (\pi t_s / D_L)}{S \rho c_p U} \right)^{1/2} (x - x_o)^R \qquad (2.27)$$

where:

ψ = solar insolation factor which was chosen arbitrarily as:

0.1 for very low insolation

0.3 for low insolation

0.6 for moderate insolation and

1.0 for strong insolation

H_c = 20% of the solar constant

t_s = time since sunrise

D_L = length of day

R = a variable exponent

h_o = initial depth of TIBL at downwind distance x_o -- allows for changes in TIBL shape

h = depth of TIBL at downwind distance x

Once again Equation 2.27 has a singularity problem with S approaching 0.

Additional problems arise from questions of determining ψ, x_o and R. Lyons et al. (1983), for example, determined R to be 0.61 based on the average of the "best fit" R for four TIBL cases. This value may be highly dependent. It appears from different analytical and dimensional approaches (Plate, 1971; Venkatram, 1977; Raynor et al., 1979) that R is equal to 0.5.

Finally, it is important to note that some coastal dispersion modelers (Van Dop et al., 1979; Misra and Onlock, 1982) prefer to simplify the TIBL equations such that:

$$h = A[X]^{0.5} \tag{2.28}$$

where:

A = a factor containing different physical parameters necessary for TIBL determination.

In this section, all the TIBL equations except that of Peters (Equation 2.10) can be written in the form of Equation 2.28. The quantity A, constant for given surface and meteorological conditions, will vary between different formulations, however. In a later section these TIBL formulations will be examined against two different data sets to determine the best TIBL equation for use in diffusion models.

2.3 IMPACT OF TIBL VARIATION ON COASTAL DISPERSION

The specific mechanisms involved in coastal dispersion will be presented in Section 3.2. In this section, however, the physical processes involving interaction between the TIBL and an elevated plume at the coastline will be discussed.

Two important physical processes concerning dispersion in coastal regions are fumigation and trapping. Plumes emitted into the stable marine air at the shoreline ($X = 0$) normally move inland with onshore flow and at some point intersect the deepening TIBL. Intense downward mixing at the point of TIBL impaction can cause high ground-level concentration. Plumes have been observed to travel 20-to-30 km downwind before fumigating (Portelli, 1982).

Trapping conditions occur when stacks are located within the TIBL at some inland distance such that plumes are emitted into the convectively mixed TIBL and are effectively capped by the TIBL interface. If a plume is sufficiently buoyant and a stack is located close to the TIBL interface the plume may actually penetrate into the stable marine air and then fumigate back into the TIBL at a point of intersection further downwind. The importance of TIBL variation on fumigation is illustrated by a practical example shown in Figure 2.3. Various parameters used in Figure 2.3 are:

H_s = 160 m (stack height)
Δh_s = 90 m (plume rise)
U_m = 5 m s^{-1}
$h_1(X) = 5.61\ (X)^{0.5}$ typical maximum (A) factor (Misra and Onlock, 1982)
$h_2(X) = 2.71\ (X)^{0.5}$ typical minimum (A) factor (Misra and Onlock, 1982)

The TIBL heights $h_1(X)$ and $h_2(X)$ were calculated using a

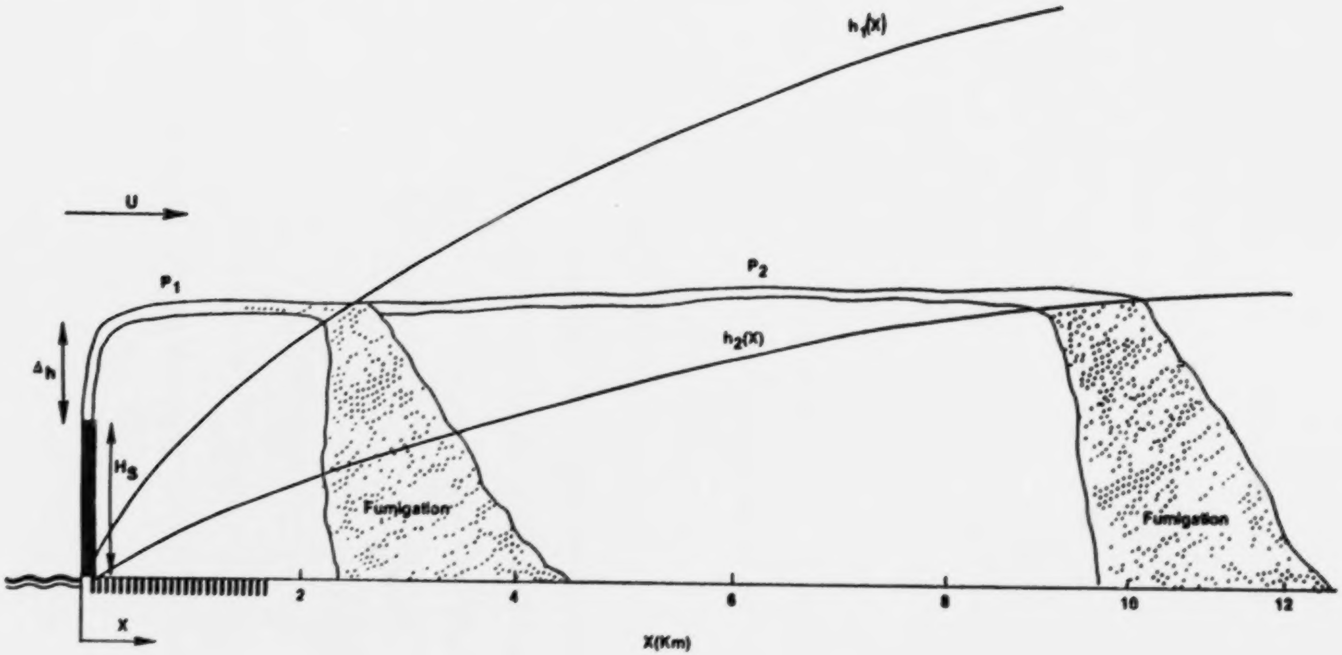
U
$h_1(X)$
P_1
P_2
$h_2(X)$
Δh
H_S
Fumigation
Fumigation
X
2
4
6
8
10
12
X(Km)

Figure 2.3: Impact of TIBL variation upon location of downwind maximum concentration. $h_1(X)$ and $h_2(X)$ refer to TIBL height 1 and height 2, respectively. P_1 and P_2 refer to plumes 1 and 2, respectively. Δh refers to plume rise and H_s refers to the stack height.

simplified TIBL equation (Equation 2.28). Minimum and maximum (A) factors were obtained from observations.

For the case of $h_1(X)$, the TIBL grows sharply from the coast, reaching a height of 250 m just after 2 km downwind. Fumigation of plume P1 begins at this point. For simplicity, it is assumed that plume P1 is mixed instantaneously into the TIBL. The fumigation zone is depicted as about 2 km long.

For the $h_2(X)$ case, the TIBL is seen to grow less sharply than for the $h_1(X)$ case. The TIBL height at 2 km is about 120 m, which is considerably below the effective stack height of 250 m. In this case plume P2 impacts the shallow TIBL around 9 km downwind. Fumigation of plume P2 begins at this point.

The difference between h_1(2 km) and h_2(2 km) is about 130 m. This simple example illustrates that even a relatively small difference in predicting TIBL height at a given downwind distance may cause serious problems in predicting the location of the ground-level fumigation and hence the location of the maximum ground-level concentration. Every coastal dispersion model must therefore have a reliable TIBL variation module in order to predict the ground-level fumigant concentration.

3.0 COASTAL DISPERSION MODELING

This chapter briefly presents the mechanics of fumigation both inland and at the coast and presents a review of the various shoreline dispersion models and modifications to each model.

3.1 THE MECHANICS OF FUMIGATION

The phenomenon of fumigation has been observed for several centuries. One of the earliest uses of the word "fumigation" was in the book by John Evelyn (1661) entitled "Fumifugium: or the Inconvenience of the Aer and Smoake of London Dissipated, Together With some Remidies" (as cited by Dooley, 1976).

In the early twentieth century numerous cases of fumigation were reported in Anaconda, Montana and San Francisco, California, among other places (Dooley, 1976). The first real study of fumigation occurred in the late 1930´s at Trail, British Columbia and is reported by Hewson and Gill (1944).

Basically, fumigation is a transitional process which involves a plume in a stable layer impinging upon an unstable turbulent lower layer. The impingement may be because of temporal or spatial turbulent layer growth. Bierly and Hewson (1962) defined three different types of fumigation:

Type I: Nocturnal inversion breakup

Type II: Flow of air over an artificial heat source

Type III: Continuous, occurring over natural heat sources such as shorelines

Type I fumigation generally occurs around mid-morning as the overnight inversion lifts to plume height level. Three factors influence the growth of this mixed layer (Lindsey and Ramsdell, 1983):

1. Surface heating
2. Increased surface level winds
3. Increased upper boundary layer winds

Increased surface heating warms the near surface air resulting in an upward transfer of sensible heat. This causes the near surface air to become unstable and turbulence is no longer suppressed by buoyancy forces. Increasing surface winds caused by the transfer of momentum between recoupling levels aids in continually increasing the turbulence, which allows for increased mixed layer height. Shear induced turbulence (aiding in mixed layer growth) is possible if higher level winds increase under stable conditions.

A typical Type I fumigation case generally results in fumigation for 1 or 2 hours. Plumes initially emitted into the stable nocturnal inversion exhibit a fanning type dispersion pattern. During early morning the nocturnal inversion layer gradually lifts until mid-morning, when it reaches the base of the plume. Fumigation results when the plume becomes entrained into the growing well-mixed layer. Assuming that complete fumigation results in uniform vertical dispersion between the plume top and the ground, the ground-level concentrations under Type I conditions may be obtained by using the Gaussian fumigation equation (Turner, 1970):

$$C = \frac{Q}{U\sigma_{yf}\sqrt{(2\pi)}} \exp[(-y^2/2\sigma_{yf}^2)(1/(H_e+2.15\sigma_z))] \qquad (3.1)$$

where σ_{yf} represents the horizontal dispersion coefficient during fumigation (in meters). A modification of this equation was used by Lyons and Cole (1973) for coastal fumigation.

Bierly and Hewson (1962) gave an approximation for obtaining the value of σ_{yf} which assumes that the plume spreads outward at an angle of 15 degrees. Turner (1970) suggested that the horizontal coefficient at plume centerline be represented by σ_y under stable (Pasquill-Turner class E or F) conditions at a point downwind (X_E) where complete fumigation has occurred. Combining these two approximations, Turner (1970) suggests:

$$\sigma_{yf} = \sigma_y(\text{stable}) + H_e/8 \qquad (3.2)$$

Type II fumigation occurs during the evening hours when rural air, which has just been stabilized by radiational cooling, reaches a shallow convective layer over an urban area. The stable air could mix down into the shallow convective layer carrying with it leftover pollutants which originated from other areas (Munn, 1959). This process is made possible by the so called "heat island effect" of a city.

The concern here is with Type III fumigation, which occurs during onshore flow and generally during daylight hours. Plumes emitted into the stable marine air eventually impinge upon the growing TIBL and fumigate downward, as briefly outlined in Chapter 2. Fumigation zones may range in size from a hundred meters to several kilometers long and from tens of meters to a few kilometers wide (Dooley, 1976).

The following sections briefly describe different coastal fumigation models that have appeared in the literature with discussion of their similarities and differences. Modifications to take into account non-instantaneous mixing conditions when the plume impacts the TIBL (the real world situation), will also be suggested.

3.2 THE LYONS AND COLE (1973) MODEL

Before dispersion models were developed, early coastal dispersion studies (Hewson et al., 1963) concentrated on photographing smoke released near shorelines. Later Lyons and Cole (1973), in a study of a large, four stack fossil fuel plant on the western shore of Lake Michigan, presented a modification of Turner's fumigation scheme (presented in the previous section) for shoreline locations. The Lyons and Cole (1973) model divides the downwind dispersion area into three zones:

Zone I: Undisturbed dispersion zone (X_1)

Zone II: Plume fumigation zone (X_2)

Zone III: Plume trapping zone (X_3)

A diagram depicting the vertical plume geometry appears in Figure 3.1. The assumptions of the model are:

(1) "Steady-state" concentration

(2) Flat terrain

(3) No initial plume dilution

(4) For a given plume, wind direction and speed are constant in space. Therefore the effect of shear cannot be incorporated.

In Zone I, where C is a function of $X,Y,Z:H_e$, the elevated plume is emitted into a homogeneous stable layer and therefore remains unmodified in shape. The basic Gaussian fumigation formulation (Equation 3.1) for finding elevated concentrations in this zone may be written as:

$$C(X_1,Y,Z:H_e) = \frac{Q}{2U\pi\sigma_y(x,s)\sigma_z(x,s)} \exp\frac{-y^2}{2\sigma_y^2(x,s)} \left[\exp\frac{-(Z-H_e)^2}{2\sigma_z^2(x,s)} + \exp\frac{-(Z+H_e)^2}{2\sigma_z^2(x,s)}\right] \qquad (3.3)$$

where $\sigma_y(x,s)$, $\sigma_z(x,s)$ are the standard deviations for plumes spreading into the stable air. Figure 3.1 shows the plume axis along with a typical $\sigma_z(x,s)$ plume spread in the zone depicted as X_1.

Zone II $(X_2,Y,Z:H_e)$ applies to the region where the plume impacts the TIBL and is being entrained into the

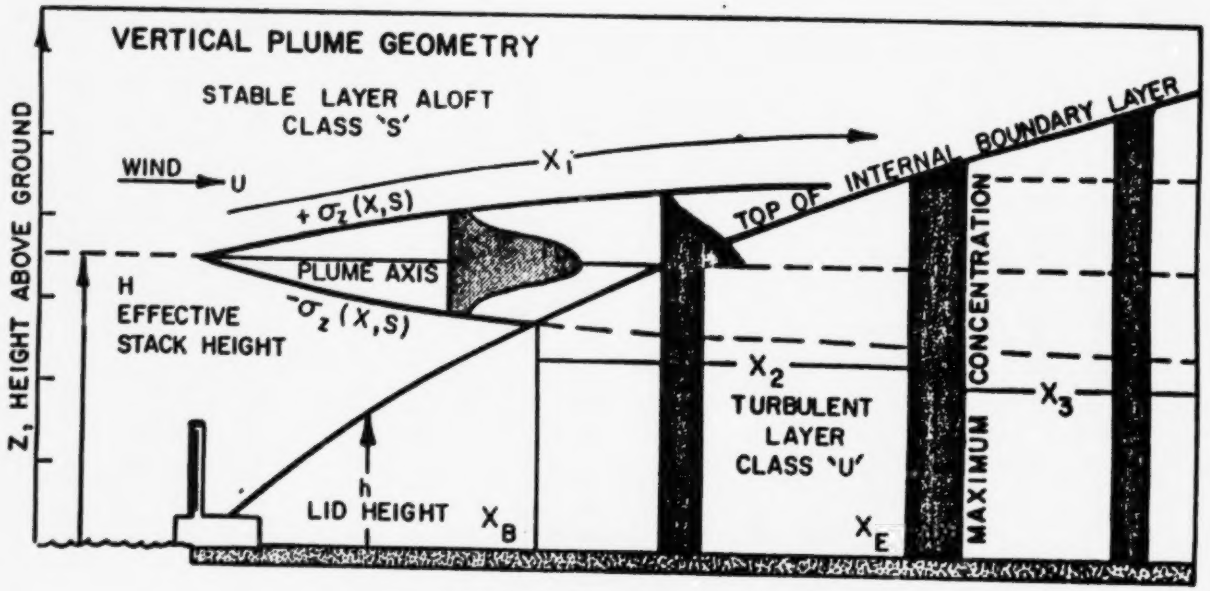
VERTICAL PLUME GEOMETRY
STABLE LAYER ALOFT CLASS 'S'
WIND → U
X_1
$+\sigma_z(X,S)$
PLUME AXIS
$-\sigma_z(X,S)$
H EFFECTIVE STACK HEIGHT
Z, HEIGHT ABOVE GROUND
h
LID HEIGHT
X_B
TOP OF INTERNAL BOUNDARY LAYER
X_2
TURBULENT LAYER CLASS 'U'
X_E
MAXIMUM CONCENTRATION
X_3

Figure 3.1: Vertical plume geometry of the Lyons and Cole (1973) model. $X_{1,2,3}$ refer to different regions described in the text. X_B and X_E refer to the beginning and ending of fumigation. Here H is the effective stack height.

TIBL. Figure 3.1 depicts this zone as falling between points X_B (beginning of fumigation) and X_E (for end of fumigation). The beginning of fumigation occurs at the point $h = H_e - 2.15\sigma_z(x,s)$, which is similar to the approach of Turner (1970). This is the point where turbulence begins to affect the lower portion of the plume. Consequently, the point at which the majority of the plume has been mixed into the TIBL is determined by $h = H_e + 2.15\sigma_z(x,s)$.

An important feature to note about Zone II is that the profile of concentrations below the TIBL is considered nearly uniform in the vertical. Horizontally, the plume is treated as Gaussian. Concentrations in Zone II can be found by using the equation:

$$C(X) = \frac{Q}{\sqrt{(2\pi)}\sigma_{yf}(x,s)\ U_m h} \left[\int_{-\infty}^{p} (2\pi)^{-0.5} \exp\left(-p^2/2\right) dp \right]$$
$$* \ \exp\left[-1/2\ \left(y/\sigma_{yf}(x,s)\right)^2\right] \qquad (3.4)$$

where $p = (h(x) - H_e)/\{\sigma_z(x,s)$ and σ_{yf} is the horizontal spread of the plume in the fumigation zone which can be represented by:

$$\sigma_{yf}(x,s) = \sigma_y(x,s) + H_e/8 \qquad (3.5)$$

Equation 3.5 states that a correction factor of $H_e/8$ is needed to represent the dispersion in the TIBL.

In the third zone the plume is assumed to be trapped with a variable TIBL lid height as an upward boundary. Concentrations once again are assumed to be uniform in the vertical below the TIBL. The choice of dispersion coefficients in this region must be done with care, since the initial standard dispersion coefficients are not valid within the TIBL. Therefore, to determine dispersion characteristics in Zone III one must choose a virtual source at some point x_o', which lies between X_B and X_E in Zone II. The plume trapping formula of Turner (1970), along with a virtual point source method to determine the new dispersion coefficient, is used in this zone.

In the mid-70's the Lyons and Cole (1973) model was modified to a regional type model for urban, coastal use. The new model was called GLUMP (Great Lakes University Mesoscale Project). The model incorporated Equation 2.19 for the TIBL parameterization and included multiple vertical atmospheric layers with independent parameters.

3.3 THE CRSTER SHORELINE FUMIGATION MODEL (CSFM)

The CRSTER Shoreline Fumigation Model (CSFM) is an interactive version of EPA's Single-Source CRSTER model which has been modified to handle shoreline dispersion conditions. The model can handle stacks located both inside and outside the TIBL. The model consists of four main modules: two plume rise modules, a diffusion module and a fumigation module. Concentration calculations can be made at 180 receptors arranged in 5 rings (at a time) of 36 receptors for each ring.

The fumigation module incorporates the Lyons and Cole (1973) scheme described in the previous section with several modifications. The model assumes that a pollutant parcel entering the TIBL from the stable layer is completely mixed in the TIBL and that this mixing takes place instantaneously. However, unlike the Lyons and Cole (1973) model, which treats dispersion in the fumigation zone as $\sigma_{yf} = \sigma_y + H_e/8$, the CSFM model assumes that the plume is gradually eroded by the TIBL such that different segments of the entrained plume disperse differently. The concentration at a particular receptor X_j is affected by all of the plume segments (subscript j) which have been entrained into the TIBL upwind.

The example (Figure 3.2) given by Cole and Fowler (1982) illustrates the concept further. Figure 3.2 shows that pollutant parcels in segment 1 have been affected by a travel distance of about 2.5 km in the stable air and 0.5 km in the TIBL. Segment 2 is shown to have a stable air travel time of 3.5 km and a TIBL travel time of 0.5 km. This means that the plume in segment 2 would be more characteristic of dispersion in stable conditions and thus interact with the TIBL differently than the plume in segment 1.

CSFM uses $\sigma_y(x,s)$ to determine the lateral spread at

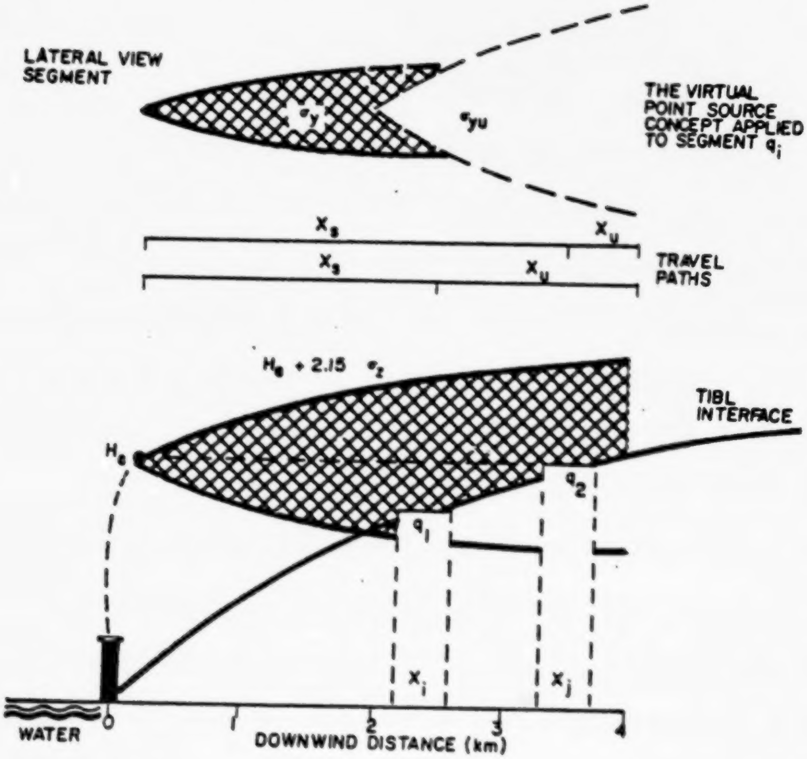

LATERAL VIEW SEGMENT
σy
σyu
THE VIRTUAL POINT SOURCE CONCEPT APPLIED TO SEGMENT q_i
X_s
X_u
X_s
X_u
TRAVEL PATHS
H_e + 2.15 σ_z
TIBL INTERFACE
H_e
q_1
q_2
x_i
x_j
WATER
0
1
2
3
4
DOWNWIND DISTANCE (km)

Figure 3.2: Plume geometry of the CSFM model showing individual entraining plume segments (q_1, q_2 refer to segments 1 and 2, respectively).

the point of TIBL plume intersection. A virtual point source is introduced at the TIBL impaction point which has a σ_y equal to $\sigma_y(x,s)$. Consequently, the concentrations at X_j are the sum of all the plume segments entrained into the TIBL upwind of X_j such that:

$$C_j = \sum_{i=1}^{n} C_{ji} \qquad (3.6)$$

and

$$C_j = \frac{Q_i}{\sqrt{(2\pi)}\sigma_{yf_{ij}} U\ h(X)} \qquad (3.7)$$

The coefficient $\sigma_{yf_{ij}}$ represents the horizontal dispersion coefficient for plume segment i as it reaches receptor X_j and is determined by the stability of the marine air and the TIBL at each receptor distance. The quantity Q_i is the mass per second contained in plume segment i and is computed for every 0.2 km interval. Q_i is determined by:

$$\begin{aligned} Q_i = Q[\int_{\infty}^{p} (2\pi)^{-0.5} \exp(-p/2)^2 dp]\Big|_{\text{at } X_i} \\ - [\int_{\infty}^{p} (2\pi)^{-0.5} \exp(-p/2)^2\ dp]\Big|_{\text{at } X_i - 1} \end{aligned} \qquad (3.8)$$

where X_i represents the downwind distance at plume segment i.

The integral in Equation 3.8 is the area under the standard normal distribution, where p is the value of a variable having a normal distribution. This gives the proportion of the normally distributed plume that has entered the TIBL at some distance x. In this case, p is defined by:

$$p = \frac{h - H_e}{\sigma_z(y,s)} \tag{3.9}$$

The p factor thus accounts for the portion of the plume that is mixing downward after TIBL impaction.

Plume rise is determined using three methods based on the stack location. If the plume is emitted into the stable air, the Briggs (1975) plume rise formula with stable $\partial\theta/\partial z$ is used. The formula is:

$$\Delta h_s = 2.4\ (F_o/U_s D)^{0.333} \tag{3.10}$$

where:

Δh_s = is the plume rise (m)

F_o = is the buoyancy flux ($m^4 s^{-3}$)
and $F_o = (g/\pi)\ v_f(T_s - T)T^{-1}$

T_s = pollutant temperature (K)

$v_f = (\pi/4)v_s d^2$ (exit velocity) (m s^{-1})

v_s = stack gas velocity (m s^{-1})

d = diameter (m)

U_s = wind speed at stack height in stable air (m s^{-1})

D = stability parameter $(g/T)(\partial\theta/\partial z)$

When the stack is located below the TIBL (i.e., an inland stack) the potential exists for either trapping or penetration. First, the final plume rise is determined using Briggs (1975) formulations with unstable $\partial\theta/\partial z$. If the resulting rise leaves the plume below the TIBL, trapping occurs, since the plume is not buoyant enough to penetrate the TIBL interface. Penetration occurs if the resulting rise is greater than the TIBL height (i.e., the plume punctures the TIBL). In this case the height of penetration is determined and a two staged plume rise model by Holzworth (1978) is utilized.

The Holzworth (1978) scheme generates 25 m interval layers up to 500 m in addition to a layer at stack height and a layer at TIBL height. Temperature and wind speed are estimated for each layer and a height (Z_n) is assigned where n represents the level number. A buoyancy flux (F) is computed at Z_s (stack height) until a negative flux is found. The initial buoyancy (F_i, $m^4 s^{-3}$) is empirically determined by (Holzworth, 1978):

$$F_i = (37 \times 10^{-6})\, E \tag{3.11}$$

where E (cal s^{-1}) is the heat emission rate and is given by:

$$E = 83.45\, E_V P_1 (T_S - T_1) T_S^{-1} \tag{3.12}$$

and where:

E_V = gas volume emission rate ($m^3 s^{-1}$)

P_1 = atmospheric pressure at stack height (mb)

T_S = effluent temperature at top of stack (K)

T_1 = air temperature at stack height (K)

Plume rise and subsequent fluxes at higher levels are calculated by formulas also given by Holzworth (1978).

After these calculations, receptor concentrations are determined as previously described.

A flowchart summarizing the most important aspects of the model appears in Figure 3.3. The model reverts to the standard CRSTER output if the input data indicates that the conditions are not appropriate for a TIBL to form (e.g., insufficient land-water temperature difference).

3.4 THE MISRA SHORELINE FUMIGATION MODEL (MSFM)

Misra (1980a) presented a model for coastal point source application based on the equation of conservation of mass. The assumptions made by Misra (1980a) include:

(1) Constant wind speed with height and independent of shoreline distance

(2) Perpendicular wind direction to the shoreline

(3) Instantaneous homogeneous mixing of the plume upon TIBL impaction

(4) Concentration distribution is Gaussian

(5) Plume is emitted into the stable marine air

(6) Dispersion coefficients are a function of w_*

Two key differences between the Misra (1980a) and the CSFM models are:

(1) The plume fumigates everywhere at the interface between the stable air and the TIBL. Thus the three-zoned approach is changed to a stable zone and a fumigating zone.

(2) After TIBL impaction, the plume is assumed to be dispersed based on the parameters of the mixed layer (such as convective velocity scaling) and not on the derived stability σ_{yf} of each plume segment as in CSFM.

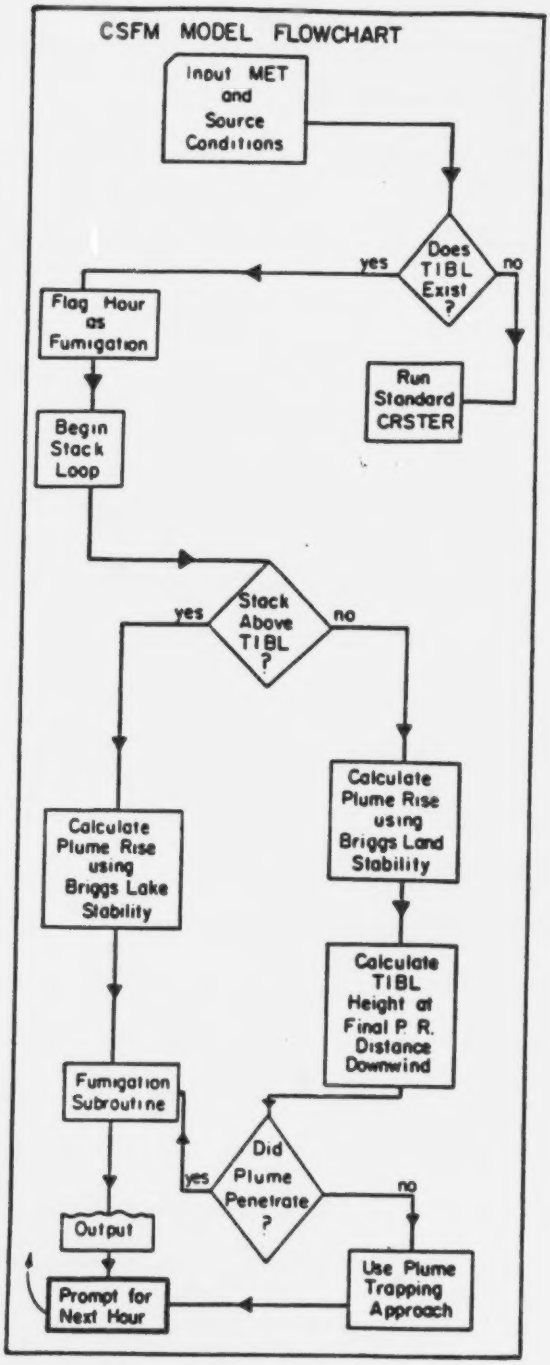
CSFM MODEL FLOWCHART
Input MET and Source Conditions
Does TIBL Exist ?
yes
no
Flag Hour as Fumigation
Run Standard CRSTER
Begin Stack Loop
Stack Above TIBL ?
yes
no
Calculate Plume Rise using Briggs Lake Stability
Calculate Plume Rise using Briggs Land Stability
Calculate TIBL Height at Final P. R. Distance Downwind
Fumigation Subroutine
Did Plume Penetrate ?
yes
no
Output
Use Plume Trapping Approach
Prompt for Next Hour

Figure 3.3: Flowchart of the CSFM model.

The model assumes that the movement of pollutants into the TIBL are caused by two mechanisms:

(1) Entrainment of the plume downwind by the growing TIBL and

(2) Processes which affect plume dispersion in stable air

The dominating mechanism is assumed to be plume entrainment. Plume dispersion in the TIBL is assumed to be described as:

$$F_e(X,Y) = C_s(X,Y,h) \left(U_s \frac{dh}{dX} + \frac{K_{zs}}{C_s} \frac{dC_s}{dZ} \right) \qquad (3.13)$$

where F_e is the entrainment flux through the TIBL interface, $C_s(X,Y,h)$ is the concentration distribution along the TIBL interface, U_s is the wind speed in the stable layer at height h and K_{zs} is the diffusion coefficient in the stable layer defined by $K_{zs} = 1/2\ d/dt(\sigma^2_{zs})$, where σ_{zs} is the vertical standard deviation of position of a particle at time t, after release from the stack.

Misra (1980a) defines (X', Y') as being points located on the TIBL interface h(x) at some downwind distance X′. An area source exists at each of these points such that $F(X',Y')dX'dY'$ represents the net flux of pollutants through that area source. The dispersion into the TIBL is assumed to occur from the elevated area source coincident with the intersection of the plume and the TIBL. The source strength is provided by the concentration field of the plume within the stable layer (C_s) coincident with the

TIBL.

Misra (1980a) uses similarity theory in order to obtain diffusion parameters both above and in the TIBL. He assumes that the parameters in the stable layer are only affected by the turbulence created by the plume itself and not by atmospherically induced turbulence. (This is a reasonable assumption since turbulence levels are low in the stable layer.) This means that σ_{ys} and σ_{zs} are both proportional to plume rise Δh_s. The stable layer dispersion parameters are:

$$\begin{aligned} \sigma_{zs} &= a_1\,(F_o/U_s)^{1/3}\,t^{2/3} && \text{for } t \leq 4.5/N \\ &= a_2 && \text{for } t > 4.5/N \qquad (3.14) \\ \sigma_{ys} &= a_3\,(F_o/U_s)^{1/3}\,t^{2/3} \end{aligned}$$

where a_1, a_2 and a_3 are experimental constants and where:

N = Brunt-Vaisalla frequency (s^{-1}) $[(g/\theta)d\theta/dz)]^{0.5}$

F_o = plume buoyancy (m^4s^{-3})

U_s = mean wind speed in the stable layer ($m\ s^{-1}$)

t = travel time (s), defined as (x/U_s) with x the downwind distance

The value 4.5/N represents a time limit and for a stable atmosphere is assumed to correspond to the time after which the plume levels off (Misra, 1980a).

Characterization of σ_y in the TIBL is a function of the convective velocity scale w_*, where:

$$w_* = (gH_oh/\rho c_pT)^{1/3} \qquad (3.15)$$

The variable w_* is a function of buoyancy, heat flux and TIBL height. The Misra (1980a) model makes the assumption that w_* is independent of downwind distance. Following Lamb (1978), σ_{yh} can be written as:

$$\sigma_{yh}(X) = 0.333\ (w_*/U_m)(X-X') \qquad \text{for } (X-X') \leq hU_m/w_* \qquad (3.16)$$

$$\sigma_{yh}(X) = 0.333\ (w_*/U_m)h^{0.333}(X-X')^{0.666} \qquad \text{for } (X-X') > hU_m/w_* \qquad (3.17)$$

This type of dispersion coefficient parameterization has also been recently used in the Maryland Power Plant Siting Program (PPSP) model by Weil and Brower (1984) with good success.

Misra (1980b) showed that the predicted and observed ground-level concentrations agreed if $w_*/U_m \geq 0.07$. However, detailed validation of the MSFM model was not undertaken at that time. A flowchart of the basic components of the MSFM model appears in Figure 3.4. Output for the MSFM type models consists of concentration values in a simple XY type format along with the meteorological data.

3.5 EMPIRICAL MODIFICATION TO MSFM

The approaches of Lyons and Cole (1973) and Misra (1980a) assume that the plume is instantaneously mixed downward after impacting the TIBL, however, variability in the TIBL (or mixed layer) height may require a longer time for total plume fumigation.

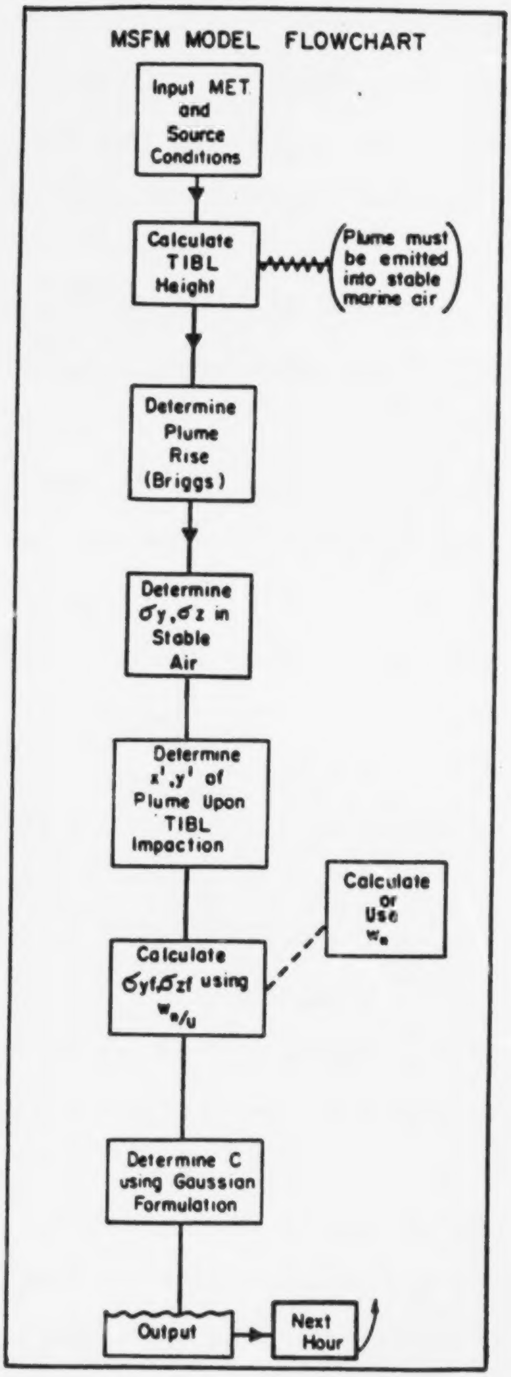
MSFM MODEL FLOWCHART
Input MET and Source Conditions
Calculate TIBL Height
Plume must be emitted into stable marine air
Determine Plume Rise (Briggs)
Determine σy, σz in Stable Air
Determine x', y' of Plume Upon TIBL Impaction
Calculate or Use w_e
Calculate σyf, σzf using w_e/u
Determine C using Gaussian Formulation
Output
Next Hour

Figure 3.4: Flowchart of the MSFM model. (Note that the plume must be emitted initially into stable marine air.)

Water tank laboratory experiments involving entrainment of a tracer into a convectively mixed boundary layer were recently performed by Deardorff and Willis (1982). The mixed layer was assumed to undulate between heights h_1 and h_2 because of the presence of convective eddies. The change in the height $(h_2 - h_1)$ was observed to be 30%. For modeling purposes, the mixed layer was assumed to be represented by a mean value.

The location X_o is where pollutants begin to entrain into the TIBL. Diffusional travel time can be related to downwind distance X so that $X - X_o = U_m(t - t_o)$. Using nondimensional distance parameters (w_*/hU_m) the dimensionless downwind distance was written as:

$$X^* = (X - X_o)\, w_*/hU_m \tag{3.18}$$

Additionally, dimensionless time was written as:

$$t^* = tw_*/h \tag{3.19}$$

and dimensionless concentration as:

$$C^* = CU_mh^2/Q \tag{3.20}$$

Two categories of entrainment (slow and fast) were examined to show the variability of ground-level concentrations.

An adjustment factor based on the laboratory results is given by Deardorff and Willis (1982). The factor takes into account the influence of a variable TIBL height and non-instantaneous vertical mixing. It is assumed that the plume has small vertical dispersion before hitting the TIBL interface. A fraction of the potential fumigant [A(t)] is entrained over a time t with $0 \leq A \leq 1$. Therefore, the mass of pollutant per unit length which is intercepted per time dt is:

$$Q \frac{\partial A}{\partial t} \, dt \tag{3.21}$$

In nondimensional notation, if the vertical "element" containing A(t) were to be mixed upon TIBL entry, the concentration distribution may be written as:

$$dC^*(0,0,t^*) = (\partial A/\partial t)[\sqrt{2\pi}\,(\sigma_y/h)]^{-1} \tag{3.22}$$

Deardorff and Willis (1982) integrated Equation 3.22 and obtained an equation which represents the summation of the various elements that had started fumigating at some arbitrary time t′:

$$C(0,0,t^*) = \sqrt{(2\pi)} \int_0^{t^*} (\partial A/\partial t')[\sigma_y(t^*-t')h^{-1}]^{-1} \tag{3.23}$$

A weighting factor $W(t^*-t')$ that parameterizes the slow downwind mixing of the pollutants was determined by the empirical functions:

$$W(t^*-t') = 3t''^2 - 2t''^3 \qquad t'' < 1 \tag{3.24}$$

$$= 1 \qquad t'' \geq 1$$

where $t'' = (t^*-t')/4$.

According to Deardorff and Willis (1982) this means that only 16% of the well-mixed value from any particular entrained parcel of fumigant is supposed to appear at ground-level one time constant (t") later, while 84% of its well-mixed value appears three time units after the entrainment and 100% after 4 time units.

The empirical adjustment of Deardorff and Willis (1982) that accounts for the delay in touchdown at ground-level of the pollutants entrained into the TIBL has been incorporated into the MSFM base model via Equation 3.13.

Another approach to account for the non-instantaneous nature of the fumigation process is based on a statistical model suggested by Misra (1982) for convective boundary layers. This approach is discussed in the next section.

3.6 DOWNDRAFT MODIFICATION OF THE MSFM MODEL

The Convective Boundary Layer (CBL) which occurs under the TIBL interface contains both updrafts (thermals) and downdrafts. Based on an analysis of the Minnesota data, Caughey (1982) has shown that the downdraft regions in the CBL were more spread out and lasted longer than updrafts. Probability density analysis of vertical velocity in the CBL (Lamb, 1982) indicates that the area under the density profile is larger for the negative half than for the positive half, meaning that downdrafts occupy more than half the horizontal reference plane through the CBL. The analysis showed that updrafts covered 40% of the area while downdrafts covered 60% of the area. Mass continuity, however, dictates that the updrafts have higher velocities than the downdrafts. Lamb (1982) shows that more energy is contained in updrafts due to surface layer shear. He also shows that turbulence within the central core of a downdraft will be low due to subsidence.

Misra (1982) proposed a revision to the Gaussian type approach based on the prevalence of these downdrafts in the CBL. The Misra (1982) downdraft model assumes that the pollutant particles are non-buoyant and that a large number of downdrafts pass over a stack during a given time period. To apply this approach to MSFM, it is assumed that no downdrafts occur in the stable air prior to TIBL penetration by the plume and that the processes related to downdrafts are responsible for vertical dispersion within the TIBL. Thus, even though entrainment at the top of the TIBL will be dominated by the characteristics of the interfacial layer (Wyngaard, 1984), it is plausible that the entrained material will be carried to ground-level by the downdraft.

Misra (1982) assumes that the vertical velocity of the downdrafts follow a function described as:

$$\overline{w}_d = a\, f_1(z) \qquad (3.28)$$

and

$$f_1(z) = -(Z/h)^{0.333}(1 - 1.1\, Z/h) \qquad 0.025 \leq Z/h \leq 0.675 \qquad (3.29)$$

$$f_1(z) = -0.225 \qquad 0.0675 \leq Z/h \leq 1 \qquad (3.30)$$

$$\sigma^2_{wd} = 2.4\, w_*^2\, (Z/h)^{0.666}[1 - 0.77(Z/h)^{0.25}]^2 \qquad (3.31)$$

It is assumed that the velocity with which the material is injected into the downdrafts is a constant in the upper 1/3 of the boundary layer. Another function g(z) which is an integral form that defines the downdraft velocity at plume-TIBL intersection can be defined as:

$$g(0.025) = h\int_{0.675}^{1}(dZ'/0.225) + h\int_{0.025}^{0.675}(dZ')/(Z^{0.333}(1 - 1.1\ Z'))$$

$$= 3.34h \qquad (3.32)$$

where $Z' = Z/h$.

It is assumed that the elemental area source as described in Misra and Onlock (1982) has a height equal to the TIBL height at that location. Since the material can mix into the TIBL from this location only when it is caught in downdrafts, the effects of updrafts are ignored. It is also assumed that a downdraft has a sufficient lifetime such that materials emitted into it remain inside until they touchdown at the ground-level.

Substituting the approximate values of $f_1(z)$, σ_w and w_d and using Equation 3.16 (from the MSFM base model), the MSFM/downdraft modification ground-level concentration may be determined by using:

$$C = (1.78\ Q/(2\pi w_*))\int_0^X[(X-X')\sigma]^{-1}\ \exp\{-[(h-H_e)/\sqrt{2}\ \sigma_{zs}]^2$$
$$- [(1.74\ U_m h)/(X-X')w_* - 0.198]^2 - y^2/2\sigma'^2\}\ d/dX'$$
$$* ((h-H_e)/\sigma_z)dX' \qquad (3.33)$$

The values of σ_{ys} and σ_{zs} are determined using the parameterizations of Lamb (1979) presented earlier.

The downdraft model was evaluated by Misra (1982) using Lamb´s (1978) numerical data input. The model was not evaluated using real air quality data.

4.0 BRIEF REVIEW OF COASTAL DISPERSION STUDIES

In this chapter coastal dispersion studies are briefly reviewed. In addition, the experimental setup of the Nanticoke study is presented. This study will be used for coastal dispersion model evaluation in Chapter 7. This chapter is concluded with a description of model data requirements.

The characterization of dispersion in coastal areas has been investigated during several field experiments. In the early 1960's substantial work was done by Prophet (1961) to characterize aerosol dispersion in coastal regions. Later studies such as the one by Munn and Richards (1967) began focusing on regulatory aspects of coastal dispersion. The dramatic increase in space flight operations during the mid-to-late 1960's created the need for several studies of toxic contaminant dispersion in coastal launch areas such as Vandenburg Air Force Base, California and Cape Canaveral, Florida (Record, 1970).

In the 1970's considerable attention was devoted to identification of coastal dispersion regimes and development of coastal dispersion models in the Great Lakes area. Lyons et al. (1974) and Lyons (1977), for example, presented data taken from power plants along the western shore of Lake Michigan and used this data for development of a regional coastal dispersion model. Rizzo (1975) conducted extensive acoustic sounder studies on the shoreline of Lake Michigan during this time period and used the data develop a regional, coastal mixing depth climatology data base.

A comprehensive study of coastal meteorological processes was undertaken by Brookhaven National Laboratory (BNL) during the mid-to-late 1970's (Raynor et al., 1975, Raynor et al., 1983). Some of the results of the BNL studies along with a similar Japanese effort in the mid-1970's appear in Chapter 6.

The SEADEX (Shoreline Environment Atmospheric Dispersion Experiment) field program was sponsored by NRC to obtain data for the evaluation of dispersion models. The field study was conducted in the vicinity of Kewaunee, Wisconsin during the period May 28 - June 8, 1982. Ten tests were run using SF6 tracer gas and oil fog. Real-time concentration distributions aloft were determined by a Cessna 337 aircraft equipped with an alpha airborne lidar instrument. Acoustic sounder units, minisonde units and a ship provided meteorological data. Preliminary results (Johnson et al., 1983) of the June 8, 1982 case indicated a three dimensional, helical lake breeze circulation pattern, however the data is not available for public distribution at this time.

The next section presents the methodology of the Nanticoke study which will be used for model validation.

4.1 NANTICOKE STUDY -- GENERAL DESCRIPTION

The Ontario Ministry of Environment (OME) in conjunction with the Canadian Atmospheric Environment Service (AES) and the Ontario Hydro Power Company conducted a comprehensive study of the Nanticoke Generating Station (NGS) plume during the summer of 1978 and 1979. NGS is located on the north shore of Lake Erie across from Erie, Pennsylvania.

The basic coastal dispersion objectives of the Nanticoke Environmental Management Program (NEMP) were:

(1) To obtain detailed meteorological measurements of the vertical structure of onshore flows

(2) To characterize the dispersion of SO_2 under fumigation conditions by developing a realistic shoreline dispersion model

The first field phase (NEMP I) occurred from May 29 to June 16, 1978. The second field phase (NEMP II) occurred from May 28 to June 14, 1979.

4.2 NANTICOKE PLANT CHARACTERISTICS

Operated by the Ontario Hydro Company, the NGS consists of two stacks, each of which is 198 m high. Each stack has four flues with a load capacity of 500 mw each. Flue diameter is 5.49 m. Total plant load capacity is 4000 mw with approximately 156,000 tons of SO_2 per year emitted under present conditions. Plume rise has been observed to average around 400 m from stack base (Ontario Ministry of Environment, 1979).

The fly ash emission rate was 150 - 220 kg h^{-1} during the study period. The plant has 99% efficient precipitators.

4.3 NEMP INSTRUMENT DEPLOYMENT - BOUNDARY LAYER MEASUREMENTS

Boundary layer measurements were taken using a combination of minisonde units (MS), acoustic sounders (AS), surface flux units (SF) and tethersonde units (TS). Figure 4.1 shows the position of these various fixed systems. Symbols A and B represent the minisonde unit positions. The numbers following A and B refer to downwind distance (km) from NGS, while numbers with other symbols are for unit identification purposes. Measuring systems TS 2, AS 2 and SF were co-located for comparison purposes. Figure 4.2 gives a more detailed cross-sectional type view of the TIBL instrument deployment.

The tethersonde units provided wind, humidity and temperature information up to 600 m and were particularly useful in the first several kilometers inland from the coast. Both continuous and vertical profiling modes were employed. The 2 kg instrumental package consisted of a pair of rod thermistors for temperature measurements, a premium hygristor for relative humidity measurements, a Feuss barometer and miniature blade/cup anemometers for wind measurements. Accuracies of the wind speed were ± 0.1 m s^{-1}. Wind direction accuracy was $\pm 3^{\circ}$. The package

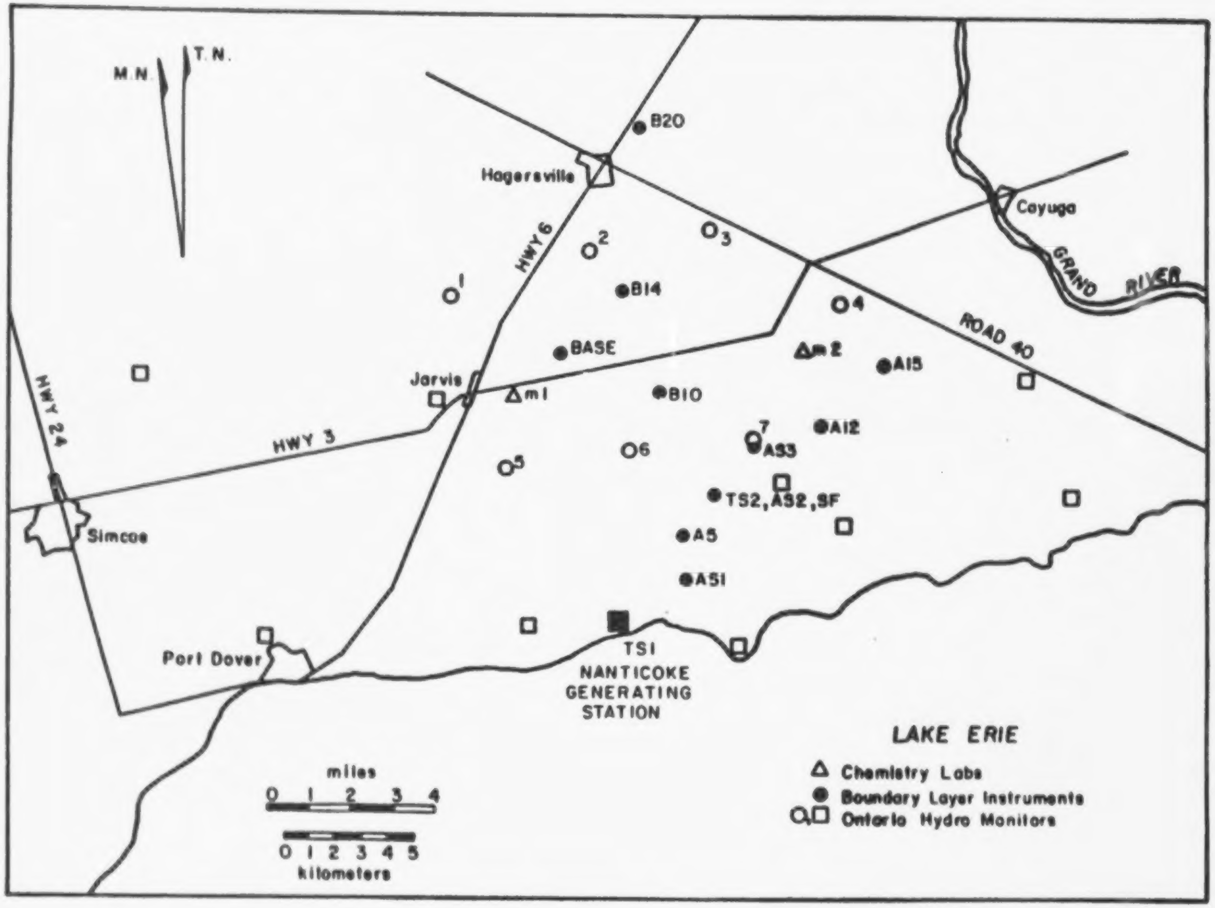
M.N.
T.N.
B20
Hagersville
Cayuga
GRAND RIVER
HWY 6
2
3
1
B14
4
ROAD 40
BASE
m2
A15
HWY 24
Jarvis
m1
B10
HWY 3
7
A12
A53
6
5
TS2, A52, SF
Simcoe
A5
A51
TS1
Port Dover
NANTICOKE
GENERATING
STATION
LAKE ERIE
miles
0 1 2 3 4
0 1 2 3 4 5
kilometers
△ Chemistry Labs
● Boundary Layer Instruments
○,□ Ontario Hydro Monitors

Figure 4.1: Deployment of the various measuring systems of the NEMP study (from Portelli, 1982).

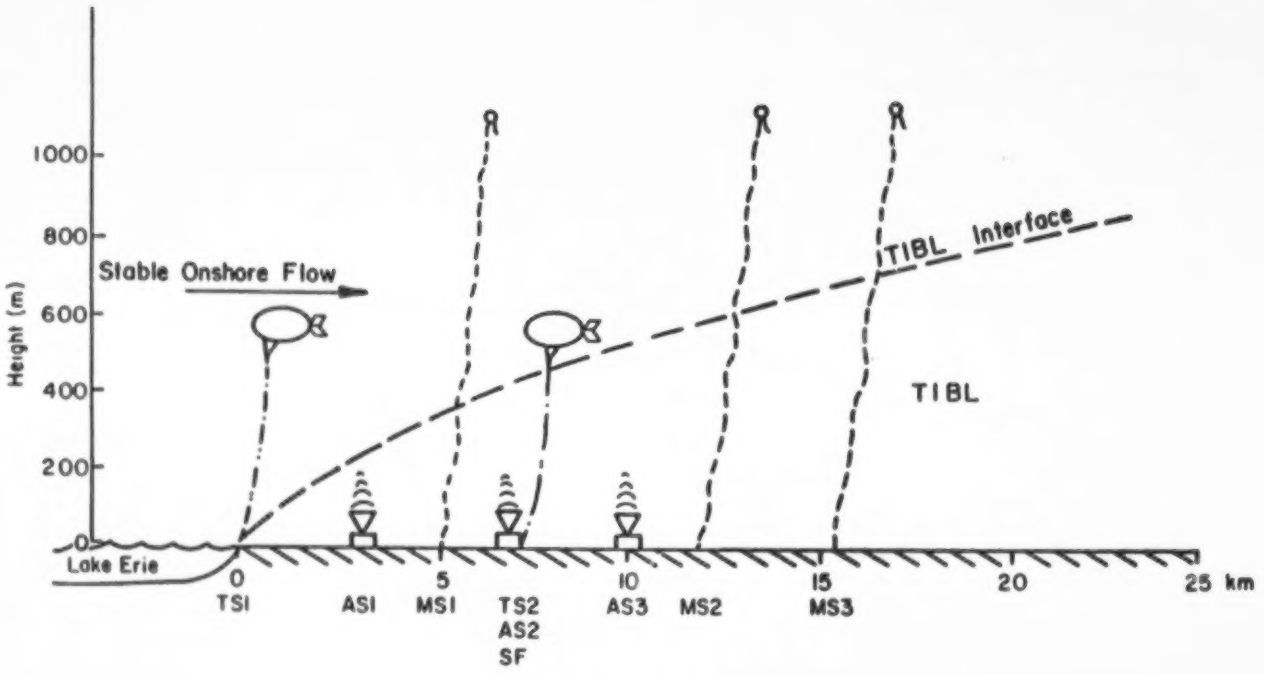
Height (m)
1000
800
600
400
200
0
Stable Onshore Flow
TIBL Interface
TIBL
Lake Erie
0
TS1
AS1
5
MS1
TS2
AS2
SF
10
AS3
MS2
15
MS3
20
25 km

Figure 4.2: Cross-sectional deployment view of the NEMP boundary layer systems (from Portelli, 1982).

was sent aloft using a large balloon. A tethersonde unit located at TS 1 determined the onshore flow prior to overland modification, while TS 2 was located at some distance inland to allow for measurements of a shallow TIBL. The acoustic sounding units located at AS 1, AS 2 and AS 3 were also able to determine the structure of the TIBL.

The MS systems were mobile, therefore allowing great flexibility in deployment and potential in terms of complementing the AS systems. Sites A5, A12 and A15 were chosen as the main launch locations, since the prevailing wind direction was from the southwest. Sites B10, B14 and B20 were used as alternate launch locations when the wind direction was south-southeast. The system consisted of an instrument package containing a temperature sensor and a transmitter attached to a free floating balloon. Wind speed and direction were obtained by a double theodolite tracking system. Launches began at 0800 hours and continued to the end of the study period.

The SF unit was located inland to determine the fluxes of momentum, sensible and latent heat and correlate these fluxes to TIBL evolution. Sensible heat flux was obtained by using platinum resistance elements which gave the necessary gradient data. Net radiation was measured by solarimeters. A three component sonic anemometer/thermometer was used to obtain measurements necessary for the eddy correlation technique. A laser scintillometer, which estimates surface heat flux from path-averaged measurements of the scintillations of monochromatic laser light, was also located at the site.

Wind measurements were taken at an 85 m tower located 10 km inland and also at the stack height. In addition, some of the mobile air quality units contained wind measuring equipment.

4.4 NEMP INSTRUMENT DEPLOYMENT -- PLUME CHARACTERISTICS AND AIR QUALITY MEASUREMENTS

The ground-based air quality measuring component consisted of eight measuring systems including both mobile, in-situ and fixed monitors. A mobile lidar unit was used to obtain plume height, bearing and dispersion characteristics (σ_y, σ_z). The laser unit consisted of a 1.0 J ruby laser with a 6 second repetition rate. The assembly was rotatable through 360 degrees of azimuth and 180 degrees of elevation (Hoff and Froude, 1978). About 300 cross-sections were made using the lidar remote sensing technique.

Three mobile correlation-spectrometer (COSPEC) units were used to obtain vertically integrated SO_2 concentrations. The COSPEC unit utilizes the UV absorption of zenith sky radiation which determines the burden of SO_2 over the unit. The voltage output of the unit is proportional to the integral of the path of gas concentration. This value is usually expressed as concentration times path length or ppm-m. Plume traverses were generally averaged over one-half hour periods and then projected onto an axis normal to the plume. One COSPEC unit was always assigned to the area within 7 km of the plant. Two other roving units were assigned to strategically important area. Over 700 COSPEC measurements were made during the study.

The two roving COSPEC units also had SIGN-X SO_2 monitors which obtained ground-level concentrations. In addition, a helicopter with a SIGN-X instrument was used to obtain vertical profiles of pollutant concentration and to direct ground units to the plume area. The helicopter runs included five traverses of five different elevation heights repeated three times. A twin engine Piper Navajo was also used for SO_2 and O_3 airborne mapping.

Sixteen Ontario Hydro Power Company Phillips SO_2 type monitors (Figure 4.1, open circles and squares) reported one hour averaged concentrations. The monitors consisted of two portable glass fiber boxes which can be placed on the ground. The measuring principle involved continuous colorimetric titration with bromine.

Mobile chemistry units (Figure 4.1, symbols M 1 and M 2) which contained gas analysis systems were deployed for plume chemistry measurements. Unit M 1 (mobile air lab) contained analyzers for SO_2, NO_x, H_2S, CO, O_3, HC, methane, sulphates, nitrates, metal particles and oxides

(Portelli, 1982). Flow was sampled at 5 m above ground. Unit M 2 (mobile chemical lab) contained an SO_2 and O_3 TECO type monitor. The labs operated in an in-situ mode upon arriving at the monitoring site. Figure 4.3 shows the typical cross-sectional deployment of the plume measuring equipment. The use of these various instrument systems has allowed detailed analysis of the plume behavior (Hoff et al., 1982).

4.5 DATA REQUIREMENTS FOR RUNNING THE MODELS

The coastal dispersion models described in Chapter 3 allow the user to compute concentration values on an hourly basis or in some cases (as with CSFM) on a monthly or yearly (climatological) basis. The coastal dispersion model input requirements can be broken into two broad areas: site specific and meteorological. Site specific variables include stack height and location, exit velocity, stack gas temperature, stack diameter, emissions rate and effective stack height (based on site specific parameters). Meteorological input variables include wind speed, surface heat flux (for TIBL and w_* calculations), TIBL height (including the A factor) and the Brunt-Vaisalla frequency (N) which is used to characterize the stable air mass. CSFM incorporates the Lyons and Cole model. Hence it was decided that the best results can be obtained by comparing CSFM and MSFM, which make different assumptions and use different methods in modeling fumigation. The input

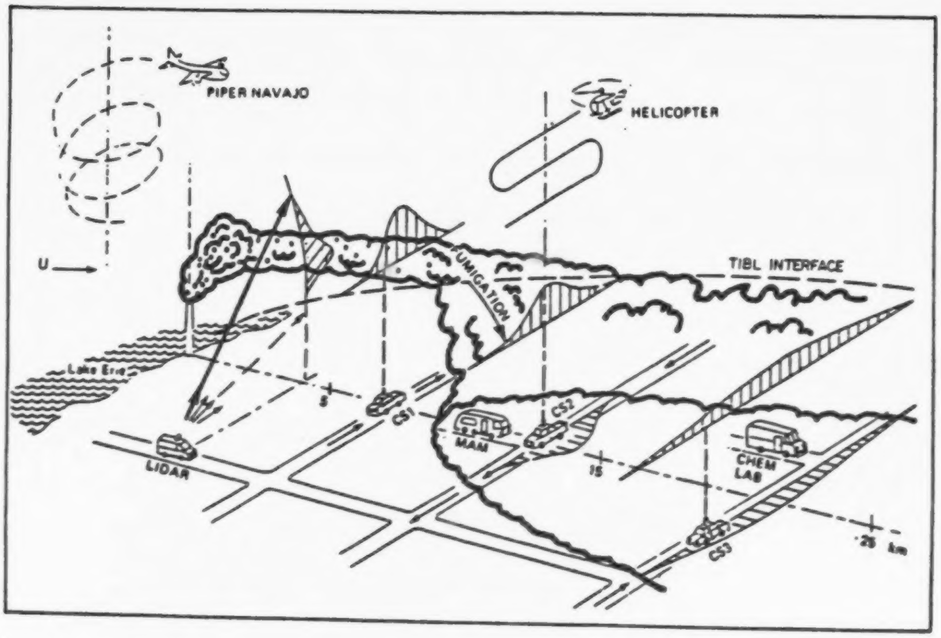
PIPER NAVAJO
HELICOPTER
U
TIBL INTERFACE
FUMIGATION
Lake Erie
5
CS1
MAM
CS2
15
CHEM LAB
LIDAR
CS3
25 km

Figure 4.3: Cross-sectional deployment view of the NEMP air quality measuring systems (from Portelli, 1982).

necessary for each model is listed in Table 4.1.

The CSFM output consists of concentration values along a "ring" (similar to the regular CRSTER model) at some distance X from the source. The model can also be used for emissions from islands, offshore sources or under offshore wind flow, although in this study the model has not been evaluated under those conditions. Output for the MSFM type models consists of concentration values in a simple X Y type grid along with the meteorological input data.

TABLE 4.1

INPUT FOR BASE MODELS

Input Factors	CSFM	MSFM
Site Specific		
Stack height	X	X
Stack location	X (can handle inland stacks; needs angle of shore)	(only for shoreline releases)
Gas exit velocity	X	uses F_o
Stack gas temperature	X	" "
Stack diameter	X	" "
Emissions rate	X	X
Effective stack height	X from Briggs, 1975	X from Briggs, 1975
Meteorological Information		
U_{speed}	X	X
$U_{direction}$	X	
Heat flux (H_o)	X	(not required but useful to determine w_* if not given)
h	Weisman (1976)	$h = AX^{0.5}$ [if measured or Weisman (1976)]
N		X
w_*/U		X

5.0 COASTAL DISPERSION MODEL EVALUATION PROTOCOL

Much attention has been given to the technical aspects of air pollution models. The ultimate concern, however, is in how well a model simulates actual measured data. In this section a brief overview of model evaluation efforts is presented, followed by the evaluation protocol and a summary of the criteria and test days chosen for model evaluation.

5.1 A BRIEF OVERVIEW OF MODEL EVALUATION TECHNIQUES

The increase in air pollution regulations during the past decade has stimulated regulatory agencies and industry to develop statistical methods for model evaluation. The meaning of the word "evaluation" itself has undergone extensive changes in definition. For the purposes of this study, "evaluation" will be defined to be the process of examining and appraising model performance by using field data to establish the accuracy of a model or technique. This is similar to the definition of Fox (1981).

The need for performance measures in air pollution model evaluation has been discussed by Johnson (1972). Brier (1975) first suggested the following general steps in model evaluation:

(1) Complete sensitivity analysis of the model

(2) Calculation of mean square errors of the residuals $(\overline{P} - \overline{O})$

(3) Completion of a regression analysis of predicted and observed concentration

(4) Examination of the frequency distribution of predicted and observed concentrations

(5) Examination of the overall model bias

In 1978, EPA published the Guideline on Air Quality Models. The guidelines gave the following broad procedures for model evaluation and comparison:

(1) Compare predicted P vs. observed O concentration values

(2) Determine the cause of discrepancies

(3) Correct and improve data bases as needed

(4) Change the model if required to reflect better mathematical representation of physical reality

(5) Document procedures

A dispersion model performance workshop in 1980 brought together the American Meteorological Society and EPA to discuss evaluative procedures for air quality models. Fox (1981) summarized recommendations made at the workshop. The participants agreed on four key areas that would limit air quality model calculations:

(1) Quality of meteorological data

(2) Quality of comparative ambient air quality measurements

(3) Emissions data quality

(4) Algorithmic capability to reproduce natural events

Fox (1981) suggested, with the above limiting factors in mind, that:

(1) Plume data be grouped into observed and predicted concentration field values, paired for a particular location in space at a particular time

(2) Plume data be developed into a peak concentration data set with various degrees of time and space pairing

(3) Cumulative frequency distributions of unpaired (in time) observed and predicted concentration values be developed

The specific performance measures outlined by Fox (1981) included both residual (difference) analysis, which allows a quantitative estimate of ($\overline{P} - \overline{O}$) and correlation, which allows a quantitative measure of agreement between O and P. The residual analysis methods from Fox (1981) include:

(1) Mean Bias Error (MBE)

$$MBE = N^{-1} \sum_{i=1}^{n} (P_i - O_i) \tag{5.1}$$

or Mean Absolute Error (MAE)

$$MAE = N^{-1} \sum_{i=1}^{n} |P_i' - O_i'| \tag{5.2}$$

(2) Variance of the difference

$$S_d^2 = (N-1)^{-1} \sum_{i=1}^{n} (P_i - O_i - MBE)^2 \tag{5.3}$$

(3) Gross error of the difference
Mean Square Error (MSE)

$$MSE = N^{-1} \sum_{i=1}^{n} (P_i - O_i)^2 \tag{5.4}$$

or Root Mean Square Error (RMSE)

$$RMSE = [N^{-1} \sum_{i=1}^{n} (P_i - O_i)^2]^{0.5} \tag{5.5}$$

The correlation analysis methods of Fox (1981) include:

(1) time correlation ($r \Delta t$)

(2) space correlation $r_s = f[C_o(X,t);C_p(X,t)]$

(3) time and space combined (r)

The recommended correlation equation is:

$$r = \frac{(C_o - C_o)(C_p - C_p)}{\sqrt{[\Sigma (C_o - C_o)^2 \, \Sigma (C_p - C_p)^2]}} \qquad (5.6)$$

Fox (1981) also notes that future research is required to establish the statistical tests needed for different air quality models.

5.2 STATISTICAL EVALUATION PROTOCOL

Willmott (1982a) proposed several modifications to the Fox (1981) recommendations. In particular, Willmott (1982) argues strongly against using the Pearson moment correlation coefficient (r) with the Fisher statistic confidence interval or its companion, the coefficient of determination (r^2), as an "ultimate" means of predicted vs. observed value association. The statistics r and r^2 do describe proportional changes (either increasing or decreasing) with regard to the means of the two quantities in question. However, distinctions between the type or magnitudes of variables are not indicated by the value of r. Willmott (1981) for instance presented a simple hypothetical example of an evaluation of model A and model B. The hypothetical plot of model A and model B output (shown in Figure 5.1) indicated that the curves for models A and B both fell equidistant (one on the positive Y and one on the negative Y axis) from the observed curve. This means that a perfect correlation (r = 1.0) exists between the two models. In this case the r = 1.0 value does not account for differences in proportionality or additive constant

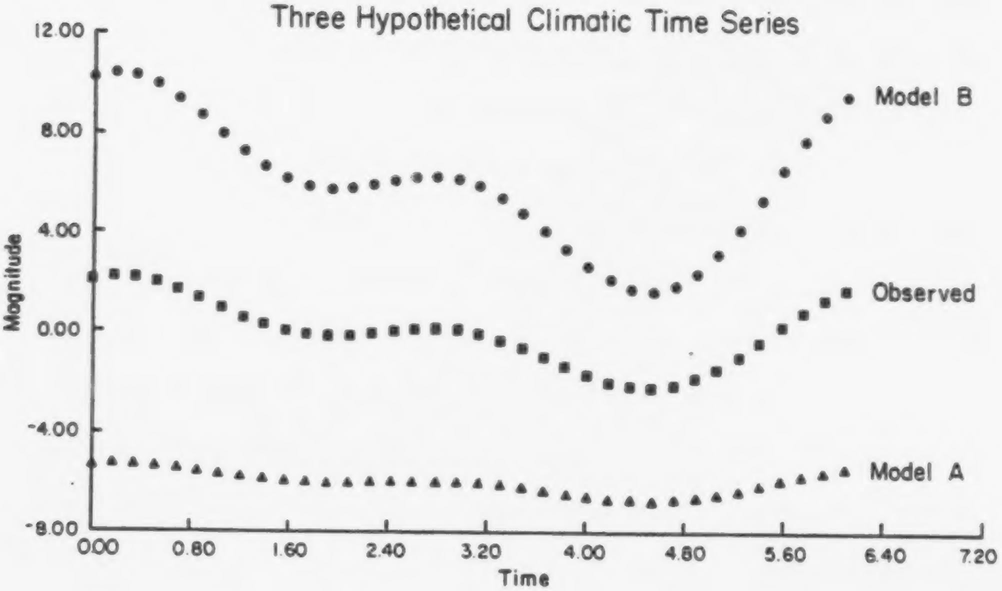

Figure 5.1: Hypothetical model output showing deceptive perfect correlation. Great differences in magnitude exist, however, tnat the correlation coefficient cannot resolve (from Willmott, 1982a).

differences between the two models (Willmott, 1981).

Willmott and Wicks (1980) presented rainfall data that showed statistically significant r and r^2 values to be unrelated to the O - P differences. They have shown that small differences between O and P could occur with low or negative values of r. Other studies (Willmott, 1982b) also indicate as to how the use of r and r^2 can be misleading. Venkatram and Vet (1981) have indicated that the correlation analysis is of little value if the observed variance is close to the expected variance between model predictions and measurements.

In addition, Willmott (1982) is generally critical of the MBE (Equation 5.1) and S_d^2 (Equation 5.3). MBE represents the mean of the difference between $\overline{O}$ and $\overline{P}$ which really does not indicate as much as a comparative analysis of $\overline{O}$ and $\overline{P}$ alone. The parameter S_d^2 is shown to be approximately equal to MSE - $(\overline{P} - \overline{O})^2$, which adds little additional information. Both parameters also describe the frequency distribution of the difference and do not identify the sources of error when compared to the perfect prediction line.

Willmott (1981, 1982) suggests using the index of agreement (d) and the Root Mean Square Error (RMSE) to circumvent the problems associated with correlation coefficients MBE and S_d^2 type parameters. The index of agreement can be interpreted as a measure of how error free a model predicts a variable. Thus the index (d) determines the extent to which magnitudes and signs of the observed values about $\overline{O}$ are related to the predicted deviations about $\overline{O}$. It is assumed that O and O are error free. The maximum possible difference between the predicted and observed values may be described by:

$$|P_i - \overline{O}| + |O_i - \overline{O}| \qquad (5.7)$$

Squaring this maximum possible difference and summing over all observations one obtains a potential error (PE) variance (Willmott, 1981) and therefore the condition $0 \leq (RMSE)^2 \leq N^{-1}(PE)^2$ is satisfied. The statistical, descriptive relative error measure which indicates the degree to which predicted values approach the observed values can then be written as:

$$d = \frac{1-N(RMSE)^2}{(PE)^2} \qquad (5.8)$$

and expanded to,

$$d = 1-\sum_{i=1}^{n}(P_i-O_i)^2 / \sum_{i=1}^{n}(|P_i'| + |O_i'|)^2 \qquad 0 \leq d \leq 1 \qquad (5.9)$$

where $P_i' = (P_i - \overline{O})$ and $O_i' = (O_i - \overline{O})$.

The unexplained error that is leftover is contained in the numerator of Equation 5.9. The d index is standardized such that cross comparisons of magnitudes can easily be made between models. A value of 1.0 indicates perfect agreement between O and P values.

Willmott and Wicks (1980) caution that d should not be interpreted exclusively, since d becomes unstable when the denominator is small. Difference measures provide the most rigorous and useful information regarding overall model performance (Willmott, 1981). However, models contain both systematic and unsystematic errors. The d index should therefore be used in-conjunction with the difference measures such as the mean square error and its components the systematic MSE (MSE_s) and the unsystematic MSE (MSE_u). Systematic errors result from causes which persist or are consistent. Unsystematic errors consist of a number of small effects such as the imprecision of a constant. Some of these effects are positive and some are negative in terms of affecting the final output value.

The best model, therefore, has a systematic difference of zero, since it should explain most of the systematic variation in O, while the unsystematic difference should approach the MSE. The value of MSE should be minimized so that the model is predicting at peak accuracy. A larger value of MSE_u when compared to MSE_s may indicate that the model is as good as possible under present conditions. In terms of statistical notation, the systematic mean square error is the error caused by model additive or proportional problems and can be expressed as:

$$MSE_s = N^{-1}\sum(\hat{P} - O_i)^2 \qquad (5.10)$$

where $\hat{P} = a + bO_i$.

The unsystematic mean square error is expressed by:

$$MSE_u = N^{-1}\sum_{i=1}^{n}(P_i - P_i)^2 \qquad (5.11)$$

The total MSE can therefore be written as:

$$MSE = MSE_s + MSE_u \qquad (5.12)$$

The values of RMSE (square roots of the MSE) are generally computed to make the numbers easier to use for qualitative or quantitative comparisons. The total RMSE may be written as:

$$RMSE = \sqrt{RMSE_s{}^2 + RMSE_u{}^2} \qquad (5.13)$$

The use of the RMSE is advantageous because it is a conservative measure of accuracy. The analysis of RMSE also has an advantage over an analysis of r or r^2 since errors in r may be hidden by high values of observed and predicted variances or appear significant due to low magnitudes of observed and predicted variances (Willmott, 1981).

Finally, in addition to $RMSE_s$, $RMSE_u$ and d, Willmott (1982) suggests that summary measures such as $\overline{O}$, $\overline{P}$, S_o^2 and S_p^2, along with simple linear regression, should be reported since they are easily understood.

In this study, while following the general philosophical recommendations of Fox (1981) in terms of using several statistical measures, the more precise approach of Willmott (1982a) is adopted. Therefore the parameters and procedures used for model evaluation are:

(1) Scatterplots of P vs O concentration values

(2) Univariate summary measures

a. $\overline{P}$

b. $\overline{O}$

c. S_o^2

d. S_p^2

e. $\hat{P} = a + bO_i$ (least square regression to obtain a and b)

(3) Specific difference measures

a. RMSE, $RMSE_s$, $RMSE_u$

b. Index of agreement (d)

Statistics based on traditional highest and second highest concentration values and on frequency distribution are not chosen in this study, since the data represents more of a case description of coastal fumigation as opposed to the more typical monthly or annual climatological receptor analysis.

The 13 test periods listed in Table 5.1 were selected because they have met the established criteria (Cole and Lyons, 1972; Lyons, 1975) for onshore coastal fumigation occurrences. The criteria are:

(1) Onshore flow outside ±10 degrees relative to the angle of the shoreline (e.g., the angle of the shoreline with respect to North at NGS is 80 degrees; therefore, the allowable windflow angles for fumigation to occur are 90 degrees to 250 degrees)

(2) Hours of occurrence from 7 AM to 7 PM (daytime)

(3) Hourly wind speed greater than 2 m s^{-1}

(4) Land-water temperature difference greater than 0.5 C

TABLE 5.1

LIST OF TESTS USED FOR MODEL COMPARISON

TEST	DATE	TIME (EDT)
1.	June 1, 1978	1100
2.	June 1, 1978	1200
3.	June 1, 1978	1300
4.	June 1, 1978	1400
5.	June 1, 1978	1500
6.	June 6, 1978	1200
7.	June 6, 1978	1400
8.	June 6, 1978	1500
9.	June 6, 1978	1600
10.	June 6, 1978	1700
11.	June 13, 1979	1700
12.	June 14, 1979	1400
13.	June 14, 1979	1600

It is also important to note that the tests only occurred under stable marine air conditions. No cases were observed with neutral or unstable marine air characteristics. Four models (CSFM, MSFM, Deardorff Modification and Downdraft modification) were evaluated based on the NEMP I and II experimental days listed in Table 5.1.

The summary measures combined with the specific measures should provide a good indication of the ability of a model to predict concentrations under coastal fumigation situations. Now that a protocol for statistical comparison of different models is established, it is proposed to first compare the various TIBL formulations given in Chapter 2 and determine the best. This formulation will be incorporated in the two dispersion models selected for comparison and then evaluated using the Nanticoke data set.

6.0 THERMAL INTERNAL BOUNDARY LAYER EQUATION EVALUATION

Importance of the air mass modification and the development of the TIBL at the coastline were addressed in earlier chapters. Effect of variation of the TIBL height on the fumigation process and the location of maximum concentration were discussed in Chapter 2. A reasonably accurate depiction of the TIBL is necessary to simulate coastal fumigation processes. In this section an evaluation of the various TIBL formulations against comprehensive field data is made to statistically determine the best available model.

Seven TIBL data bases and reports have been identified from the literature and other sources and are shown in Table 6.1. The most complete data bases in terms of overland, overwater and aircraft measurements are the eastern Long Island and Kashimaura, Japan studies. These two data bases were used to evaluate the various TIBL formulations. NEMP studies were not used for TIBL evaluation purposes because they did not have as complete a set of overwater observations as the Brookhaven and Kashimaura studies.

First presented are two typical days (one with stable overwater conditions and one with unstable overwater conditions) to demonstrate some of the variations in the values obtained from TIBL prediction equations under different meteorological situations. The two data bases

TABLE 6.1

TIBL DATA BASES

DATA BASE	SOURCE
Brookhaven (BNL)	Raynor et al. (1979) and unpublished data
Kashimaura (Japan)	Gamo (1981); Gamo et al. (1982)
Nanticoke (Canada)	Lui (1977); Portelli (1982); Kerman et al. (1982)
Wisconsin/Lake Michigan	Lyons (1977)
Avon Lake/East Lake, Cleveland	Unpublished data
Maine	Fritts et al. (1980)
Tampa Bay	Unpublished data

are then combined to describe the TIBL prediction equation variation in terms of an overall comparison. This section is concluded with a categorization of the TIBL cases by stability and wind. Six TIBL formulas have been evaluated (Equations 2.1, 2.2, 2.7, 2.10, 2.16 and 2.17).

Twenty-nine hours (cases) of TIBL measurements spanning twenty-four days were examined. Each hour of data is considered a case. The experiments were conducted during the period from March to November. Generally, each case contained between four and twelve TIBL measurements downwind. Observed TIBL heights were determined every 2 km downwind for the Kashimaura data base and every 1 km downwind for the BNL data base. The total number of observed TIBL heights for the twenty-nine cases is 203.

6.1 THE BROOKHAVEN COASTAL METEOROLOGY EXPERIMENTS

The Atmospheric Sciences Division of the Brookhaven National Laboratory investigated development and characteristics of the TIBL over Long Island, New York during the mid-and-late 1970's as part of their coastal meteorology program. Terrain of the study area varies from sandy near the coast to shrub and tree covered further inland.

Measurements of turbulence and temperature were made from aircraft and tower-mounted instruments. These data were plotted as a vertical cross-section by combining various heights along the flight track. Observations of land and ocean surface temperatures were made with an infra-red sensor from the aircraft. Flight tracks across Long Island are shown in Figure 6.1. For this study tracks 3 and 4 were chosen since they provided the greatest overland distance for TIBL growth and were not influenced by inland bodies of water. Wind profiles were determined from pilot balloon soundings.

Methods for determining various parameters used in the TIBL equations are given in Table 6.2.. Wind speeds observed near BNL were used for overland values. A complete description of the experimental program is given by Raynor et al. (1979).

6.2 THE KASHIMAURA COASTAL METEOROLOGY EXPERIMENTS

The Japanese National Research Institute for Pollution and Resources conducted a TIBL investigation in the Kashimaura-Kujukurihama region of Japan during the 1970's. The study will be referred to as Kashimaura for simplicity. The region is located 100 km east of Tokyo and is sandy with some shrubs and farmland. Figure 6.2 shows the triangular configuration of the coast. Occasionally, the Kashimaura sea breeze joined the Kujukurihama sea breeze. These cases were not considered in the analysis. Aircraft measurements of turbulence and temperature were made from heights of 50 m to 2000 m. Pilot balloon soundings were taken inland and at various points along the coast. Tower measurements of wind and temperature were also made at several coastal and inland sites. Land and ocean surface

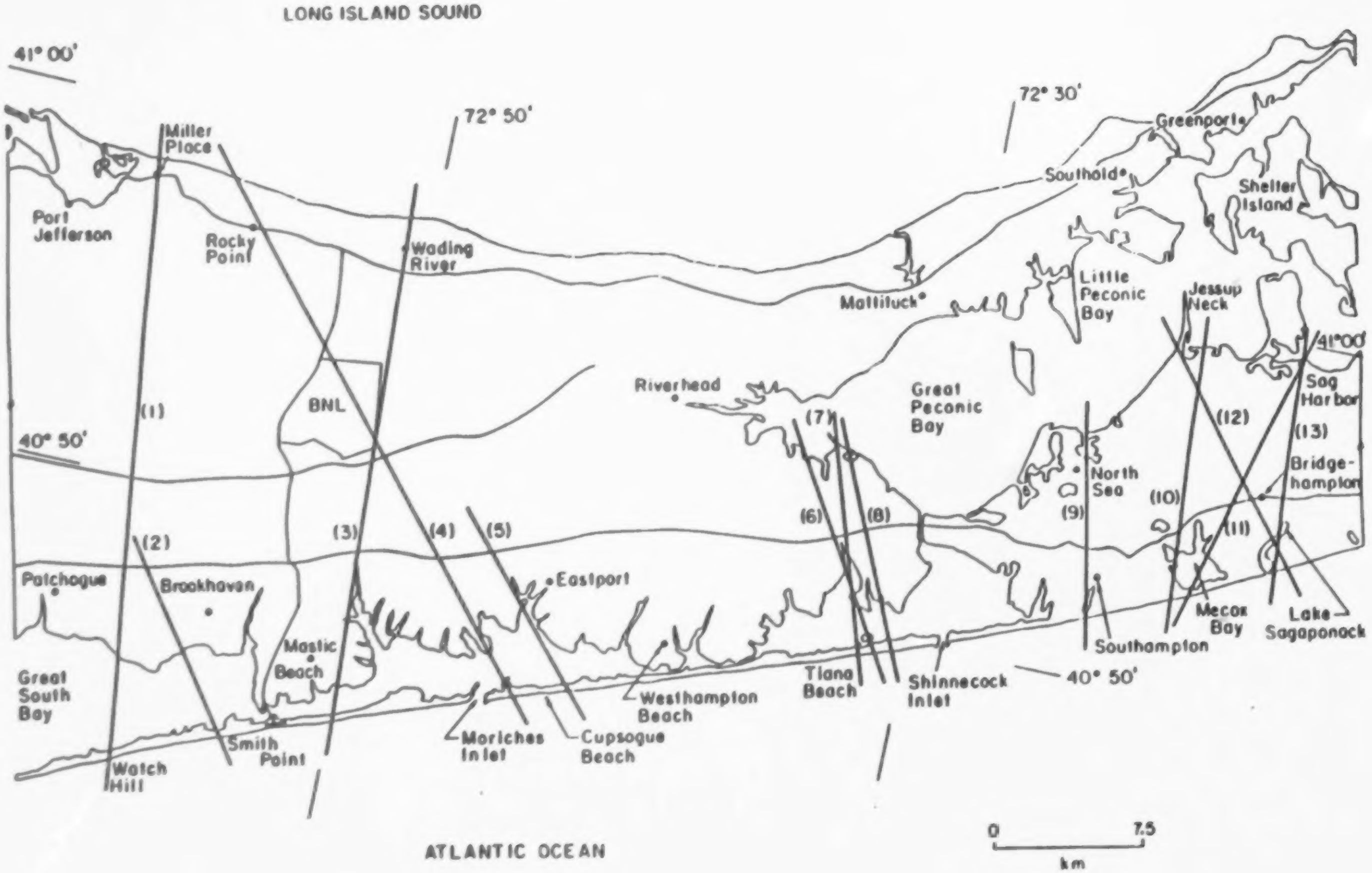
LONG ISLAND SOUND
41° 00'
72° 50'
72° 30'
Miller Place
Port Jefferson
Rocky Point
Wading River
BNL
Riverhead
Mattituck
Southold
Greenport
Shelter Island
Little Peconic Bay
Jessup Neck
41°00'
Sag Harbor
Great Peconic Bay
North Sea
Bridge-hampton
40° 50'
Patchogue
Brookhaven
Eastport
Mastic Beach
Great South Bay
Smith Point
Watch Hill
Moriches Inlet
Cupsogue Beach
Westhampton Beach
Tiana Beach
Shinnecock Inlet
40° 50'
Southampton
Mecox Bay
Lake Sagaponack
(1)
(2)
(3)
(4)
(5)
(6)
(7)
(8)
(9)
(10)
(11)
(12)
(13)
ATLANTIC OCEAN
0
7.5
km

Figure 6.1: Map of Long Island showing flight tracks for TIBL experiment. Tracks 3 & 4 were used in this TIBL study.

TABLE 6.2

TIBL PARAMETERS USED FOR THE BNL DATA BASE

Parameter	Method
$U_{10,z}$	10 meter winds from tower near BNL, U_z from wind profiles
	Overwater temperature profiles
u_*	Logarithmic profile relation with an average z_o of 0.3 m
T_L	Infra-red sensor from aircraft
T_W	Infra-red sensor from aircraft
γ,S	Overwater temperature profiles
F	0.2 (Venkatram, 1977)
H_o	Surface similarity relationship $H_o = \rho c_p u_* kz(d\theta/dz)$, where k is von Karman's constant (0.4) and z is the height over which temperature measurements were taken

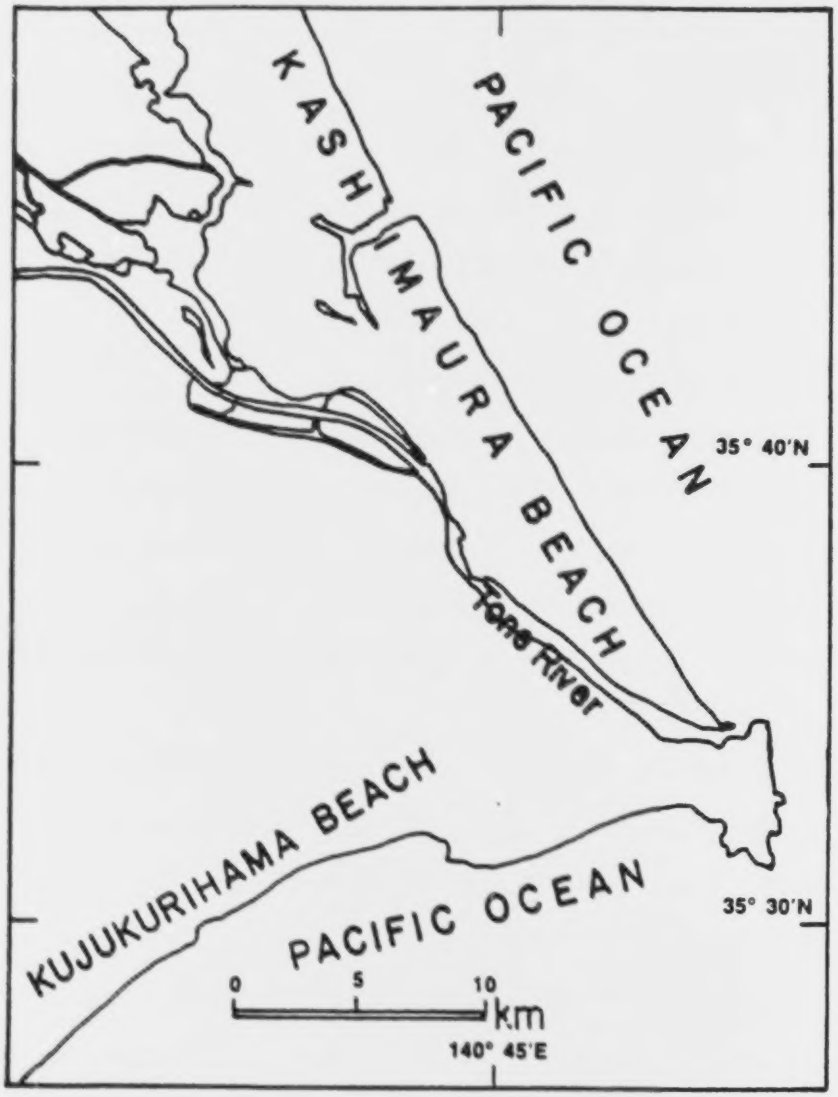
KASHIMAURA BEACH
PACIFIC OCEAN
35° 40'N
Tone River
KUJUKURIHAMA BEACH
PACIFIC OCEAN
35° 30'N
0
5
10
km
140° 45'E

Figure 6.2: Map of Kashimaura-Kujukurihama, Japan experimental TIBL areas.

temperatures (IR) were taken at 1 km intervals. Flight tracks were made across the entire region. Solar insolation data was available from the Choshi Observatory located at the apex of the triangle. Methods for determining the various TIBL parameters for this data base are listed in Table 6.3. A complete description of the experimental methods is given by Gamo et al. (1982).

6.3 THE STABLE UPWIND OVERWATER CASE

Stable conditions over water upwind of the coastline are generally observed during the spring and early summer seasons and lead to an ideal fumigation condition downwind of the coastline. Hence this was selected as one of the two examples for comparison of TIBL height values obtained using various formulations.

Upwind stable conditions over water off Long Island are very common, particularly in the spring and summer seasons. The case presented is Brookhaven experiment BL #13, which was conducted on June 16, 1979 from 1330 to 1500 EST. A listing of the meteorological data pertaining to the experiment appears in Table 6.4. A surface-based inversion was present over the water up to a level of 150 m. The water temperature was 14 K cooler than the land temperature. The presence of this strong temperature differential between the land and the water caused the TIBL to be shallow (less than 340 m high), since the warming of the marine air was gradual. TIBL observations continued out to

TABLE 6.3

TIBL PARAMETERS USED FOR THE KASHIMAURA DATA BASE

Parameter	Method
$U_{10,z}$	10 meter winds from towers, U_z from pilot balloon wind profiles
$\Delta\theta$	Overwater aircraft traverses
u_*	$\sim\sigma_w/1.3$ method. σ_w was obtained from overland aircraft flights
T_L	Infra-red sensor from aircraft
T_W	Infra-red sensor from aircraft
γ,S	Reconstruction of temperature profiles from overwater aircraft traverses
F	0.2 (Venkatram, 1977)
H_o	When H_o was not given, the relationship $H_o = 0.39S_i$ was used, where S_i = solar insolation (Misra and Onlock, 1982)
ψ	Based on solar insolation data directly

TABLE 6.4

BL #13 METEOROLOGICAL DATA

Parameter	Value
U	4.5 m s^{-1}
$\Delta\theta$	3.0 K
u_*	0.5 m s^{-1}
T_L	303 K
T_W	288.5 K
H_o	162 W m^{-2}
dT/dz	0.015 K m^{-1}
Wind direction	150°

12 km downwind, where an equilibrium height was approximately reached.

The predicted TIBL values for downwind distances up to 12 km are given in Figure 6.3, which shows that for this case Equation 2.2 (Raynor et al., 1975) predicts the TIBL height the best. Equation 2.1 (Van der Hoven, 1967) also predicts the temporal pattern of the TIBL height fairly well, but tends to systematically underpredict the height. This may be because of the lack of TIBL forcing terms such as T_L or T_W in the equation. Equation 2.10 (Peters, 1975) underpredicts the TIBL height for all downwind distances. This may be attributed to the land-water temperature difference appearing in the denominator.

Equation 2.7 (Venkatram, 1977) overpredicts the TIBL throughout. Much of this overprediction (as compared to the Raynor et al. 1975 formulation and observations) appears to have been created by a difference factor of 1.83 between the term $[2/(1-2F)]^{0.5}$, where F = 0.2 (Venkatram, 1977) and the terms in the Raynor et al. (1975) formulation. Equation 2.17 (Weisman, 1976) underpredicts the TIBL for this case.

6.4 THE UNSTABLE UPWIND OVERWATER CASE

As was discussed in a previous section, one of the controlling parameters for TIBL growth is the upwind thermal stability over water. An upwind, thermally unstable case is selected for evaluation in this section in contrast

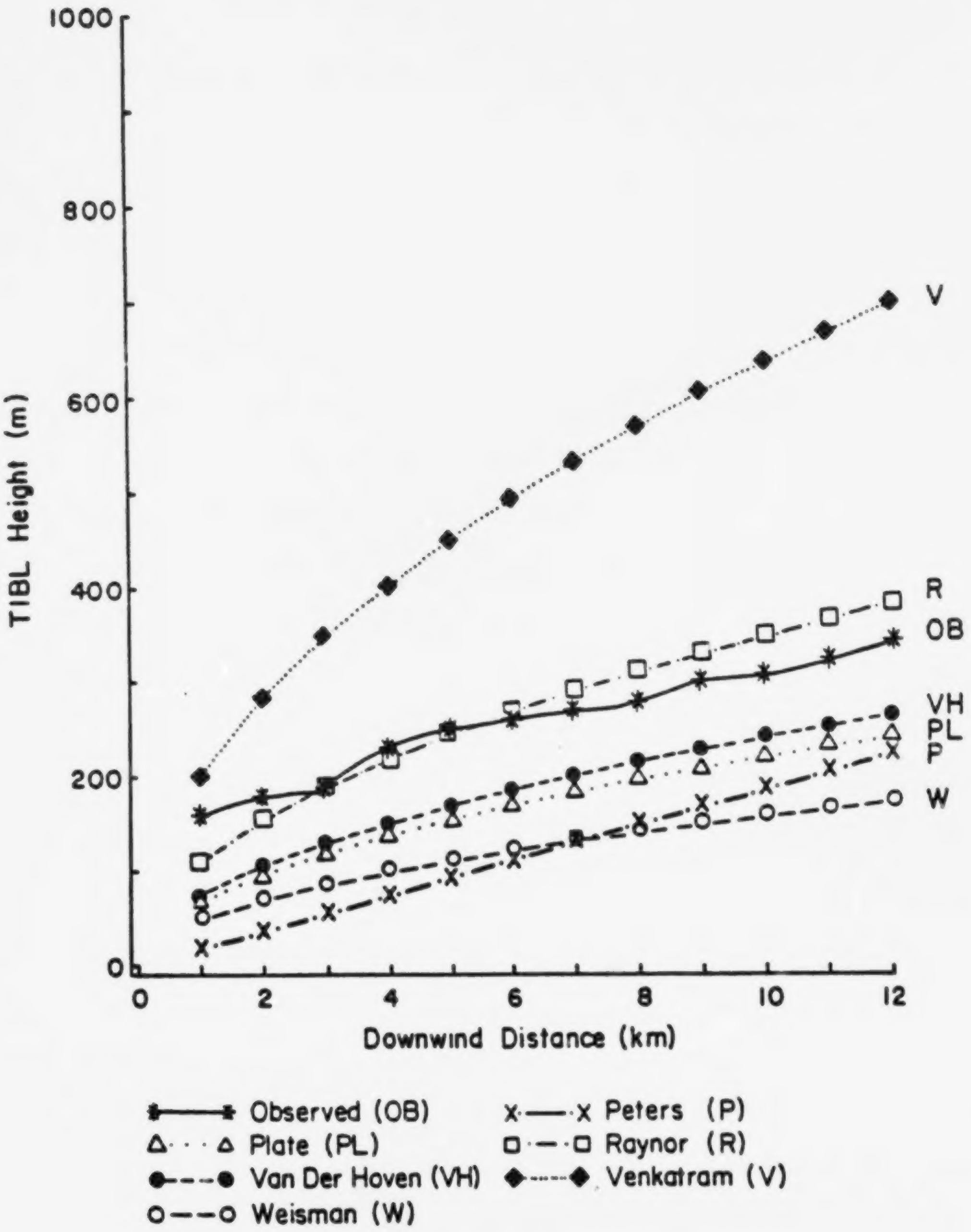

Figure 6.3: Observed vs predicted TIBL heights for BL #13.

to the stable case in the previous section because of the existence of an initial, shallow mixed layer over the ocean, capped by an elevated thermal inversion.

The upwind unstable case is most common in winter and early spring. The case selected for unstable condition analysis was Brookhaven experiment BL #6, which occurred on March 18, 1975, 1130 to 1330 EST. A listing of the meteorological data pertaining to the experiment appears in Table 6.5. The sounding shown in Figure 6.4 indicates that a shallow, superadiabatic layer existed over the ocean near the surface, capped by a stable layer. The TIBL equations are therefore modified by adding a constant h_o to the original equation. For example, Equation 2.2 now becomes:

$$h = h_o + (u_*/U)(X|T_L - T_W|/\gamma)^{0.5} \qquad (6.1)$$

This modification is made because the equations assume that offshore conditions are stable. The h_o in this case was determined to be 150 m based on the overwater temperature profile. Table 6.6 gives an interesting comparison of the predicted values of the TIBL with and without h_o. The TIBL prediction equations without h_o greatly underpredict the TIBL.

The TIBL grew very rapidly for this case after 2 km because of the development of intense overland convection. Figure 6.5 shows the TIBL height with downwind distance X. Weisman's (1976) formulation with the h_o modification predicts the best along with Venkatram's (1977)

TABLE 6.5

BNL #6 METEOROLOGICAL DATA

Parameter	Value
U	4.5 m s^{-1}
$\Delta\theta$	5.0 K
u_*	0.5 m s^{-1}
T_L	290 K
T_W	281.3 K
H_o	276 W m^{-2}
dT/dz	-0.0131 K m^{-1}
h_o	150 m: h_o is the initial TIBL height due to unstable or near-neutral overwater conditions
Wind direction	150°

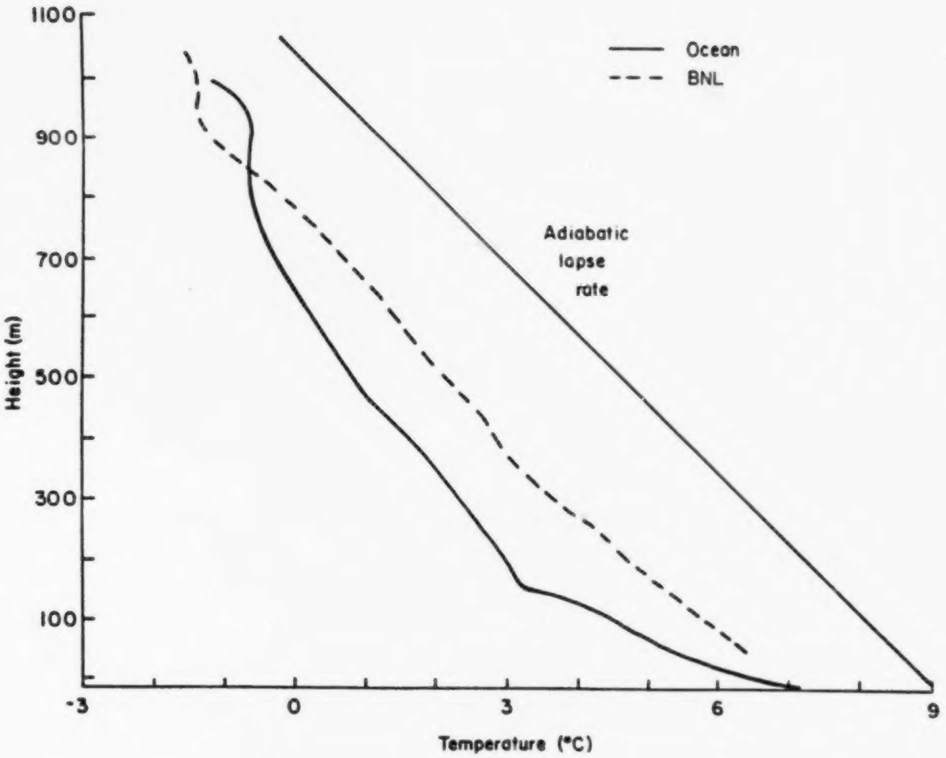

Figure 6.4: Sounding for BL #6.

TABLE 6.6

COMPARISON OF h (m) VS h + h_o (m)

km	Observed TIBL (m)	TIBL Height	Van der Hoven	Raynor	Peters	Weisman	Venkatram	Plate
1	250	h	62	102	53	186	185	263
		h+h_o	212	252	203	336	335	413
2	450	h	88	146	105	263	262	372
		h+h_o	238	296	255	413	412	522
3	575	h	108	176	158	323	321	457
		h+h_o	258	326	308	473	471	607
4	600	h	124	204	211	373	371	527
		h+h_o	274	354	366	523	521	677
5	650	h	139	228	263	417	415	590
		h+h_o	289	378	413	567	565	740
6	700	h	152	250	316	456	454	645
		h+h_o	302	400	466	606	604	795
7	750	h	165	270	369	493	491	697
		h+h_o	315	420	519	643	641	847
8	770	h	176	288	421	527	524	745
		h+h_o	326	438	571	677	674	895
9	775	h	187	306	474	554	556	790
		h+h_o	337	456	624	704	706	940

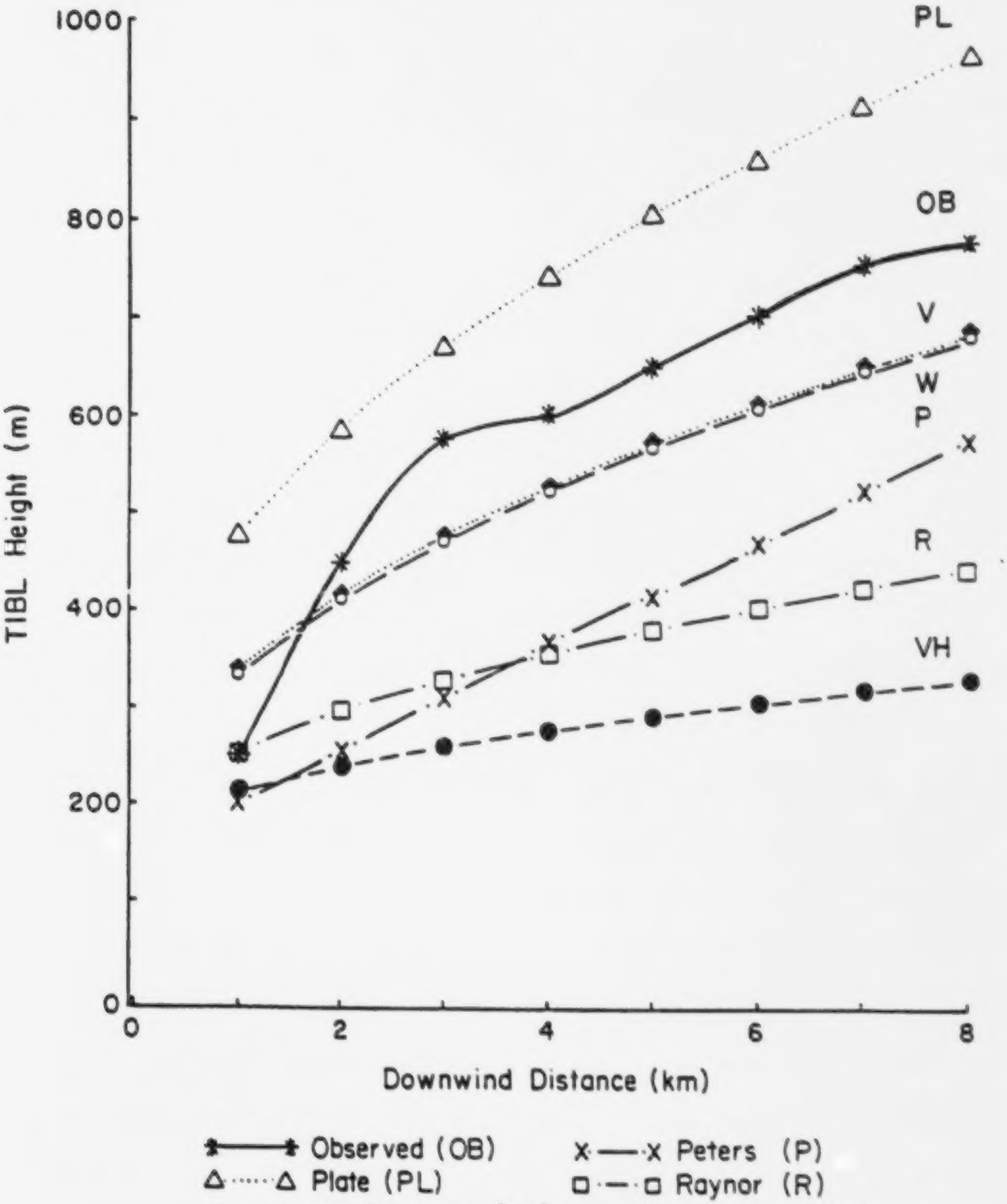

Figure 6.5: Observed vs predicted TIBL heights for BL #6.

formulation. It is possible that Venkatram's (1977) formulation predicts better values than in the previous case because of the relatively uniform winds in the lowest levels. The average h difference between the Weisman (1976) formulation and the Venkatram (1977) formulation was about 10 m, which is within observational error.

Two typical cases of differing upwind stability have indicated mixed results in terms of the predictive capabilities of the various TIBL equations. This would suggest that some caution be exercised when applying even the determined, best predictive equation. Statistical evaluation of these equations using the two data bases should allow for a better evaluation of the effectiveness of the various TIBL equations.

6.5 EVALUATION OF TIBL EQUATIONS

A statistical analysis of the predicted and observed TIBL values was first undertaken to determine the best overall predictive equation. The data was not categorized according to wind speed, stability and so forth at this point. The summary measures, regression coefficients and difference measures appear in Table 6.7. An analysis of $\overline{O}$ vs. $\overline{P}$ values indicates that the Plate (1971), Venkatram (1977) and Raynor et al. (1975) formulations all on average overpredicted the TIBL height. Equation 2.7 (Venkatram, 1977) has the most deviation from the observed value. The greatest scatter (based on the comparison of S_p) is

TABLE 6.7

OVERALL TIBL ANALYSIS

(N = 203)

Equations	Summary Measures				Linear Regression			Difference Measures			
	$\overline{O}$	$\overline{P}$	S_o	S_p	a	b	r	RMSE	$RMSE_u$	$RMSE_s$	d
Van der Hoven	359	226	184	135	86	0.39	0.28	208	114	174	0.61
Raynor et al.	" "	376	" "	216	261	0.32	0.32	242	207	126	0.55
Peters	" "	305	" "	219	175	0.36	*0.08	245	208	129	0.58
Weisman	" "	309	" "	207	121	0.52	0.45	208	182	101	0.68
Plate	" "	437	" "	292	171	0.74	0.44	273	257	92	0.62
Venkatram	" "	495	" "	250	366	0.36	0.22	300	240	180	0.50

Note: Units are in meters except for the slope b, index d and correlation coefficient (r). The correlation coefficient has been included for completeness. (*) indicates not significant at the 95% confidence interval (in this case $r_{crit} = 0.14$).

exhibited by the Plate (1971) equation. All equations, however, show a rather large scatter.

The linear regression coefficients present a rather confused picture of small "a" values, yet small "b" values. It is very difficult to draw conclusions from examining the coefficients alone. The correlation coefficients have been included for completeness, although they either show minimal significance or are not significant at the 95% confidence level. The difference measures indicate that the Weisman (1976) and Plate (1971) equations are performing the best. The equations are ranked from best predictor to worst predictor as follows:

(1) Weisman (1976)
(2) Plate (1971)
(3) Van der Hoven (1967)
(4) Peters (1975)
(5) Raynor et al. (1975)
(6) Venkatram (1977)

The decision to rank the Weisman (1976) equation first is based on the index of agreement value of 0.68, which is the highest value of any model. This means, for example, that 68% of the potential for error is explained by the model. Secondly, even though both the Weisman (1976) and Van der Hoven (1967) equations have identical RMSEs, the real differences between the two approaches lie in the systematic and unsystematic errors. The systematic errors of the Weisman (1976) model, for example, are much lower than the systematic errors of the Van der Hoven (1967) model.

An examination of the regression coefficients also shows that the Weisman (1976) and Plate (1971) models outperform all the other models. The summary measures indicate that the Weisman (1976) and Plate (1971) models underpredict or overpredict, respectively, with regard to $\overline{O}$ vs $\overline{P}$. The other three rankings are based on a combined analysis of the difference measures, summary measures and regression coefficients.

The Peters (1975) model (ranked fourth overall) makes the physically unrealistic assumption that the TIBL is linear, with no entrainment at the TIBL interface. Peters (1975), of course, also cautions that his equation should not be used for long downwind distances. This is because of the linear rapid growth of the predicted TIBL height. The Raynor et al. (1975) formulation cannot handle the neutral case and the results were affected by those particular observations close to neutral conditions. The Venkatram (1977) model, which contains state-of-the-art analytical reasoning, surprisingly finishes last in overall rank. There may be several reasons contributing to the poor performance of the model. First, the model is to be used under steady-state conditions, meaning that it can only be applied when the atmosphere is in an "equilibrium state," which lasts for a few hours during daytime conditions. Unfortunately, the coastal meteorological processes do not always satisfy steady-state conditions. The amount of heat flux could be cut back by clouds for a time in mid-day, thus causing sudden temporary collapse of the TIBL. Secondly, the inversion (i.e., TIBL interface) heat flux controlling the TIBL height is assumed to be a fixed part of the surface heat flux. This assumption may be restrictive as the strength of the TIBL interface decreases with decreasing thermal stratification of the marine air. This is similar to the argument of Zilitinkevich (1975). Also, the use of a fixed entrainment factor (F_R) may limit the applicability of the equation to varying entrainment rates along the TIBL interface.

6.6 ANALYSIS BY WIND CATEGORY

The TIBL data base contained different meteorological conditions in terms of water temperature, thermal stability over water and wind speed. It will be of interest to determine if some of the models do better under certain meteorological conditions. The data base was divided into smaller segments depending on wind speed and thermal stability and the statistical analysis was carried out. In this section classification by wind speed is made. In the next section data are classified according to thermal stability. Classification by wind speed allows linking the TIBL models somewhat to the different mesoscale (i.e., higher winds under sea breeze conditions) and synoptic scale conditions (i.e., gradient winds due to the location of high pressure systems) in the study area. Category U1 contained 101 cases and included wind speeds of 4.0 m s^{-1} or less. Category U2 contained 102 cases and included wind speeds greater than 4.0 m s^{-1}. Lower wind speeds will generally lead to near-free convection conditions and higher TIBL heights as shown by Raynor et al. (1979). Table 6.8 a-b shows the various evaluative statistics for the U1 and U2 categories.

It appears that the formulation of Weisman (1976) performs the best under low wind conditions, based on analysis of d and RMSEs. The rankings are:

(1) Weisman (1976)
(2) Van der Hoven (1967)
(3) Plate (1971)
(4) Peters (1975)
(5) Raynor et al. (1975)
(6) Venkatram (1977)

It is also interesting to see that the top three rankings for the U1 case are relatively consistent with the general analysis given in Section 6.5. In this category the Venkatram (1977) model does very poorly, finishing last in rank.

The inherent difficulty with most of these models is that the effects of advection are represented by one

TABLE 6.8a

TIBL ANALYSIS CATEGORIZED BY WIND

CATEGORY U 1

(N = 101)

Equations	Summary Measures				Linear Regression			Difference Measures			
	$\overline{O}$	$\overline{P}$	S_o	S_p	a	b	r	RMSE	$RMSE_u$	$RMSE_s$	d
Van der Hoven	399	282	203	129	125	0.39	0.38	197	101	170	0.62
Raynor et al.	" "	458	" "	213	418	0.10	0.35	285	211	191	0.43
Peters	" "	334	" "	212	197	0.34	0.33	248	199	148	0.60
Weisman	" "	379	" "	211	202	0.44	0.42	222	190	114	0.67
Plate	" "	536	" "	299	286	0.63	0.41	311	269	156	0.60
Venkatram	" "	534	" "	258	531	0.01	*0.18	353	257	242	0.37

* See Table 6.7 for notes. Here $r_{crit} = 0.20$.

TABLE 6.8b

TIBL ANALYSIS CATEGORIZED BY WIND

CATEGORY U 2

(N = 102)

Equations	Summary Measures				Linear Regression			Difference Measures			
	$\overline{O}$	$\overline{P}$	S_o	S_p	a	b	r	RMSE	$RMSE_u$	$RMSE_s$	d
Van der Hoven	319	170	155	117	91	0.25	0.33	294	149	253	0.62
Raynor et al.	" "	295	" "	186	0.47	0.46	*0.15	342	271	209	0.51
Peters	" "	276	" "	223	165	0.35	0.27	345	293	183	0.57
Weisman	" "	240	" "	177	81	0.50	0.44	293	247	158	0.65
Plate	" "	340	" "	251	115	0.71	0.41	386	349	163	0.60
Venkatram	" "	457	" "	236	178	0.87	0.24	424	320	278	0.49

* See Table 6.7 for notes. Here $r_{crit} = 0.19$.

horizontal wind velocity which is assumed constant with height. Even the Venkatram (1977) model, which requires a mean mixed layer wind, does not take into account marine stable air wind velocities. Thus, wind shear effects are not accounted for in any of the models. Readings et al. (1973) have shown, however, how wind shear at the CBL - stable air interface is important in entraining sensible heat and momentum.

Table 6.8 b displays the evaluative statistics for the higher wind category, U2. The results are markedly similar to the U1 results. Under higher wind conditions the Weisman (1976) formulation once again performs well. The rankings are:

(1) Weisman (1976)
(2) Plate (1971)
(3) Van der Hoven (1967)
(4) Peters (1975)
(5) Raynor et al. (1975)
(6) Venkatram (1977)

The Van der Hoven (1967) formulation is shown to underpredict the TIBL height. The Venkatram (1977) formulation is consistently last in rank for both categories.

6.7 ANALYSIS BY STABILITY CATEGORY

The combined data base was divided into four stability categories labelled S1, S2, S3 and S4. The partitioning of the data is in accordance with the recommendation of

Fox (1981) regarding data interpretation using small network comparison by meteorological categories. The division of each stability category is as follows:

S1: $dT/dz < -0.012$ K m^{-1} (fairly unstable)
S2: $-0.012 < dT/dz < -0.005$ K m^{-1} (near neutral)
S3: $-0.005 < dT/dz < 0.005$ K m^{-1} (isothermal)
S4: $dT/dz < 0.005$ (stable)

The dT/dz values refer to the lapse rates over the water, therefore the TIBLs are classified by overwater boundary layer characteristics.

It is important to note that category S1 contained only nine observations. Conclusions based on this category should be used with some caution because of this small number of observations. Category S3 was observed only in the BNL data base. Table 6.9 a - d gives the statistical measures used to evaluate the equations under all four stability classifications.

The statistics for the S1 case appear in Table 6.9 a. The ranks for the various TIBL models are:

(1) Weisman (1976)
(1) Venkatram (1977)
(3) Plate (1971)
(4) Peters (1975)
(5) Raynor et al. (1975)
(6) Van der Hoven (1967)

It would appear from the evaluative statistics that

TABLE 6.9a

TIBL ANALYSIS CATEGORIZED BY STABILITY

CATEGORY S 1

(Limited Number of Data)

Equations	Summary Measures				Linear Regression			Difference Measures			
	$\overline{O}$	$\overline{P}$	S_o	S_p	a	b	r	RMSE	$RMSE_u$	$RMSE_s$	d
Van der Hoven	613	283	173	42	140	0.23	0.93	353	10	353	0.46
Raynor et al.	" "	369	" "	68	135	0.38	0.93	265	16	265	0.56
Peters	" "	413	" "	144	61	0.77	0.86	209	50	203	0.70
Weisman	" "	550	" "	125	120	0.70	0.97	85	29	80	0.91
Plate	" "	777	" "	177	169	0.99	0.96	169	41	164	0.79
Venkatram	" "	548	" "	124	120	0.70	0.94	87	29	82	0.91

* See Table 6.7 for notes. Here $r_{crit} = 0.67$.

both the Weisman (1976) and Venkatram (1977) formulation best predict TIBL height under unstable marine conditions. This may be because of the inclusion of an h_o term to each equation, which would account for the initial TIBL height caused by offshore convective conditions. It is hard to draw inferences, however, on such a limited S1 category data base.

The statistics for the S2 category (near neutral case) appear in Table 6.9 b. The rank for the models are:

(1) Peters (1975)
(2) Weisman (1976)
(3) Raynor et al. (1975)
(4) Venkatram (1977)
(5) Van der Hoven (1967)
(6) Plate (1971)

It is not surprising to see the Peters (1975) equation performing well for this category since the equation does not contain any direct stability type terms and instead relies on T_L-T_W and heat flux terms, which would not be affected by temperature gradient singularity. It is interesting to note that most of the equations tend to overpredict the TIBL height on average. This cannot be directly accounted for, except to say that perhaps difficulties in determining h_o may have aided in the process.

The evaluation statistics for the S3 category (isothermal) appear in Table 6.9 c. The ranks of the

TABLE 6.9b

TIBL ANALYSIS CATEGORIZED BY STABILITY

CATEGORY S 2

(N = 51)

Equations	Summary Measures				Linear Regression			Difference Measures			
	$\overline{O}$	$\overline{P}$	S_o	S_p	a	b	r	RMSE	$RMSE_u$	$RMSE_s$	d
Van der Hoven	394	288	157	149	178	0.28	0.29	256	141	214	0.51
Raynor et al.	" "	392	" "	233	243	0.38	*0.25	268	224	147	0.53
Peters	" "	405	" "	238	203	0.50	*0.11	252	224	116	0.60
Weisman	" "	468	" "	242	326	0.36	0.62	267	234	129	0.56
Plate	" "	662	" "	343	461	0.50	0.62	438	331	287	0.41
Venkatram	" "	395	" "	211	329	0.17	*0.23	247	208	134	0.51

* See Table 6.7 for notes. Here $r_{crit} = 0.28$.

TABLE 6.9c

TIBL ANALYSIS CATEGORIZED BY STABILITY

CATEGORY S 3

(N = 72)

Equations	Summary Measures				Linear Regression			Difference Measures			
	$\overline{O}$	$\overline{P}$	S_o	S_p	a	b	r	RMSE	$RMSE_u$	$RMSE_s$	d
Van der Hoven	373	234	202	158	48	0.50	0.40	301	170	249	0.62
Raynor et al.	" "	434	" "	255	395	0.11	*0.39	388	315	226	0.47
Peters	" "	270	" "	214	21	0.16	*0.17	358	282	220	0.54
Weisman	" "	301	" "	166	162	0.37	0.45	305	245	181	0.60
Plate	" "	426	" "	234	229	0.53	0.45	437	347	265	0.51
Venkatram	" "	495	" "	257	389	0.29	0.56	375	304	220	0.51

* See Table 6.7 for notes. Here $r_{crit} = 0.23$.

models are:

(1) Van der Hoven (1967)
(2) Weisman (1976)
(3) Peters (1975)
(4) Plate (1971)
(5) Venkatram (1977)
(6) Raynor et al. (1975)

The Van der Hoven (1967) formulation has one of the highest RMSE values, which implies that most of the error involved in the equation is systematic and can be attributed to the coefficient in Equation 2.1. The Raynor et al. (1975) equation, which ranks last in this category, appears to do so because of the lapse rate term and singularity problems as discussed before.

Finally, the more typical overwater stable category (S4) results indicate that the Weisman (1976) equation performs the best. The ranks of the models are:

(1) Weisman (1976)
(2) Van der Hoven (1967)
(3) Peters (1975)
(4) Raynor et al. (1975)
(5) Plate (1971)
(6) Venkatram (1977)

and the statistical results appear in Table 6.9 d. It is apparent that the Van der Hoven (1967) formulation contains a large systematic error, even for the stable

TABLE 6.9d

TIBL ANALYSIS CATEGORIZED BY STABILITY

CATEGORY S 4

(N = 71)

Equations	Summary Measures				Linear Regression			Difference Measures			
	$\overline{O}$	$\overline{P}$	S_o	S_p	a	b	r	RMSE	$RMSE_u$	$RMSE_s$	d
Van der Hoven	287	166	146	64	112	0.19	0.42	352	180	302	0.60
Raynor et al.	" "	306	" "	142	0.13	0.62	0.40	410	335	236	0.53
Peters	" "	255	" "	191	1	0.39	*0.23	414	337	240	0.54
Weisman	" "	173	" "	82	97	0.27	0.47	352	257	240	0.60
Plate	" "	245	" "	116	137	0.38	0.47	462	364	285	0.53
Venkatram	" "	495	" "	257	146	259	0.40	508	366	352	0.51

* See Table 6.7 for notes. Here $r_{crit} = 0.23$.

overwater case. The closeness of the 3rd, 4th and 5th ranks makes interpretation difficult. It is clear, however, that the Venkatram (1977) formula performs poorly under the prevalent conditions of a stable overwater boundary layer.

Based on these three different types of analyses, using the two available data bases, it appears that Weisman's (1976) formulation predicts the TIBL heights best. Weisman's equation was used in the TIBL modules for the various fumigation models that are compared statistically in the next chapter.

7.0 COASTAL DISPERSION MODEL EVALUATION

In this section results of both the overall model evaluation (all data) and specific cases (daily data) are presented. In addition, attempts are made to gain insight into the reasons for better model performance for certain meteorological conditions. The CSFM, MSFM and two variations of MSFM (empirical and downdraft) models are examined.

7.1 OVERALL EVALUATION

7.1.1 RESULTS

Scatterplots (Figures 7.1 a-d) of the predicted vs. observed values of each model were generated since they represent an initial means of readily displaying the various relationships between O and P values. The various general error patterns of the models are apparent with respect to the a = 0 (intercept), b = 1 (slope) prediction line. The MSFM model appears to have the least scatter about the perfect prediction line although all models exhibit considerable scatter, especially in predicting large concentration values. Three of the models tend to show an underprediction of concentration values while the MSFM model gives slight overprediction of concentration values. These scatterplots provide a qualitative initial means of determining under and overprediction, but they say nothing about the quantitative magnitude of error or the accuracy.

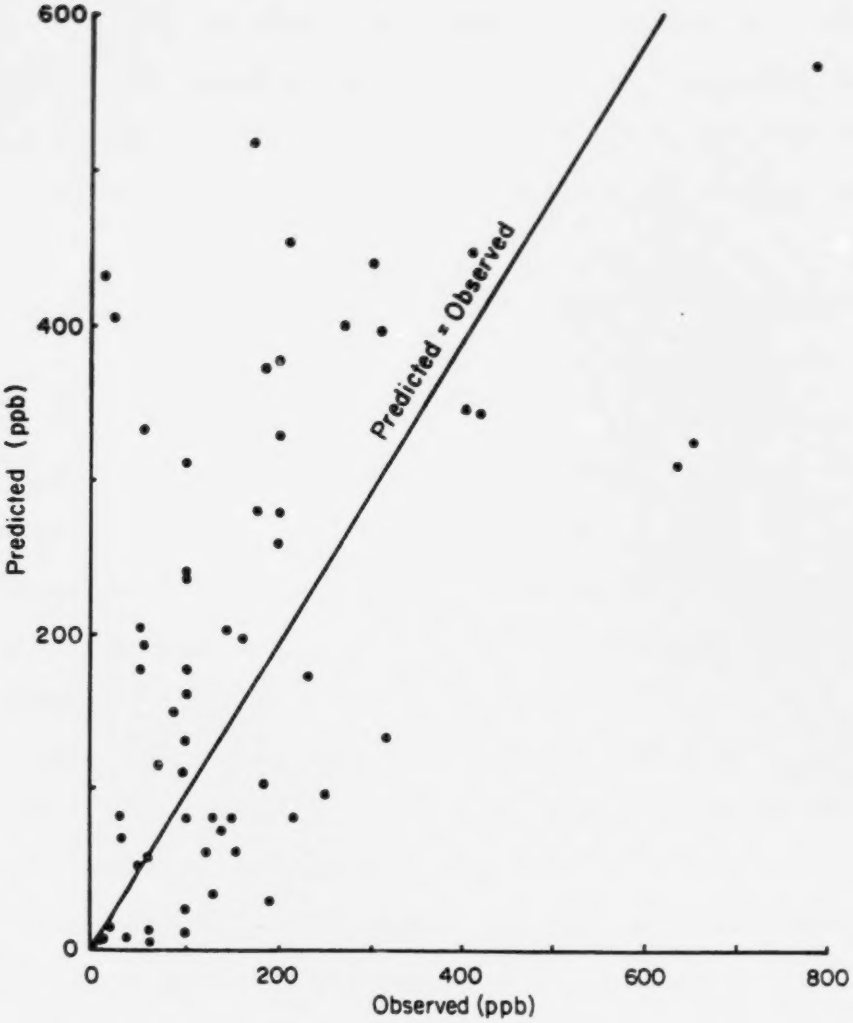

Figure 7.1a: Observed vs predicted concentration values for the MSFM model.

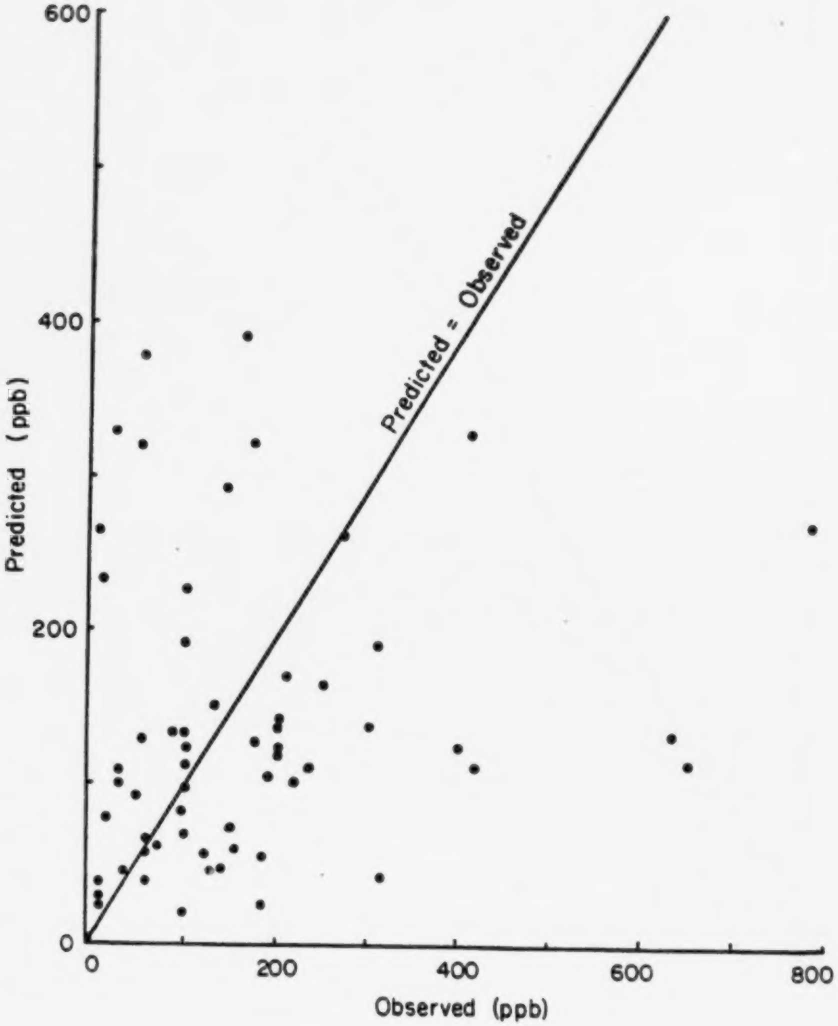

Figure 7.1b: Observed vs predicted concentration values for the CSFM model.

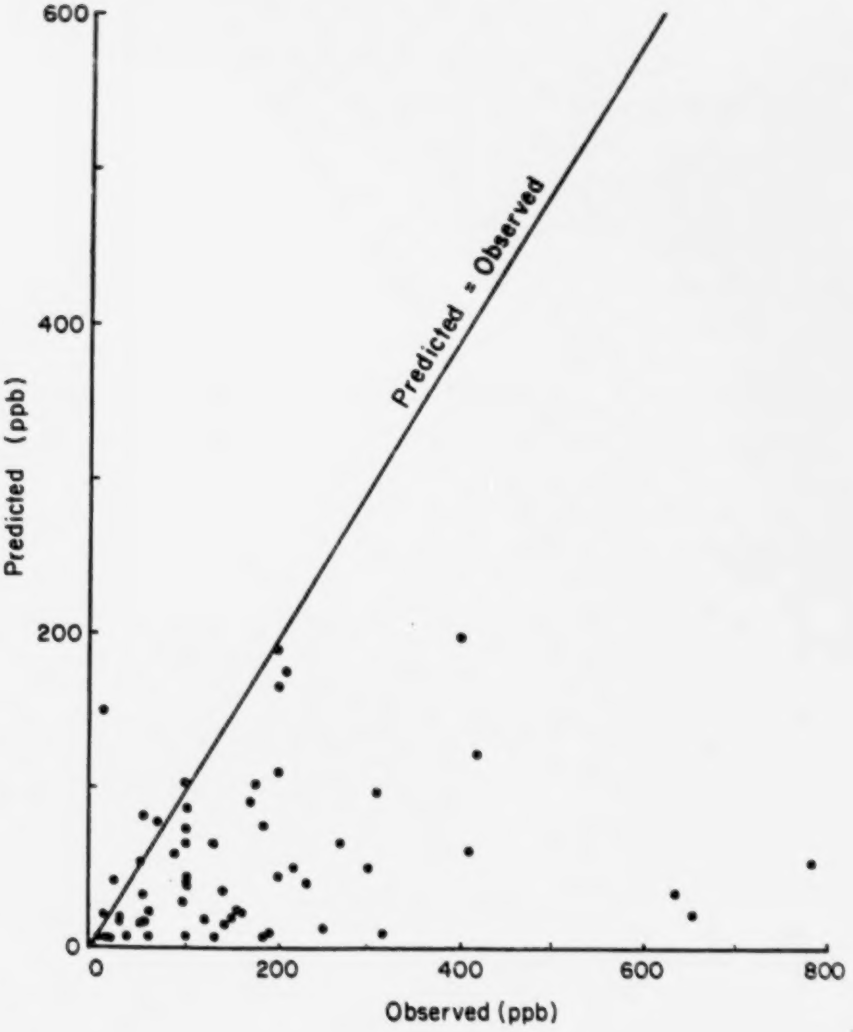

Figure 7.1c: Observed vs predicted concentration values for the empirical model.

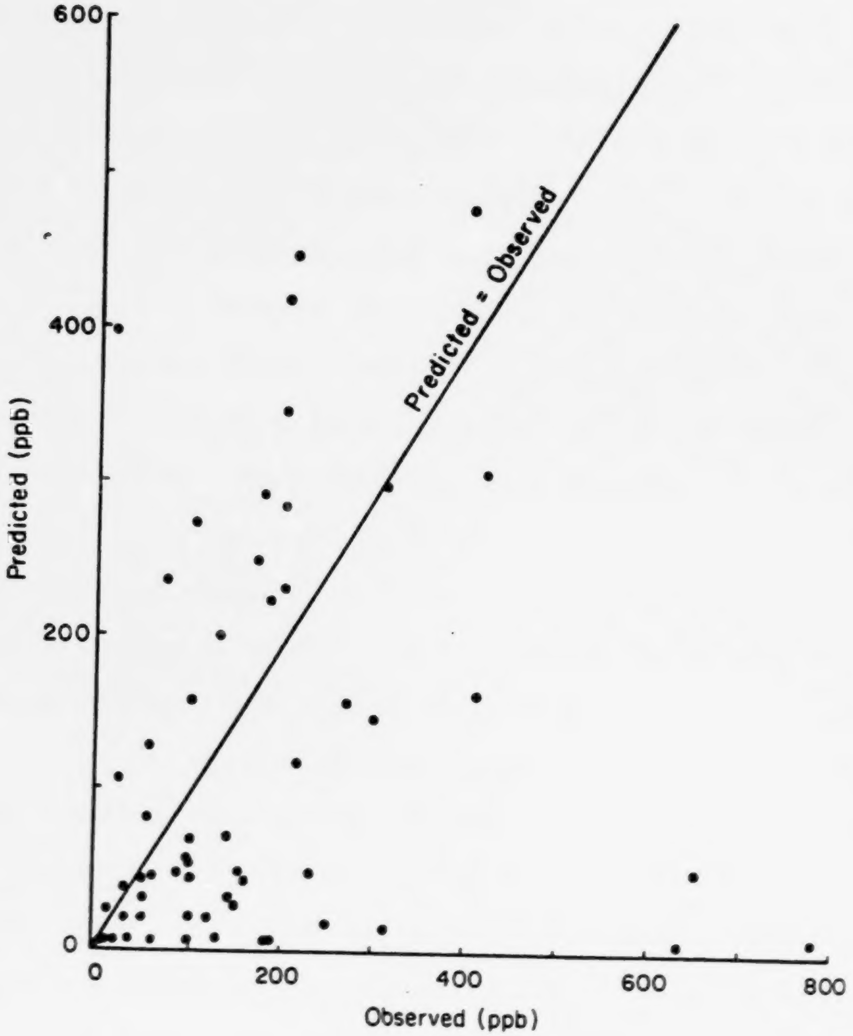

Figure 7.1d: Observed vs predicted concentration values for the downdraft model.

A listing of the various summary measures, regression coefficients and difference measures that give a better understanding about the degree of error appear in Table 7.1. The $\overline{O}$ vs $\overline{P}$ summary measures indicate that on the average the CSFM, MSFM/empirical modification and MSFM/downdraft modification underpredict concentration values while MSFM slightly overpredicts. The MSFM model exhibited the smallest average error of 26, while the empirical modification had the largest average error of -117. A comparison of S_o and S_p with regard to how close the two standard deviations approach each other gives a relative indication of how well a model performs. Thus, from Table 7.1 it appears that the MSFM model is best able to describe the observed variability. The MSFM/empirical modification deviation difference is over 100 (large compared to the other three models), which suggests that this modification is not able to completely describe some of the larger concentrations and variability.

The two measures which are not univariate summary or difference statistics are the regression coefficients. They have been included for completeness, since they are used to compute the more representative measures such as RMSEs. Willmott (1984) mentions two problems in the interpretation of a and b. The first problem is that the two coefficients are not independent of one another and the second, related problem, involves correlation analysis

TABLE 7.1

QUANTITATIVE MEASURES OF COASTAL DISPERSION MODEL PERFORMANCE

OVERALL MODEL PERFORMANCE

Equations	Summary Measures				Linear Regression			Difference Measures			
	$\overline{O}$	$\overline{P}$	S_o	S_p	a	b	r	RMSE	$RMSE_u$	$RMSE_s$	d
CSFM	164	134	158	95	118	0.10	*0.28	193	128	145	0.46
MSFM	" "	190	" "	156	99	0.56	0.32	148	128	74	0.76
Empirical Modif.	" "	47	" "	50	36	0.10	*0.25	193	48	187	0.45
Downdraft Modif.	" "	108	" "	131	84	0.15	*0.13	172	93	144	0.57

Note: Units are in ppb except for the slope b, index d and correlation coefficient (r). The correlation coefficient has been included for completeness. (*) indicates not significant at the 95% confidence interval (here $r_{crit} = 0.25$).

between the coefficients and other summary variables. Ideally, however, an outcome of $a = 0.0$ and $b = 1.0$ is desired. This condition is most closely met by the MSFM model. It is difficult to interpret the other model coefficient values since some of the "a" values are rather large, yet the "b" values are extremely small (see for example the MSFM/empirical modification, Table 7.1).

The difference measures such as RMSE generally agree with the univariate summary measurements with regard to the capabilities of the various models to predict concentration values. Table 7.1 indicates that the MSFM model has the least overall RMSE. The MSFM model also fits the criteria of the systematic error being comparatively small (although not "close" to zero) and of the unsystematic error approaching the overall RMSE.

The difference measures of the CSFM model show the $RMSE_s$ to be comparatively similar to the downdraft model, but still comparatively higher than the MSFM model. The MSFM/empirical modification has a small difference between overall RMSE and $RMSE_s$, which implies that this modification might contain numerous systematic errors. Table 7.1 also indicates that the MSFM/downdraft modification performs better in terms of both overall RMSE and $RMSE_s$ values than the MSFM/empirical modification.

The relatively comprehensive difference measure of a coastal dispersion model's ability to predict the downwind concentration, the index of agreement (d), suggests (following Willmott, 1982) the percentage of the potential for error in predicting concentrations that has been explained by the model. Thus for the MSFM model, 76% of the potential for error has been explained by the model. The d values for the other models are in the middle-to-upper 40th percentile range, which is considerably less than the MSFM model.

7.1.2 DISCUSSION OF RESULTS

The above results suggest that the appropriate rankings of the models in terms of performance should be:

(1) MSFM

(2) MSFM/downdraft modification

(3) CSFM

(4) MSFM/empirical modification

The high d value clearly stands out as the most striking difference measure in supporting the relative accuracy of the MSFM model. The high d value implies that there is low error in the MSFM model results when compared to the other models. Most of this error in MSFM is comparatively unsystematic and would therefore be harder to correct than a systematic error.

The two variations of the MSFM model (empirical and downdraft modifications) in fact show higher degrees of systematic error, which would suggest that these variations do little to enhance the concentration predictability of

MSFM. The univariate summary measures also imply that MSFM is the most accurate model, especially given the ability of S_o to emulate S_p.

The MSFM/downdraft model ranks second in terms of potential accuracy for several reasons. The d value of the MSFM/downdraft model, when compared to the two remaining models (MSFM/empirical modification and CSFM), is higher. Secondly, even though the systematic error of both the downdraft and CSFM models is equal, the unsystematic errors do indicate a big discrepancy, with the downdraft model having the better RMSE value. Thirdly, comparative values of the slope of the predicted vs observed best fit line alone suggest that the MSFM/downdraft model outperforms the remaining two models. Lastly, the summary univariate statistics, although not showing a closeness in the average sense of $\overline{O}$ and $\overline{P}$ for the downdraft model compared to the CSFM model, certainly show the better ability of the downdraft model to reproduce the scatter as evidenced by the S_o and S_p values.

The CSFM model, while ranking a close third behind the MSFM/downdraft model, outperforms the empirical modification, particularly in the areas of univariate summary measures and RMSEs. In terms of univariate summary measures, the CSFM model clearly shows a closer agreement when comparing $\overline{O}$ and $\overline{P}$ than the MSFM/empirical modification. The CSFM model also shows a somewhat closer agreement between S_o and S_p values than the MSFM/empirical modification. A RMSE comparison between the two models illustrates the quantitative problems associated with the empirical modification. The $RMSE_s$ nearly approaches the overall RMSE, indicating the possibility of systematic errors in the empirical modification, particularly given the wide difference in the univariate summary measures of $\overline{O}$ and $\overline{P}$ and also S_o and S_p. For these reasons, the empirical modification is ranked fourth.

It is important not to base the argument for the best performing model just on the quantitative description of model results. Significant physical differences exist between the two base models (i.e., CSFM and MSFM) and between MSFM and its variations (empirical modification and downdraft modification). These physical differences can only be adequately presented in the qualitative, descriptive sense by looking at the common physical parameters (such as treatment of dispersion coefficients) that are used by these models.

Physical differences between the base models of CSFM and MSFM are found in the treatment of the dispersion coefficients (σ_y and σ_z) in both the stable marine air and the convective TIBL. Other physical differences involve the utilization of a point source type of modeling approach for the CSFM model versus an areal type modeling approach used in the MSFM model. Physical differences between the two base models and the MSFM variations stem from the use of uniform, instantaneous vs non-uniform, non-instantaneous mixing assumptions.

The problem of the change in dispersion coefficients across the TIBL interface was addressed as early as the original Lyons and Cole (1973) model. The split sigma concept used in CSFM relies on the basic premise that the horizontal dispersion in the stable zone can be characterized by a dispersion coefficient σ_{ys}, which is determined by the standard Pasquill-Gifford (PG) curve. The PG coefficients were constructed from data taken over flat terrain and refer to ground-level, neutrally buoyant tracer sources, not elevated sources. The averaging time to determine the coefficients was three minutes and the concentration measurements were made out to only about 800 meters from the ground-level release.

Pasquill and Smith (1983) caution against the application of the PG coefficients without regard to terrain or circumstances. Use of the PG type coefficients has been shown in summary form to be unrepresentative of diffusion in coastal areas (see, for example, MacRae et al., 1983). In addition, an application of the EPA RAM model, modified by using the Lyons and Cole (1973) approach for a power plant in Wisconsin (Ellis et al., 1979), indicated that the PG coefficients were not helpful in predicting ground-level concentrations under fumigation conditions. In addition, use of Turner's stability criteria by CRSTER has been shown to be biased toward neutral stability by Weil and Jepson (1977) and Weil (1979).

The MSFM approach, on the other hand, allows for direct calculation of σ_{ys} based on the influence of self-induced plume turbulence created by plume momentum and buoyancy. This means that, following Briggs (1975), σ_{ys} is proportional to plume rise only, since ambient turbulence in the stable air is negligible. This is physically more realistic than the method for determining σ_{ys} by CSFM, which relies on the empirical PG curves that are not expected to be valid for the above conditions.

If the plume remains in the stable layer a long time then low frequency eddies could cause significant meander. Observations indicate σ_y to initially vary as $t^{1/2}$ (where t is the travel time) and then vary with respect to t directly (Briggs, 1985). In the shoreline environment plumes generally intercept the TIBL quickly, but in the case of a shallow TIBL, plumes may travel a considerable distance inland above the TIBL. Once again, the PG curves may not represent plume dispersion adequately under these conditions.

The determination of σ_{yfi}, which represents the CSFM model's ability to predict the individual stability of each entrained plume segment in the convective TIBL, is accomplished by adding a factor $H_e/8$ (where H_e is the effective stack height) to the dispersion coefficient σ_{yfi}. This factor (H_e/8) is based on empirical arguments given in Chapter 3.0 by Turner (1970), who assumed that the plume spreads outward at 15 degrees and that σ_{yfi} is independent of source height.

The more realistic and useful "state of the art" method of determining horizontal diffusion in the unstable convective TIBL has been outlined by Lamb (1978) and Willis and Deardorff (1978). The dispersion coefficient is both physically obtained from the w_* parameter, which represents the convective velocity scale in the TIBL and by assuming that $\sigma_y \sim X$. The assumption that $\sigma_y \sim X$ has shown to be valid by Maul et al. (1980). Venkatram and Vet (1981) suggest that the enhanced plume spreading in the convective boundary layer is caused by a conversion of downdraft vertical kinetic energy into horizontal kinetic energy upon the air hitting the ground. Venkatram (1977) has shown, however, that heat flux decreases with downwind distance; thus w_* is basically invariant. This assumption may need further field testing.

Both base models assume instantaneous, uniform vertical mixing of fumigant within the TIBL (i.e., σ_{zh} = h). This assumption has been questioned by several authors (see, for example, Deardorff and Willis, 1982). In the CSFM model, under low wind speeds, the slope of the TIBL would be steeper than that under higher wind conditions.

Thus the amount of plume interception by the TIBL is a maximum, since the plume is entrained into the TIBL fairly soon after being emitted into the stable marine air. However, if the TIBL is not as steep, the plume entrains through a greater TIBL surface area and thus can become non-uniform and not mix down instantaneously. In addition, the fumigant may not become instantaneously entrained over a large downwind distance and could wind up "smeared out" over a large downwind distance.

The MSFM/empirical modification assumes that at the initial plume-TIBL intersection (point where the lower part the plume first intersects the TIBL interface), the rate of interception is small and similar to the final plume-TIBL interception rate. The rates of mixing between initial and final plume-TIBL intersections are dependent on water tank empirical values for fast and slow entrainment.

The plume is expected to exhibit higher ground-level concentrations closer to the stack under fast entrainment conditions. Under slower entrainment conditions the plume concentration will be more spread-out since the fumigant is entraining over a broad TIBL interface. Under increasing thermal stratification the plume will exhibit less growth and thus have faster entrainment in the marine air, yielding higher concentrations (Kerman, 1982). Increasing TIBL stratification, however, aids in decreasing TIBL growth and therefore decreasing entrainment. One can see how difficult it is to determine qualitatively whether fast or slow entrainment is occurring and then apply the appropriate non-dimensional t^* to represent fumigant dispersion in the convective TIBL. Kerman (1983), in fact, states that the normalized entrainment rates for the NEMP experiments ranged from 0.055 to 0.21. The rates were consistently larger than those obtained by Deardorff and Willis (1982) in their water tank experiments.

Deardorff and Willis (1982) also make the assumption that entrainment is constant throughout the convective boundary layer. This assumption may not qualitatively hold all the time, however, since in a TIBL the entrainment rate could vary as a function of TIBL interface structure.

In the case analysis sections to follow it has also been noticed that the point of maximum concentration for the MSFM/empirical modification has been pushed downwind considerably farther than either observed values or the other model's output values. This observation is consistent with the faster observed entrainment argument of Kerman (1983) above. The reason given by Deardorff and Willis (1983) for the displacement of the fumigation zone downwind is the representation of the initial laboratory plume as being compact at the point of TIBL interception, such that $\sigma_{ys}/\overline{h}_i$ and $\sigma_{zs}/\overline{h}_i$ both equal 0.05. Here $\overline{h}_i$ is the mean TIBL height where the plume initially impacts the TIBL.

The NEMP plume on the average had a ratio of σ_{ys} to $\overline{h}_i$ of about 1.7 and a σ_{zs} to $\overline{h}_i$ ratio of 0.18 based on lidar measurements of Hoff et al. (1982). The compact, initial laboratory plume condition along with slow entrainment rates therefore produced a very dispersed plume, as typified by the underprediction of concentration values.

It is somewhat surprising that the downdraft model does not improve upon the base MSFM model, especially given the fact that more physics is incorporated into the model. Part of the reason for the lack of improvement may result from the treatment of dispersion in the convective TIBL under short time diffusion theory. The downdraft model is based on the assumption that the maximum ground-level concentration is observed close to the source in the convective TIBL. However, Misra (1982) mentions that the short time diffusion theory may not be valid farther away from the stack than a distance H_eU/w_*. This distance-averaged quantity for the NEMP experiments is about 1.5 km downwind. Thus, the same problem that plagues the CSFM model when the TIBL is shallow may be influencing the concentration distribution and slow TIBL growth.

In this section, both quantitative and qualitative arguments were presented to justify the rank order of the various coastal dispersion models. In the next several sections a detailed analysis of the individual case studies is presented, keeping in mind the above quantitative and qualitative arguments.

7.2 THE JUNE 1, 1978 CASE

The mesoscale meteorology associated with the NEMP-I group of experiments has been described by Kerman et al. (1982), Hoff et al. (1982) and Misra and Onlock (1982). In summary, June 1, 1978 was characterized by high pressure over the NEMP area which produced light northerly winds during the very early morning hours, shifting to southwest winds by 0900 EDT.

The 0800 EDT plume lidar profile taken at the stack indicated the plume bearing to be 165 degrees, or offshore. Lidar measurements taken at 1030 EDT indicated a plume bearing of 12 degrees, or onshore. This was also confirmed by 10 meter tower winds which shifted to a southwesterly direction (onshore) around 0900 EDT. The land-water temperature difference at this time was 3 degrees (increasing to 10 degrees by day's end), which aided in the development of the TIBL.

Data presented by Kerman et al. (1982) indicated that the TIBL reached a maximum between 1000 and 1100 EDT and then gradually decayed during the afternoon period. Kerman et al. (1982) suggests that early morning light winds along with rapid surface heating aided in the development of a deep initial TIBL. He also attributes the sharp increases in wind speed aloft to the suppression of the TIBL during the day. One interesting note from the boundary layer study is the observation of a shallow inversion layer at the shoreline through 1200 EDT replaced by the creation of a shallow superadiabatic layer by 1300 EDT. This could be attributed to the presence of warmer water close to the shore creating a shallow superadiabatic layer. It is believed that its depth (h_o) was not significant enough, as compared to the h_o observed by Gamo et al. (1982) and SethuRaman et al. (1984), to influence the ground-level concentration.

Plume measurements described by Hoff et al. (1982) indicate that no fumigation occurred until the time period 1000 to 1100 EDT. This is confirmed by lidar measurements which showed the effective plume height to be 410 m at a distance of 2.65 km while MS based TIBL heights at that point were 200 m. Assuming no further spread in the Z direction, the plume would be expected to impact the TIBL around 6.5 km downwind.

Lidar measurements taken later in the day (e.g., the 1445 EDT lidar profile) indicated the effective plume height to be 380 m at a distance of 1.24 km from the stack. Now, however, the TIBL has decreased to a height of 325 m at 7.1 km downwind thus allowing the fumigation zone to move inland and increase in size (Kerman et al., 1982). Plots of effective stack height related to TIBL height appear in Figure 7.2. Isopleths of observed ground-level concentrations appear in Figure 7.3 (a-h), adopted from

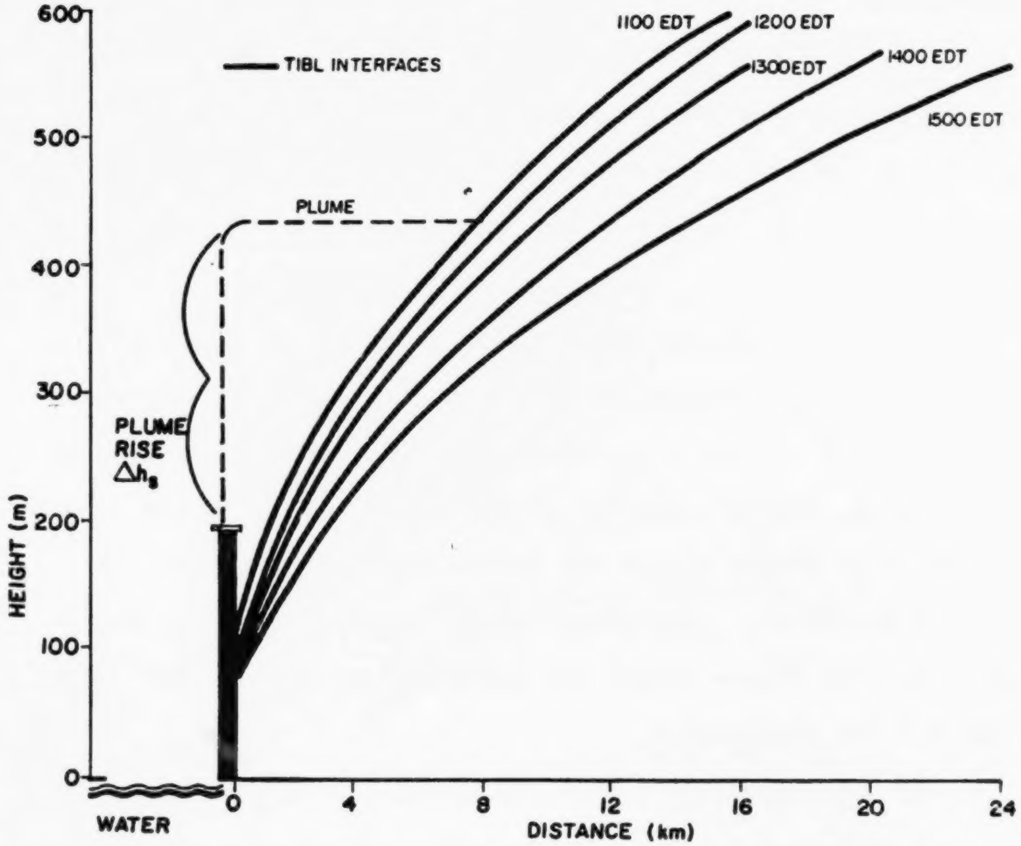

Figure 7.2: Plume-TIBL relationship for June 1, 1978.

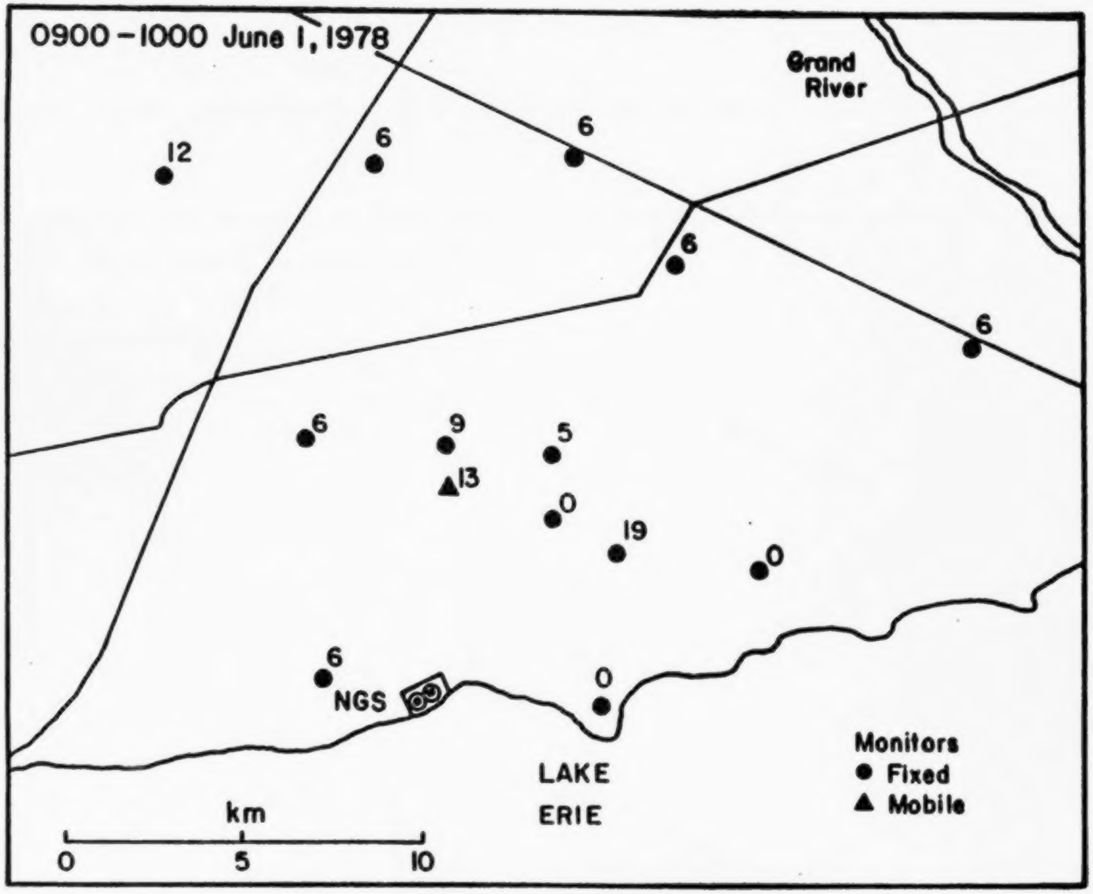
0900-1000 June 1, 1978
Grand River
12
6
6
6
6
6
9
5
▲13
0
19
0
6
NGS
0
LAKE ERIE
Monitors
● Fixed
▲ Mobile
km
0
5
10

Figure 7.3a: Concentration isopleths for June 1, 1978 -- 0900-1000 EDT.

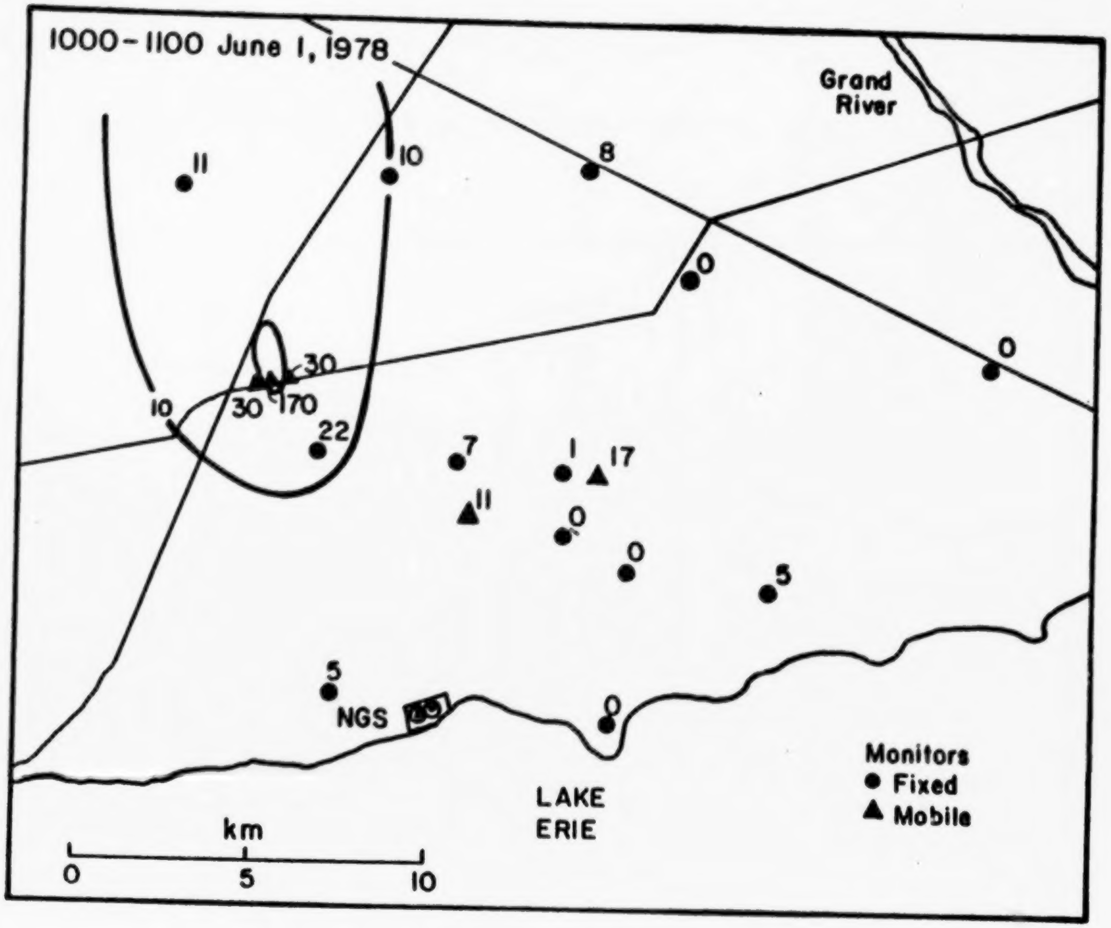
1000-1100 June 1, 1978
Grand River
11
10
8
0
0
30
10
30
170
22
7
1
17
11
0
0
5
5
NGS
0
LAKE ERIE
Monitors
● Fixed
▲ Mobile
km
0
5
10

Figure 7.3b: Concentration isopleths for June 1, 1978 -- 1000-1100 EDT.

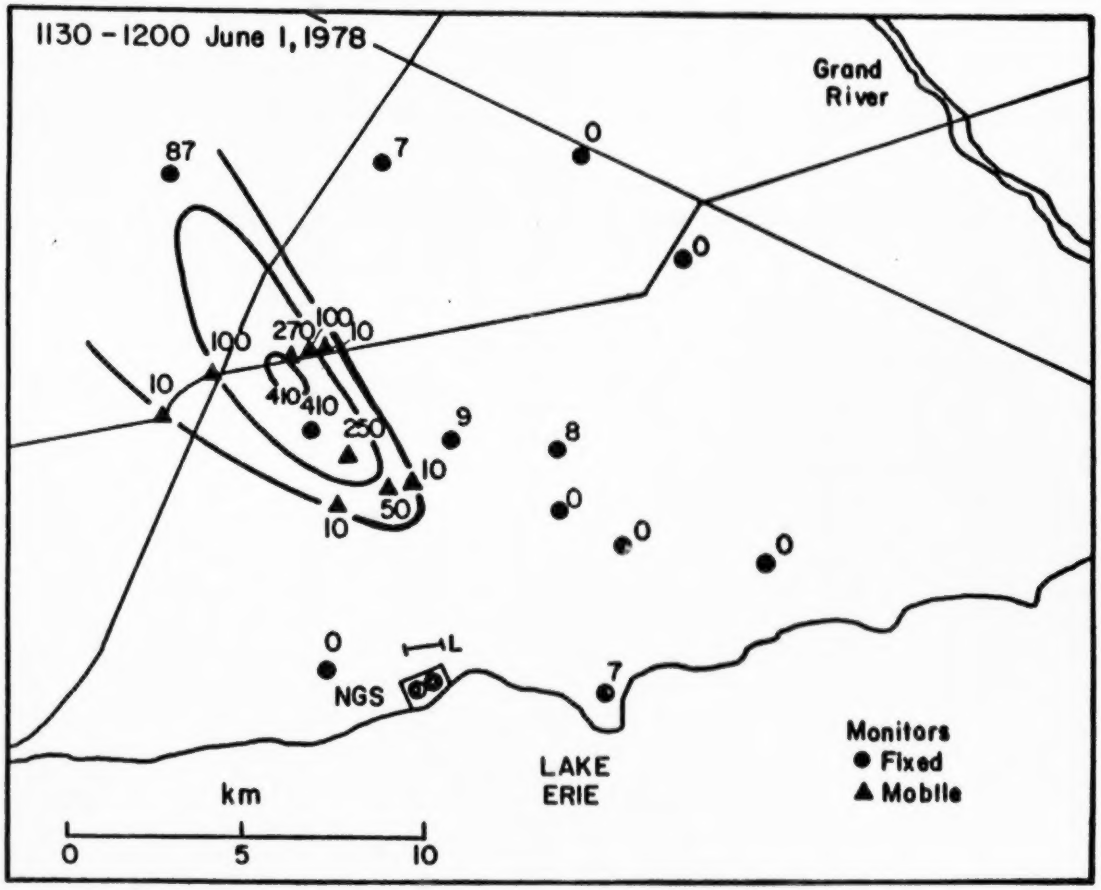
1130 - 1200 June 1, 1978
Grand River
87
7
0
0
100
270
100
10
10
410
410
250
9
8
0
0
0
10
50
10
0
L
NGS
7
LAKE ERIE
Monitors
● Fixed
▲ Mobile
km
0
5
10

Figure 7.3c: Concentration isopleths for June 1, 1978 -- 1130-1200 EDT.

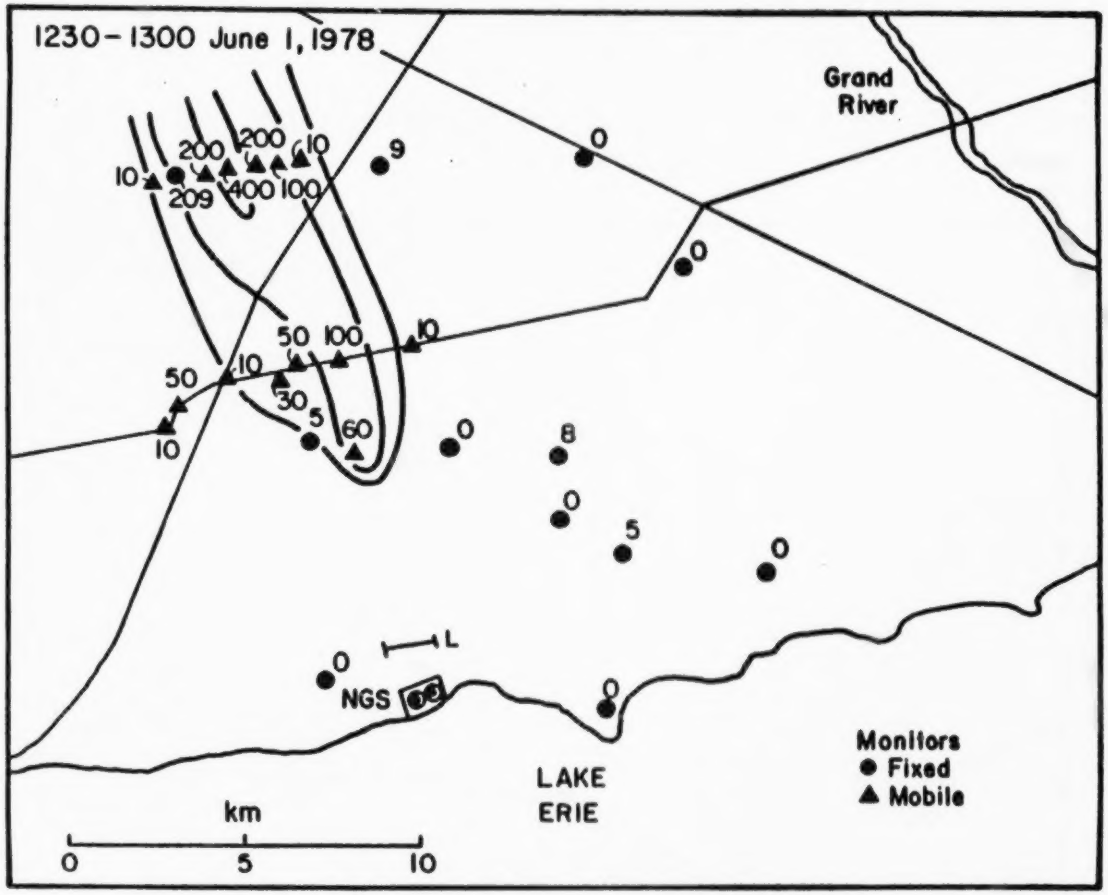
1230-1300 June 1, 1978
Grand River
10
200
209
400
200
100
10
9
0
0
50
100
10
50
10
30
5
60
10
0
8
0
5
0
L
0
NGS
0
LAKE ERIE
Monitors
● Fixed
▲ Mobile
km
0
5
10

Figure 7.3d: Concentration isopleths for June 1, 1978 -- 1230-1300 EDT.

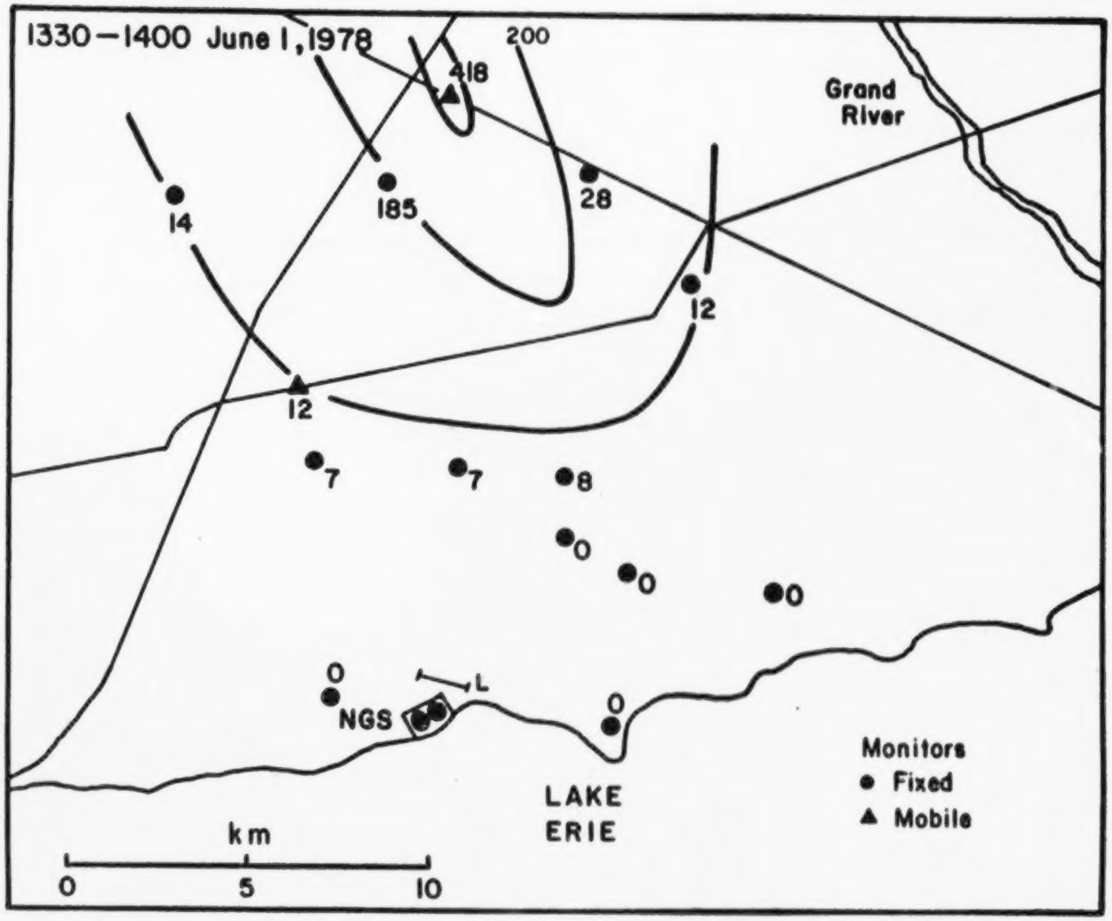
1330-1400 June 1, 1978
200
418
14
185
28
Grand River
12
12
7
7
8
0
0
0
0
0
NGS
L
LAKE ERIE
Monitors
● Fixed
▲ Mobile
km
0
5
10

Figure 7.3e: Concentration isopleths for June 1, 1978 -- 1330-1400 EDT.

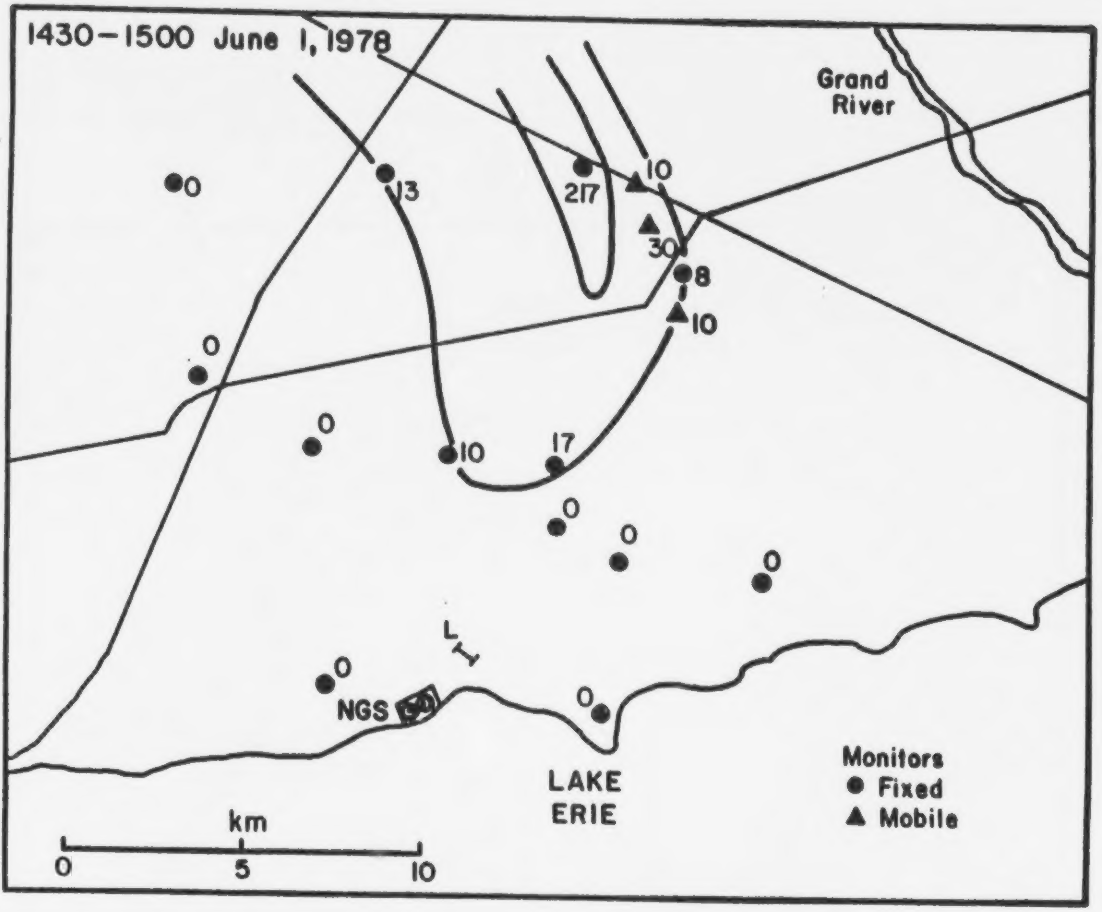
1430-1500 June 1, 1978
Grand River
0
13
217
10
30
8
10
0
0
10
17
0
0
0
0
NGS
0
LAKE ERIE
Monitors
● Fixed
▲ Mobile
km
0
5
10

Figure 7.3f: Concentration isopleths for June 1, 1978 -- 1430-1500 EDT.

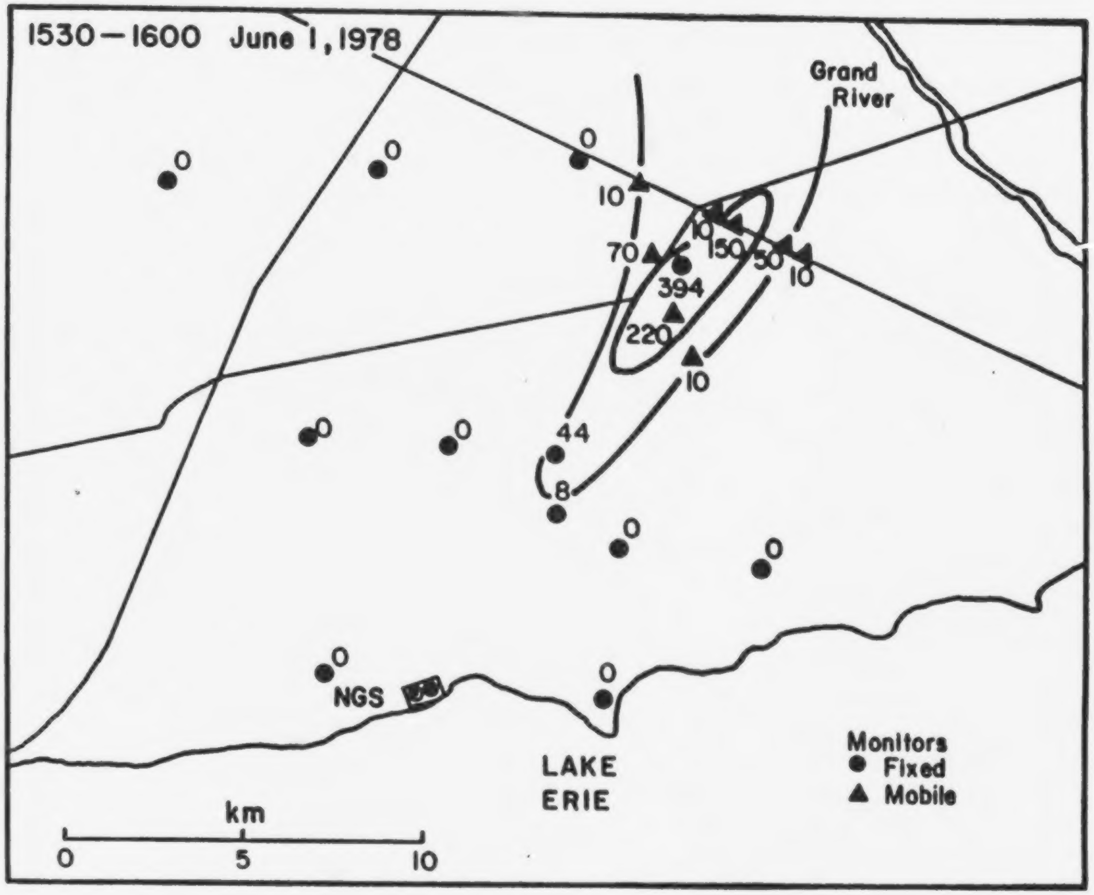

1530—1600 June 1, 1978
Grand River
0
0
0
10
10
70
150
50
10
394
220
10
44
8
0
0
0
0
0
0
NGS
LAKE ERIE
Monitors
● Fixed
▲ Mobile
km
0
5
10

Figure 7.3g: Concentration isopleths for June 1, 1978 -- 1530-1600 EDT.

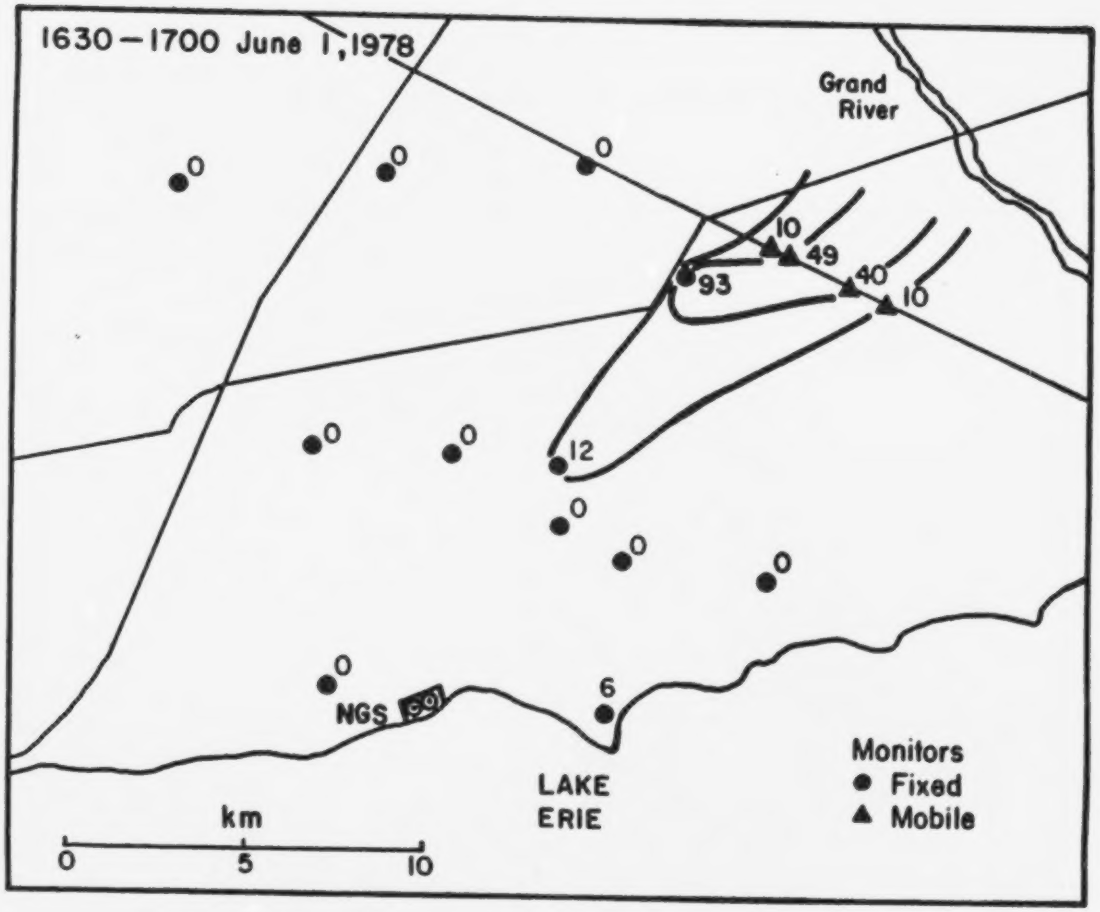
1630–1700 June 1, 1978
Grand River
0
0
0
10
49
40
10
93
0
0
12
0
0
0
0
NGS
99
6
LAKE ERIE
Monitors
● Fixed
▲ Mobile
km
0
5
10

Figure 7.3h: Concentration isopleths for June 1, 1978 -- 1630-1700 EDT.

Hoff et al. (1982). Stack emissions for the day were about 6000 g s^{-1} of SO_2 and the plant was generating an average of one-third its capacity (1300 MW).

The MSFM/downdraft model is shown (based on the summary statistics of Table 7.2) to best predict the downwind concentrations. Even though the index of agreement value of the MSFM/downdraft model is relatively close to that of the MSFM model and the slopes appear to be closely related, it is believed the other measures such as O vs P (MSFM overpredicts on average by almost 100 ppb) and RMSE suggest the superiority of the downdraft model under these conditions.

One should note that the overprediction of the concentration values by the MSFM model during the afternoon period may be because of the instantaneous mixing assumption not being valid when the TIBL is suppressed by higher wind speeds aloft and when the plume is becoming more spread-out in the X and Y directions (see, for example, the isopleths of Figure 7.3 e and f).

In addition, under higher wind speeds (and lower TIBL heights) the downdraft velocities will increase since the downdraft velocity (w_d) is proportionally related to $f_1(Z)$, which is a function of (Z/h). This implies that more fumigant will be brought down to the ground by downdrafts; however, this is mitigated by the fact that less fumigant is available at any time because of the shallow nature of

TABLE 7.2

QUANTITATIVE MEASURES OF COASTAL DISPERSION MODEL PERFORMANCE

MODEL PERFORMANCE FOR JUNE 1, 1978

Equations	Summary Measures				Linear Regression			Difference Measures			
	$\overline{O}$	$\overline{P}$	S_o	S_p	a	b	r	RMSE	$RMSE_u$	$RMSE_s$	d
CSFM	142	166	126	118	147	0.14	*0.12	158	115	110	0.48
MSFM	" "	221	" "	169	124	0.69	*0.26	168	89	143	0.67
Empirical Modif.	" "	59	" "	64	23	0.26	*0.25	135	124	54	0.59
Downdraft Modif.	" "	130	" "	156	37	0.66	*0.28	137	44	130	0.72

* See Table 7.1 for notes. Here $r_{crit} = 0.38$.

the TIBL.

Finally, the ground-level concentration isopleths (Figure 7.3 a-h) also indicate that the plume veered with the wind. This can be observed by eye and more closely observed by mentally placing a line from the power plant (NGS) through the pronounced kinks in the coastline side of the concentration isopleths and finally to the maximum concentration point (i.e., mentally duplicate the plume centerline). The fumigation zone rotated 50 degrees during the day. Lyons (1977) suggests two reasons for the veering of plumes in coastal environments. The first reason is that as the plume experiences vertical mixing due to convection, the vertical wind shear enhances spreading in the Y direction. Secondly, flow meander caused by low frequency eddies may cause variations in plume spread downwind.

Both base models totally ignore the effect of wind shear. This means that spatial determinations of model accuracy are limited to downwind location (in terms of distance) of the maximum concentration as opposed to downwind location of the maximum in terms of both distance and direction from the stack. Better future parameterizations of the wind sheer should aid in characterizing the veering of coastal plumes.

7.3 THE JUNE 6, 1978 CASE

The mesoscale meteorology associated with the June 6, 1978 case is similar to the June 1, 1978 case. The high pressure system which was over the NEMP area earlier in the week had by June 6th moved eastward, providing a general southwesterly gradient flow over the NEMP area during the morning hours. Winds aloft at 850 mb were west-southwesterly at 10 m s^{-1}.

The TIBL was observed to grow during the morning hours, collapse during the early afternoon and then grow again later in the day. Collapsing of the TIBL has been attributed (Kerman et al., 1982) to the turning of the boundary layer winds from the southwest during the morning hours to the south by noon, thus contributing to an increase in stability of the marine air during this time period. Heat flux data (Kerman et al, 1982) indicated a drop in the amount of heat flux around noon, with a short rise after 1300 EDT. Kerman et al. (1982) suggest that the strong heat flux persisted (although decreased) throughout the afternoon and contributed to TIBL regrowth.

Plume fumigation was observed as early as 1000 EDT although the first model runs were made based on 1200 EDT data due to a lack of some meteorological input parameters. The advent of boundary layer collapse is evident both from Figure 7.4 and from an examination of plume rise data. Lidar data indicated a negative plume rise around 1230 EDT and a suppressed and comparatively small plume rise by 1400 EDT. This is a result of the increased thermal

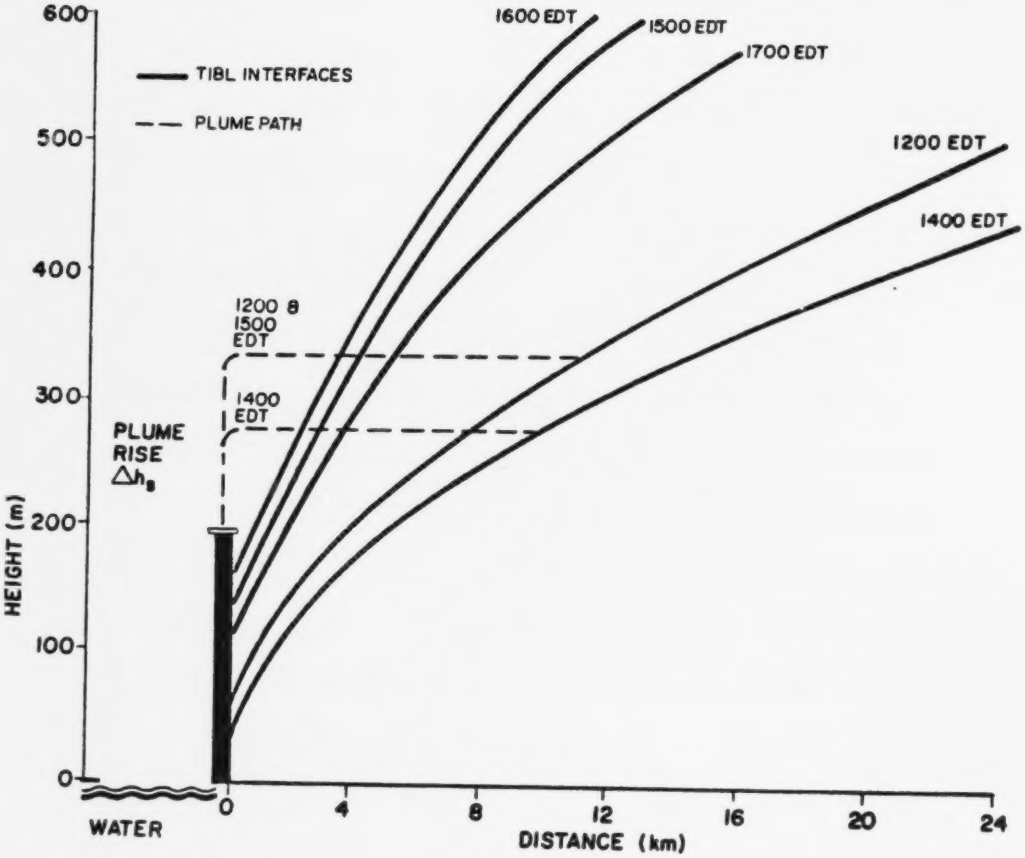

Figure 7.4: Plume-TIBL relationship for June 6, 1978.

stratification mentioned earlier.

Figure 7.5 a-h (Hoff et al., 1982) show the observed concentration isopleths for June 6, 1978. Figures 7.5 b and c show observed concentrations for the pre-TIBL collapse and TIBL collapse time periods, respectively. Modeling results during the pre-collapse period indicated that the MSFM model was able to predict concentrations quite well (see Figure 7.6 for the 1200 EDT model predictions). The CSFM model totally overpredicts the concentration values, particularly immediately after 1400 EDT. It is difficult to attribute the overprediction in the immediate post-TIBL collapse period to any one factor. In addition, the CSFM model predicted σ_y (estimated to be 285 m) cannot adequately represent the true σ_y of about 800 m.

Fumigation became very intense (Figure 7.5 g - h), with ground-level concentrations recorded as high as 782 ppb after TIBL regrowth. The MSFM model, while not able to match the exact intensity of the fumigation event, was able to reproduce both the propagation of the fumigation zone closer to the stack and the relative increase in ground-level concentration. The CSFM model was once again unable to handle the increase in concentration and the change in concentration location toward the stack. This is illustrated in Table 7.3, which summarizes the peak ground-level concentration locations for June 6th.

A complete summary of the overall statistics for

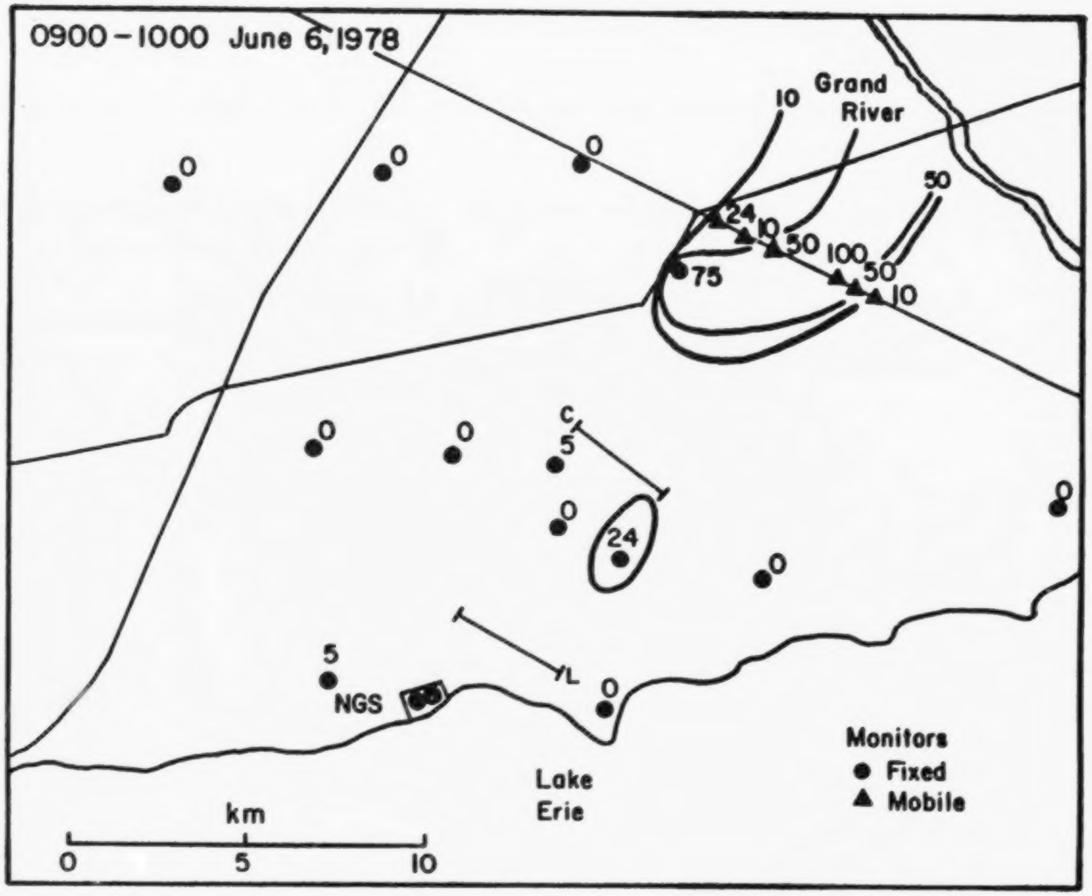
0900-1000 June 6, 1978
10
Grand
River
50
24
10
50
100
50
10
75
0
0
0
0
0
5
C
0
24
0
0
5
NGS
L
0
Lake
Erie
Monitors
● Fixed
▲ Mobile
km
0
5
10

Figure 7.5a: Concentration isopleths for June 6, 1978 -- 0900-1000 EDT.

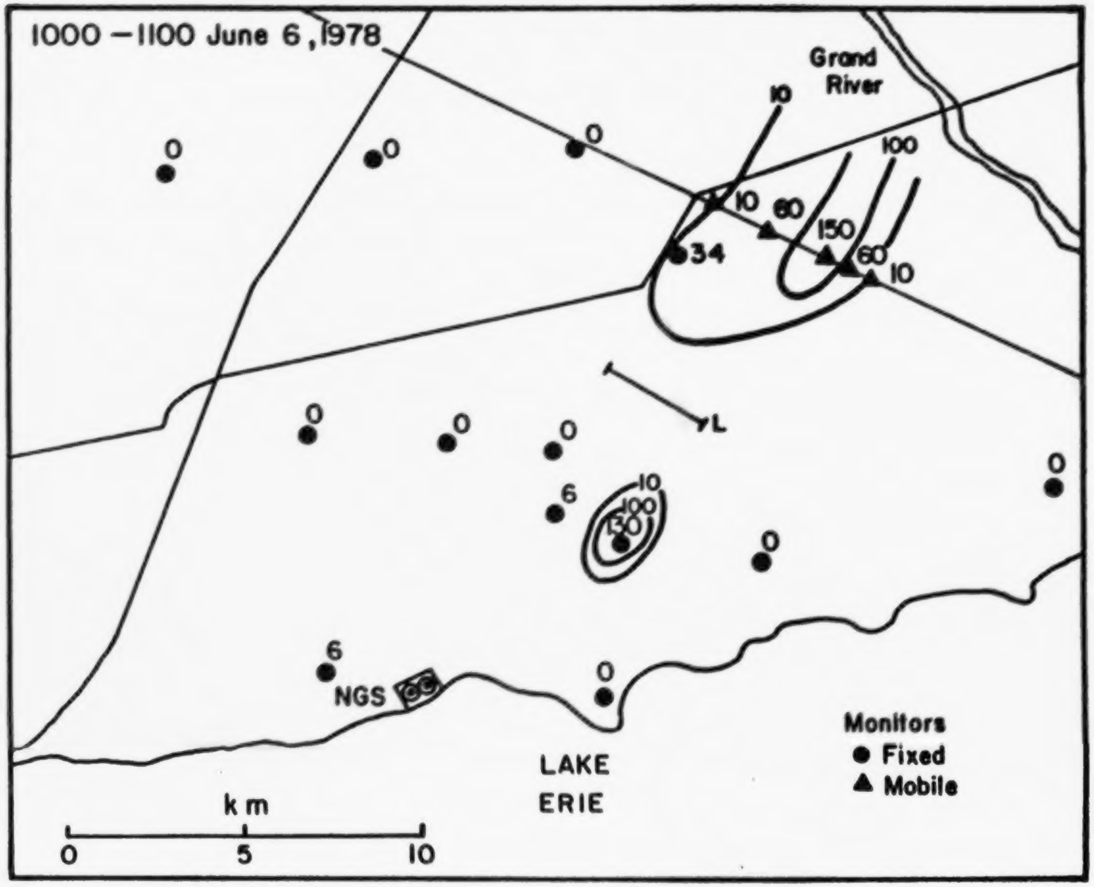
1000 –1100 June 6, 1978
Grand River
10
10
60
150
60
10
100
34
0
0
0
0
0
0
0
6
10
100
130
0
0
6
NGS
0
L
LAKE ERIE
Monitors
● Fixed
▲ Mobile
km
0
5
10

Figure 7.5b: Concentration isopleths for June 6, 1978 -- 1000-1100 EDT.

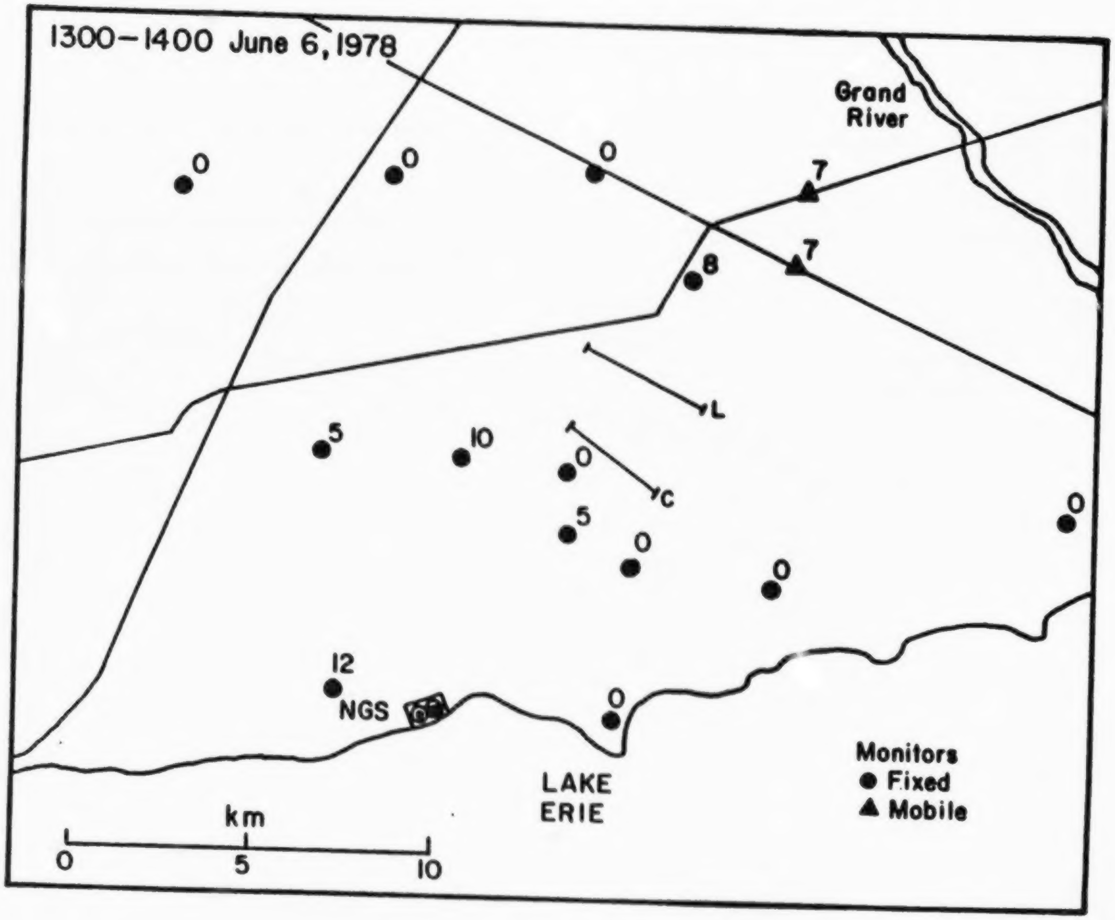
1300-1400 June 6, 1978
Grand River
0
0
0
7
7
8
L
5
10
0
C
5
0
0
0
12
NGS
0
LAKE ERIE
Monitors
● Fixed
▲ Mobile
km
0
5
10

Figure 7.5c: Concentration isopleths for June 6, 1978 -- 1300-1400 EDT.

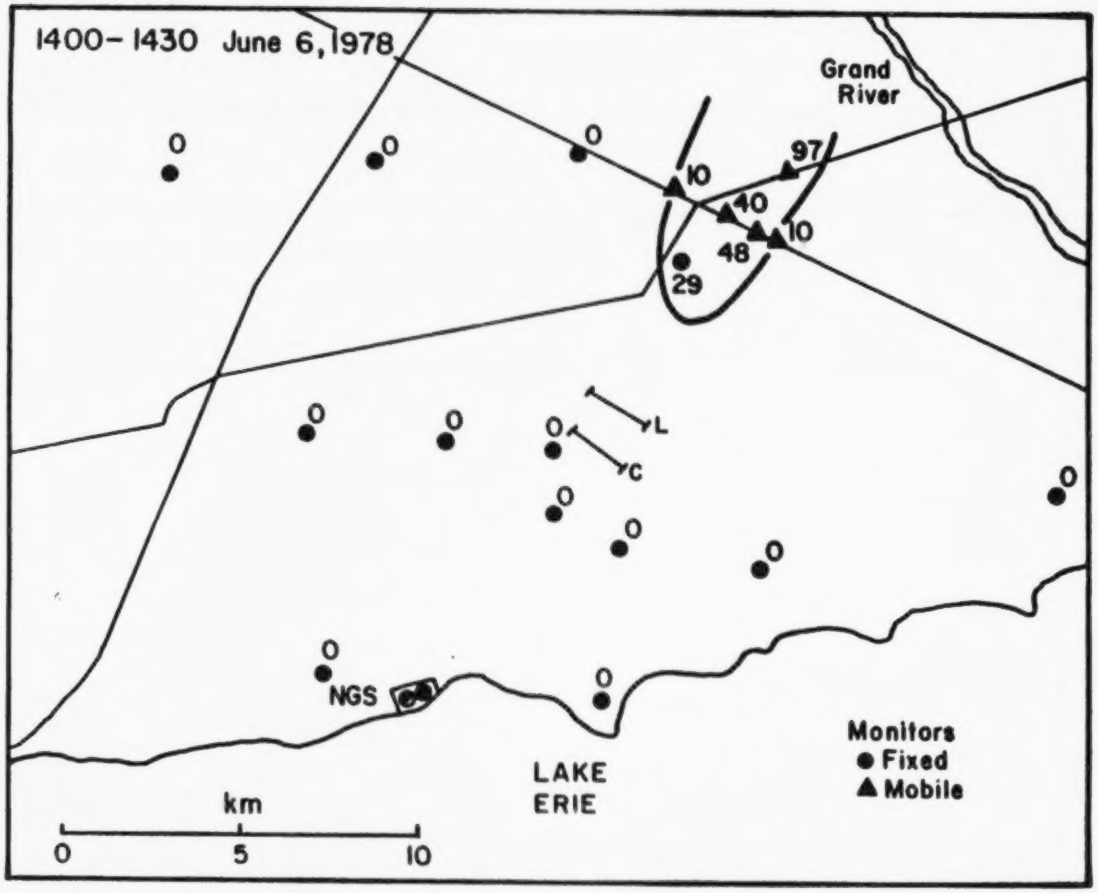
1400- 1430 June 6, 1978
Grand River
0
0
0
10
97
40
48
10
29
L
C
0
0
0
0
0
0
0
0
0
NGS
LAKE ERIE
Monitors
● Fixed
▲ Mobile
km
0
5
10

Figure 7.5d: Concentration isopleths for June 6, 1978 -- 1400-1430 EDT.

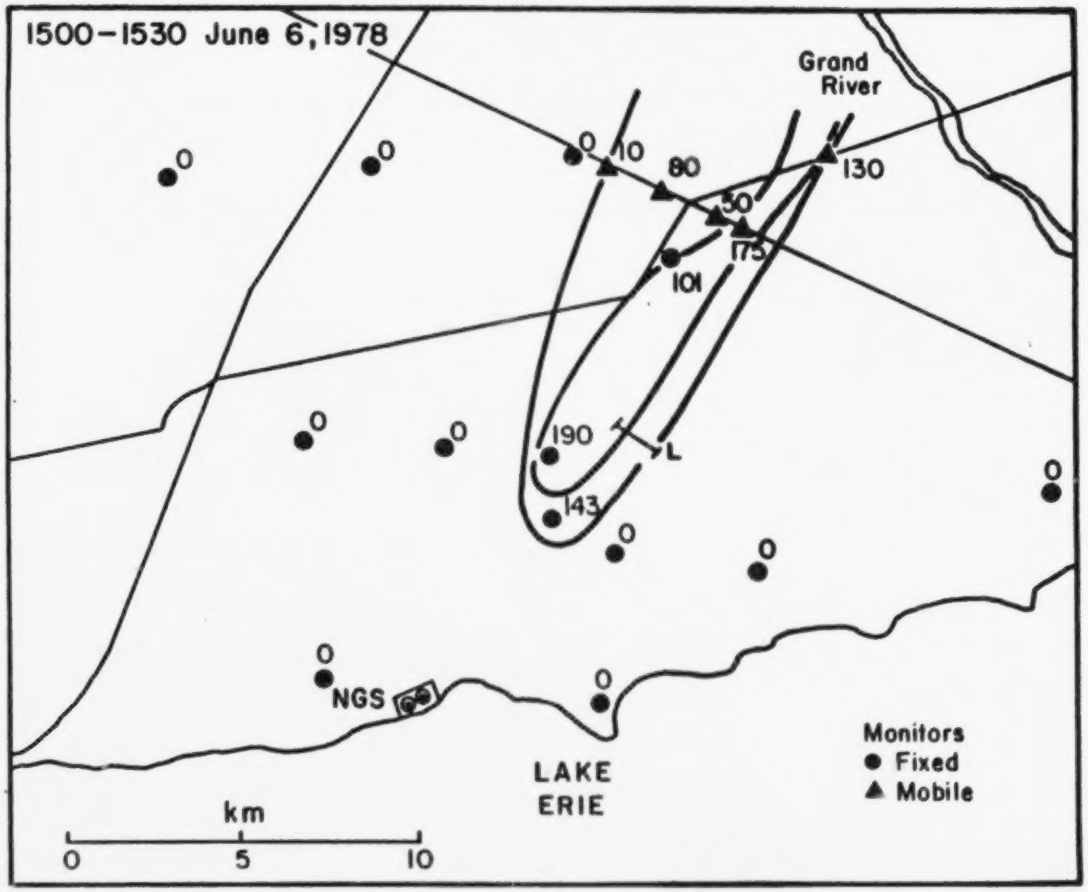
1500-1530 June 6, 1978
Grand River
0
0
0
10
80
30
130
101
175
0
0
190
L
143
0
0
0
0
NGS
0
LAKE ERIE
Monitors
● Fixed
▲ Mobile
km
0
5
10

Figure 7.5e: Concentration isopleths for June 6, 1978 -- 1500-1530 EDT.

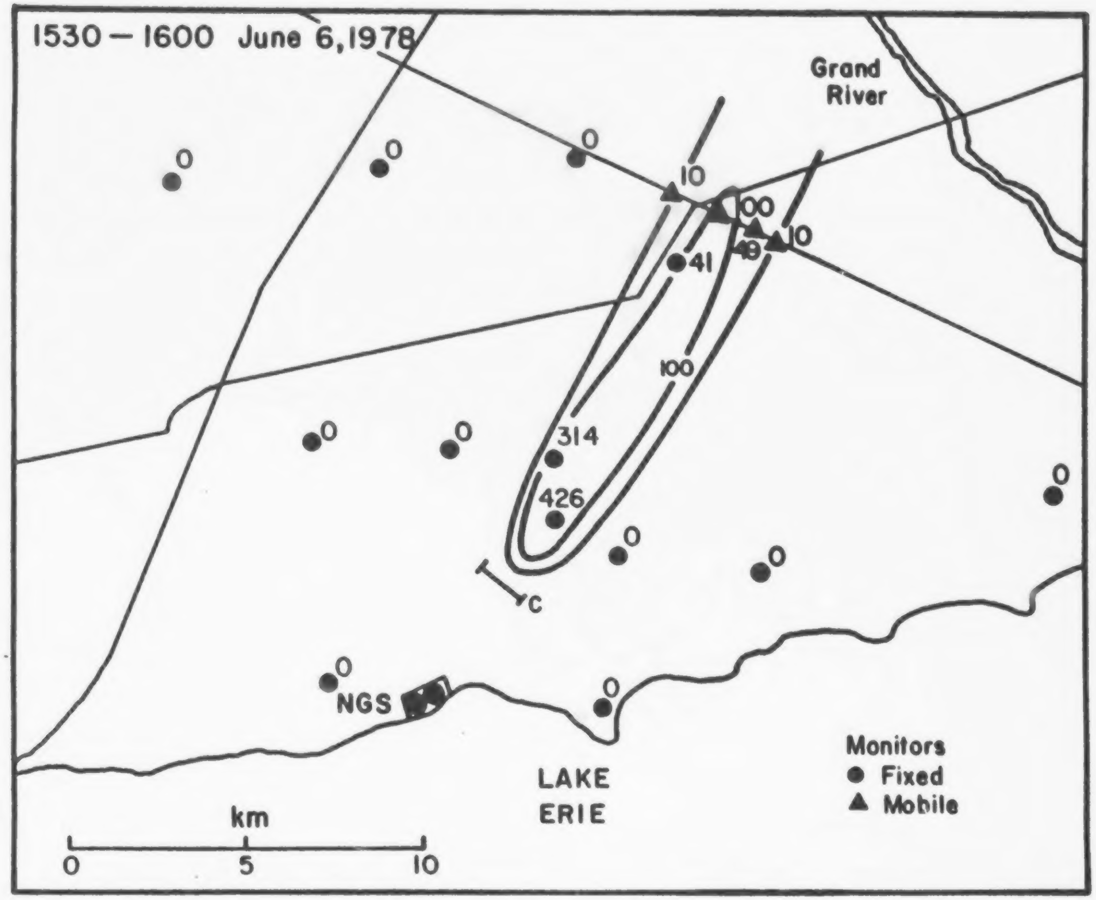
1530 — 1600 June 6,1978
Grand River
10
100
10
49
41
100
314
426
c
0
NGS
LAKE ERIE
Monitors
● Fixed
▲ Mobile
km
0
5
10

Figure 7.5f: Concentration isopleths for June 6, 1978 -- 1530-1600 EDT.

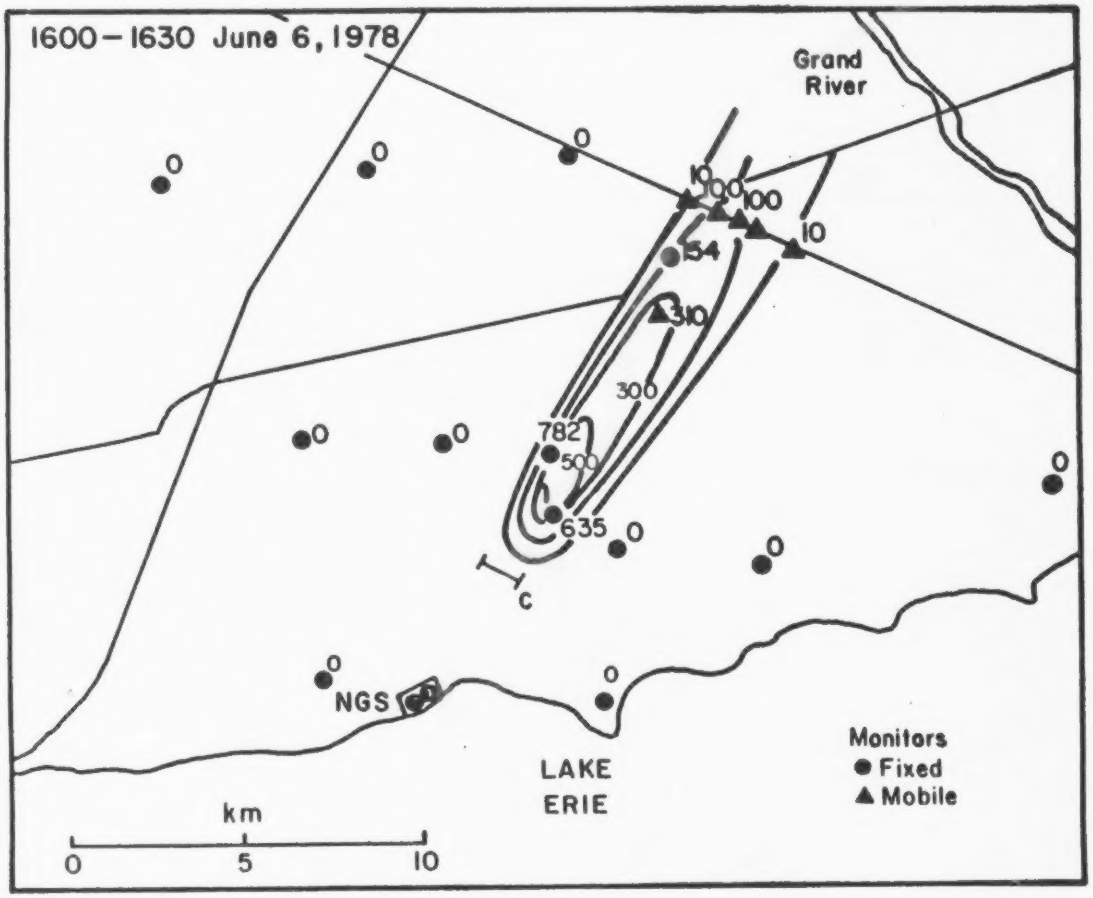
1600-1630 June 6, 1978
Grand River
10
100
100
10
154
310
300
782
500
635
c
0
NGS
LAKE ERIE
Monitors
● Fixed
▲ Mobile
km
0
5
10

Figure 7.5g: Concentration isopleths for June 6, 1978 -- 1600-1630 EDT.

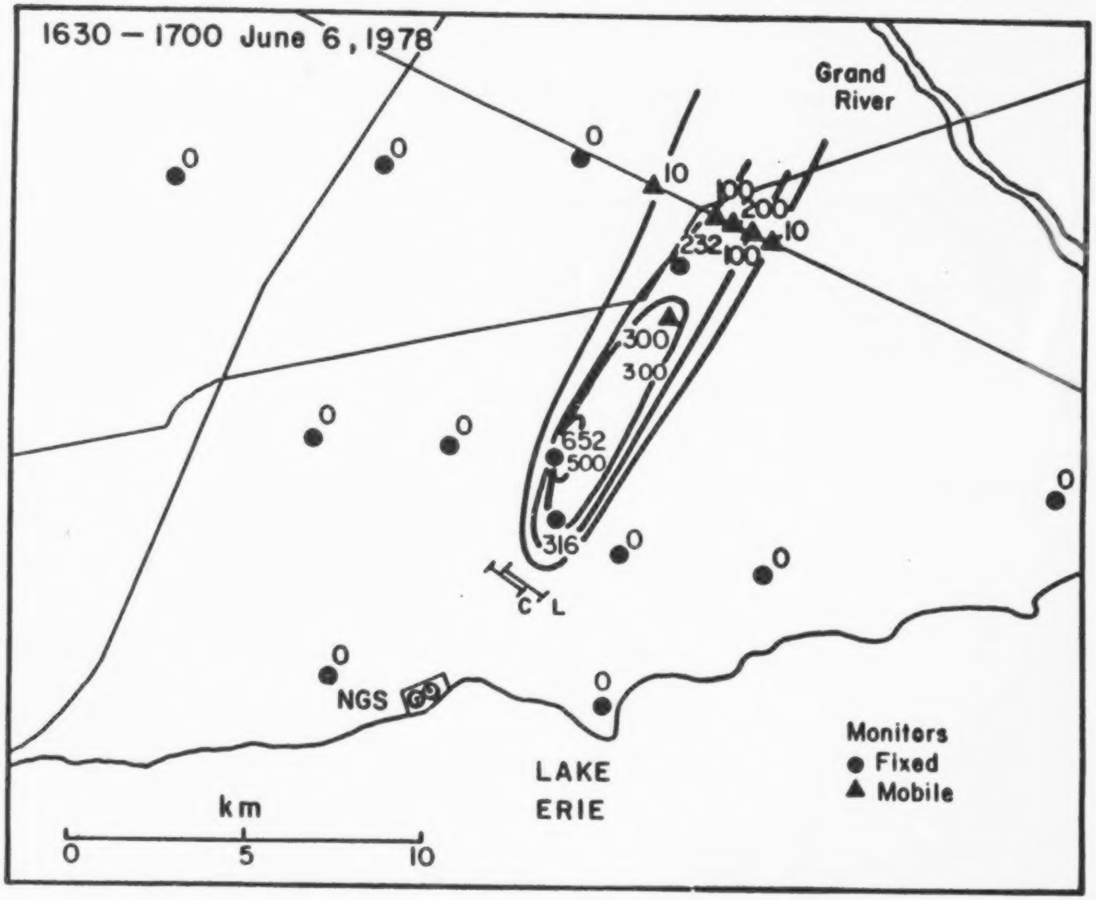
1630 — 1700 June 6, 1978
Grand River
0
0
0
0
10
100
200
10
232
100
300
300
0
0
652
500
316
0
0
0
C L
0
NGS
0
LAKE ERIE
Monitors
● Fixed
▲ Mobile
km
0
5
10

Figure 7.5h: Concentration isopleths for June 6, 1978 -- 1630-1700 EDT.

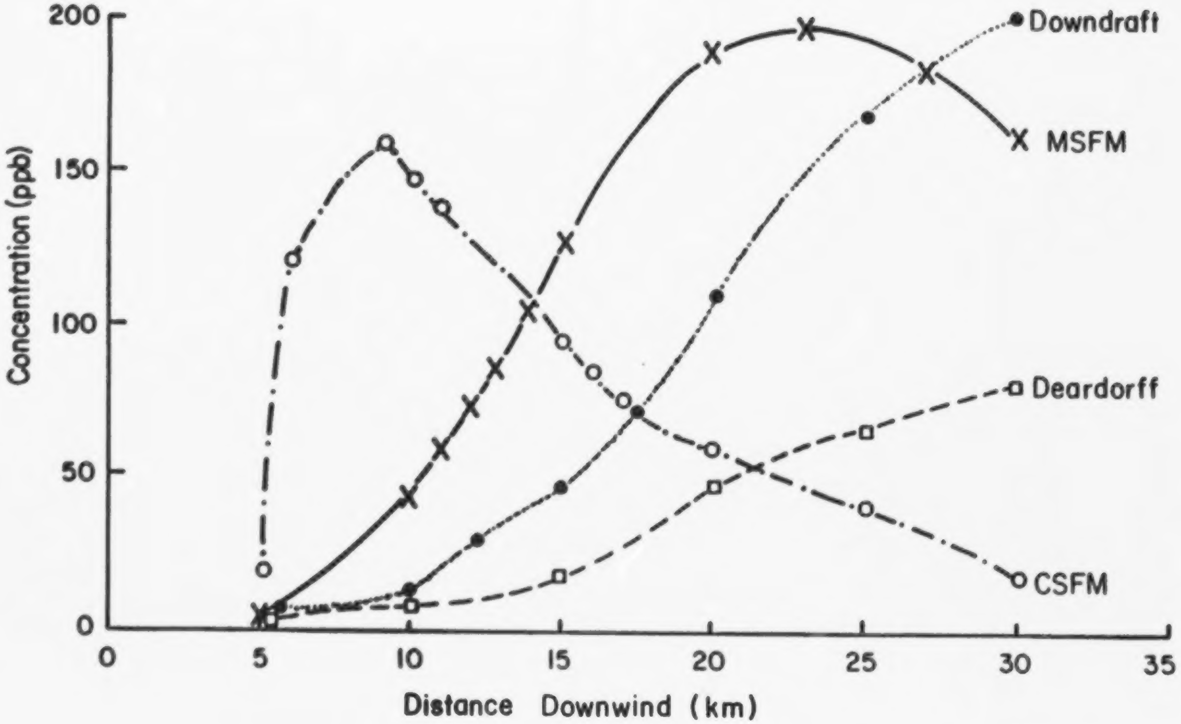

Figure 7.6: Model results for 1200 EDT June 6, 1978. Results show progressive movement of maximum concentration downwind with the MSFM variations.

TABLE 7.3

QUANTITATIVE MEASURES OF COASTAL DISPERSION MODEL PERFORMANCE

LOCATION OF MAXIMUM CONCENTRATION DOWNWIND (km)

TIME (EDT)	MSFM	CSFM	EMPIRICAL MODIF.	DOWNDRAFT MODIF.	OBSERVED
1200	25	8	30	30	17
1400	28	6	30	30	16
1500	11	7	20	30	7
1600	9	8	15	30	9
1700	13	12	25	29	10

June 6th appears in Table 7.4. From the table one can readily see that the MSFM model outperforms the other models in several key areas. The index of agreement value alone is almost two times the values for the other models, indicating that the MSFM model explains 80% of the error. Secondly, the total RMSE is lower than the other models total RMSE. Finally, the P and O values are very close together. Qualitatively, it would appear that the MSFM model is more suited to the "steady-state" (in terms of non-rotating fumigation zone) case than the MSFM/downdraft model.

7.4 THE JUNE 13, 1979 CASE (NEMP-II)

June 13, 1979 was characterized by a general west-southwesterly flow. There were a few cloudy periods which inhibited the growth of the TIBL. Fumigation began relatively late in the day (after 1500 EDT) because of the variable nature of the TIBL. The plume was found to be patchy and spread-out over the length of a traverse taken at 17.8 km downwind. Unfortunately, the NEMP-II study did not have the spatial resolution of the NEMP-I study, so detailed surface concentration isopleths cannot be presented. It was observed, however, that the plume was nonrotating and not greatly influenced by wind shear.

Figure 7.7 shows the plume rise related to the TIBL for 1700 EDT (judged to be the most complete meteorological hour). All four models show substantially less

TABLE 7.4

QUANTITATIVE MEASURES OF COASTAL DISPERSION MODEL PERFORMANCE

MODEL PERFORMANCE FOR JUNE 6, 1978

Equations	Summary Measures				Linear Regression			Difference Measures			
	$\overline{O}$	$\overline{P}$	S_o	S_p	a	b	r	RMSE	$RMSE_u$	$RMSE_s$	d
CSFM	197	124	197	64	106	0.10	*0.08	199	60	190	0.44
MSFM	" "	188	" "	152	84	0.53	0.47	142	92	108	0.80
Empirical Modif.	" "	37	" "	35	35	0.01	*0.15	252	249	35	0.42
Downdraft Modif.	" "	83	" "	109	87	-0.02	*0.10	252	228	107	0.40

* See Table 7.1 for notes. Here $r_{crit} = 0.43$.

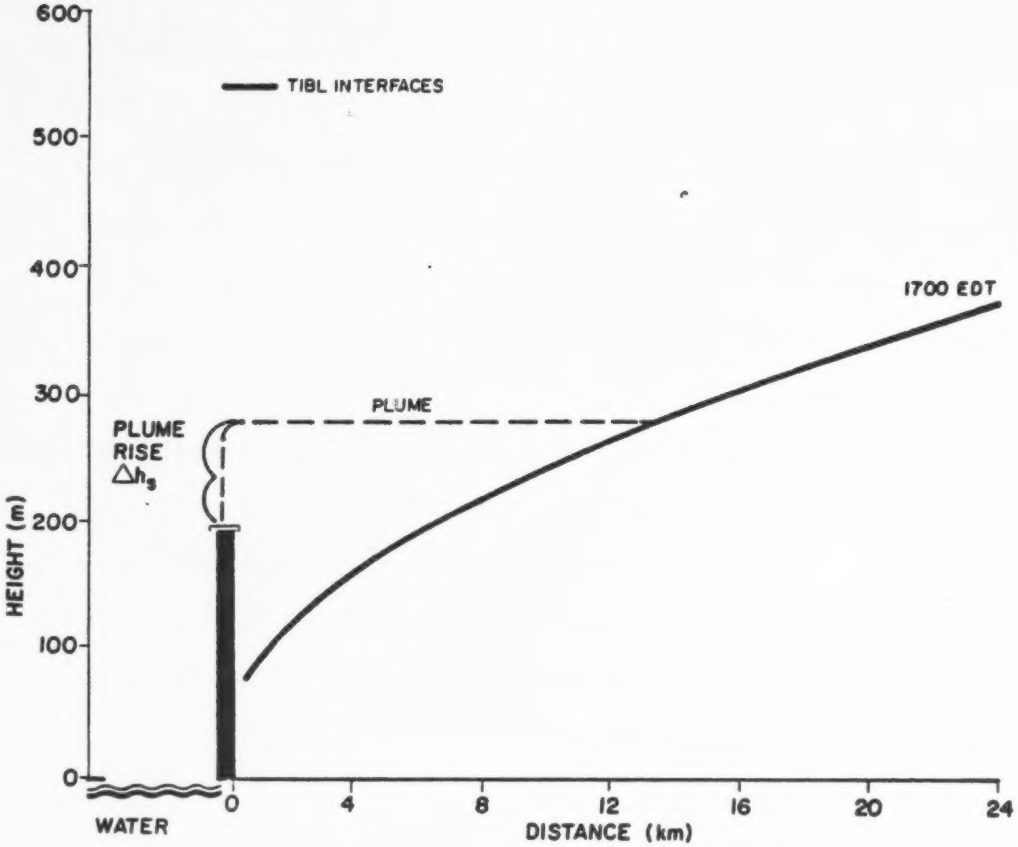

Figure 7.7: Plume-TIBL relationships for June 13, 1979.

concentration values than that observed under the NEMP-I study. The lesser concentration values may be attributed to meteorological differences, but may also be attributed to a considerable reduction in plant load during NEMP-II.

Table 7.5 indicates that the MSFM model is best able to represent the dispersion of the plume under these conditions, although it is not as able to reproduce the good results of NEMP-I. It is very curious to note that all four models have a high systematic error, which means that some variable within each model is causing an error. Sensitivity analysis (Section 7.6) may allow some insight into the important input variables. From Table 7.5 it is also observed that the $\overline{P}$ values fall generally a factor of two below the $\overline{O}$ values. This is particularly true of the MSFM/empirical modification case, where it is believed that the very slow entrainment process, with a comparatively shallow TIBL, diffuses the plume appreciably, thus creating small ground-level concentrations.

7.5 THE JUNE 14, 1979 CASE

June 14, 1979 was characterized by a south-southeasterly wind early in the day. Later, the winds shifted from south to southwest, which caused the plume to veer during the afternoon similar to the June 1, 1978 case. The hours of 1400 EDT and 1600 EDT were chosen since those hours provided the most comprehensive set of meteorological and plume measurements.

TABLE 7.5

QUANTITATIVE MEASURES OF COASTAL DISPERSION MODEL PERFORMANCE

MODEL PERFORMANCE FOR JUNE 13, 1978

Equations	Summary Measures				Linear Regression			Difference Measures			
	$\overline{O}$	$\overline{P}$	S_o	S_p	a	b	r	RMSE	$RMSE_u$	$RMSE_s$	d
CSFM	119	544	41	8	68	0.12	*0.35	77	6	76	0.36
MSFM	" "	61	" "	8	48	0.10	*0.30	67	6	67	0.46
Empirical Modif.	" "	21	" "	7	13	0.05	*0.08	105	6	105	0.35
Downdraft Modif.	" "	44	" "	22	30	0.12	*0.05	84	18	82	0.39

* See Table 7.1 for notes. Here $r_{crit} = 0.38$.

Figure 7.8 shows the plume rise related to the TIBL for this case. The point of plume-TIBL interception is around 4 km. The point of highest ground-level concentration cannot be determined because of the spatial limitations placed on NEMP-II, however, it is known that the fumigation zone extended at least 4 km based on SIGN-X and helicopter data.

Table 7.6 indicates that both the CSFM and MSFM/downdraft models perform the best based on index of agreement and RMSE values. The table shows that the CSFM model on average underpredicts and the MSFM model overpredicts the concentration values. It is seen again that most of the error associated with the models is systematic and therefore can only truly be described by a more comprehensive analysis than given here.

The MSFM model is unable to adequately reproduce the concentrations of this day. It appears (from model output) that the model senses the plume at 4 km and then brings the plume down much too fast.

7.6 SENSITIVITY ANALYSIS

The sensitivity analysis of the base models (MSFM and CSFM) examines the impact of the model input data on the calculated concentrations. The sensitivity analysis will allow identification of the most critical model variables. An evaluation of these critical model variables will aid in the collection of data (i.e., what type of data are

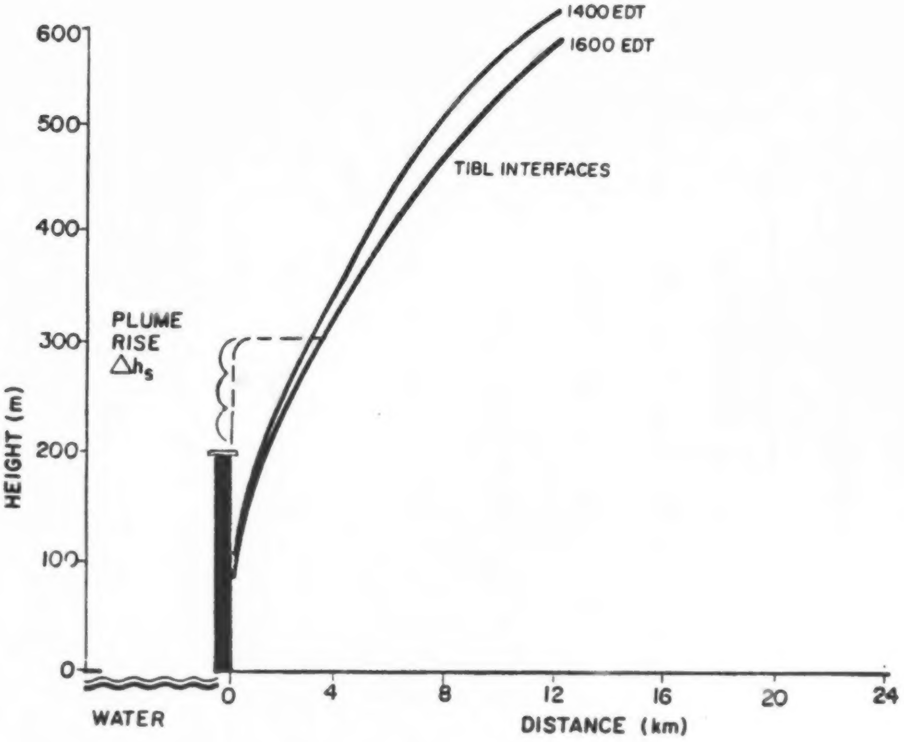

Figure 7.8: Plume-TIBL relationships for June 14, 1979.

TABLE 7.6

QUANTITATIVE MEASURES OF COASTAL DISPERSION MODEL PERFORMANCE

MODEL PERFORMANCE FOR JUNE 14, 1978

Equations	Summary Measures				Linear Regression			Difference Measures			
	$\overline{O}$	$\overline{P}$	S_o	S_p	a	b	r	RMSE	$RMSE_u$	$RMSE_s$	d
CSFM	129	51	57	10	58	-0.06	*0.15	92	6	92	0.39
MSFM	" "	99	" "	17	113	-0.11	*0.13	61	13	60	0.23
Empirical Modif.	" "	70	" "	7	74	-0.09	*0.04	76	6	75	0.41
Downdraft Modif.	" "	219	" "	18	234	-0.12	*0.14	105	14	104	0.39

* See Table 7.1 for notes. Here $r_{crit} = 0.45$.

needed for predicting concentrations), quality assurance procedures and model applicability in the future.

The sensitivity analysis consisted of variations in the magnitude of each input variable. June 1, 1978 (1300 EDT) was chosen as an arbitrary model hour. The variables considered for sensitivity analysis were:

(1) w_*/U: ratio of convective velocity to mean wind speed (allows for some representation of turbulence)

(2) A: as in $h = A X^{0.5}$ (TIBL height sensitivity)

(3) F_o: Buoyancy flux (allows for some representation of plume rise)

(4) N: Brunt-Vaisalla frequency (allows for plume characterization in stable air)

The sensitivity parameters to be studied for the CSFM model were chosen on the basis of what is unique to this version of CRSTER. Previous sensitivity studies such as Freas and Lee (1977) have shown CRSTER to be more sensitive to source parameters than to meteorological parameters. Thus, only the A factor in the TIBL formulation has been chosen for CSFM sensitivity analysis since this is really the only non-CRSTER input variable.

The parameter w_*/U has been used as a scaling variable by several authors (see, for example, Deardorff and Willis, 1978). An increase in the value implies increased heat flux (i.e., solar radiation) which also implies increased plume instability. This means that higher values of w_*/U create more of a crosswind dispersion, thus moving the maximum concentration spot closer to the stack and reducing ground-level concentrations. In the MSFM model w_*/U is used in the calculation of the TIBL crosswind dispersion coefficient (σ_{yh}).

The sensitivity analysis of w_*/U on normalized concentration, C/Q, appears in Figure 7.9. It appears from Figure 7.9 that the physical reasoning of the previous paragraph holds true. The smallest w_*/U factor (.1) corresponds to both the highest concentration value (C/Q) and the farthest downwind peak. This means that the plume is not as dispersed (resulting in higher ground-level concentrations) and is advected comparatively farther downwind. Consequently, higher values of w_*/U indicated lower concentrations. A gradual shift in the maximum concentration location toward the stack is also seen from Figure 7.9. This agrees with the physical reasoning of Lamb (1979) with regard to σ_{yh} parameterized by w_*/U. However, use of w_*/U as a dispersion type parameter requires good heat flux data input as suggested by Weil and Brower (1984).

The factor A takes into account all of the physics necessary for computation of the TIBL height. Thus the factor A directly represents the affect of the TIBL height variations on concentration. Figure 7.10 indicates the MSFM model sensitivity to varying TIBL heights. Higher values of A mean that the TIBL is steep and therefore high

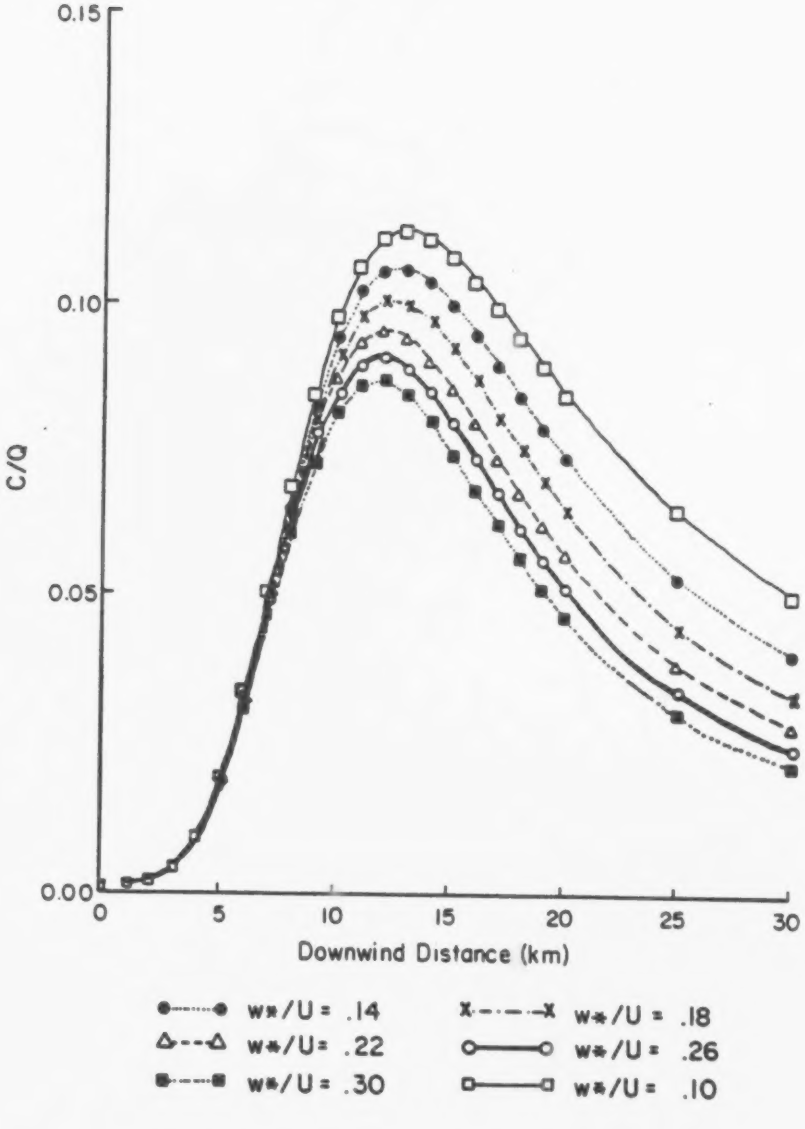

Figure 7.9: w_*/U sensitivity analysis with normalized concentration. Lower w_*/U values yield higher concentrations.

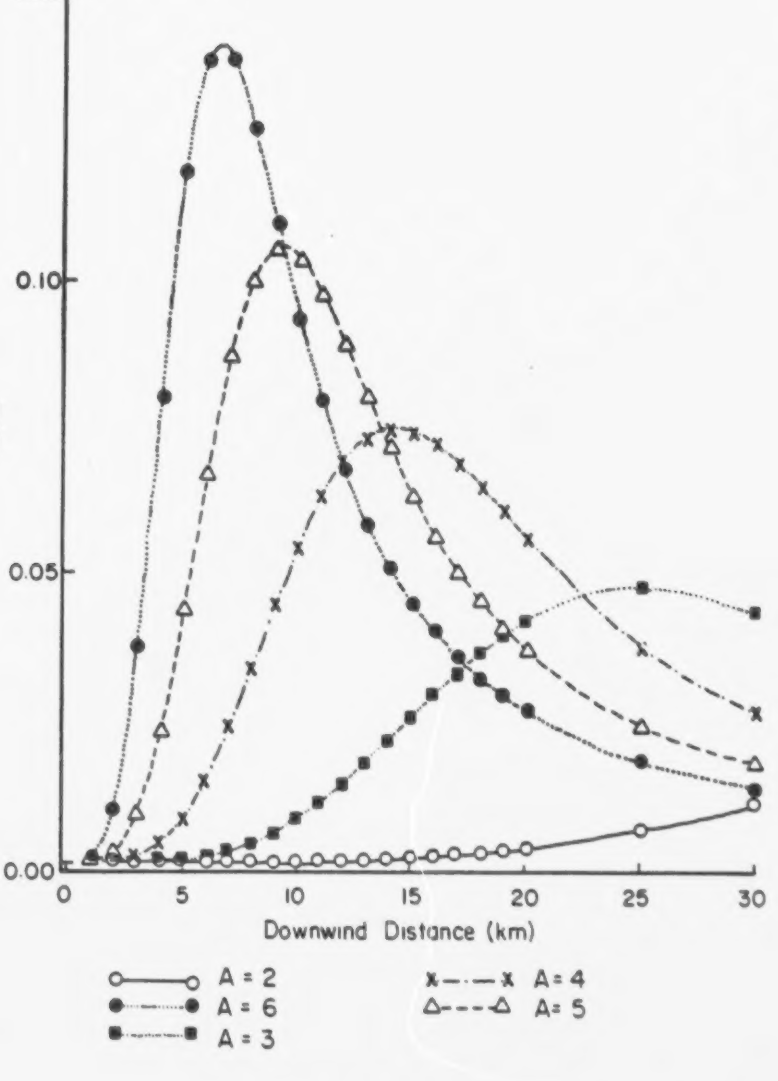

Figure 7.10: "A" sensitivity analysis with normalized concentration. Higher A values mean a steeper TIBL, thus higher and closer to shoreline concentration maximums.

concentrations of pollutant should result close to the source and in a short fumigation zone. This is shown in Figure 7.10 by the curve going up sharply to $C/Q = 0.14$. Lesser values of A are shown to push both the magnitude of the maximum concentration downward and the location further downwind. Very shallow TIBLs ($A = 2$) are shown by Figure 7.10 to cause peak concentrations at or beyond 30 km. This is particularly important in strong, thermally stratified onshore flow where the TIBL is suppressed and the plume will travel far downwind. This analysis supports the contention in Chapter 2 that TIBL height determination is critical in coastal dispersion modeling.

The use of F_o (plume buoyancy) allows one to implicitly draw conclusions about the behavior of the plume in the stable air since F_o is used in the calculation of σ_{ys} and σ_{zs}. Figure 7.11 shows the concentration distribution for various F_o values about a mean F_o value (585 m^4s^{-1}) determined from all NEMP-I and II study hours. Lower F_o and hence less σ_{ys} or σ_{zs} generated by internal plume turbulence would indicate higher ground-level concentrations since the plume would tend to be more spread-out (σ_{ys} and σ_{zs} would be less). The point of maximum concentration is also shifted farther downwind.

The final sensitivity test involves the Brunt-Vaisalla frequency (N), which is used to quantify the stability of the stable air. The Brunt-Vaisalla frequency can be

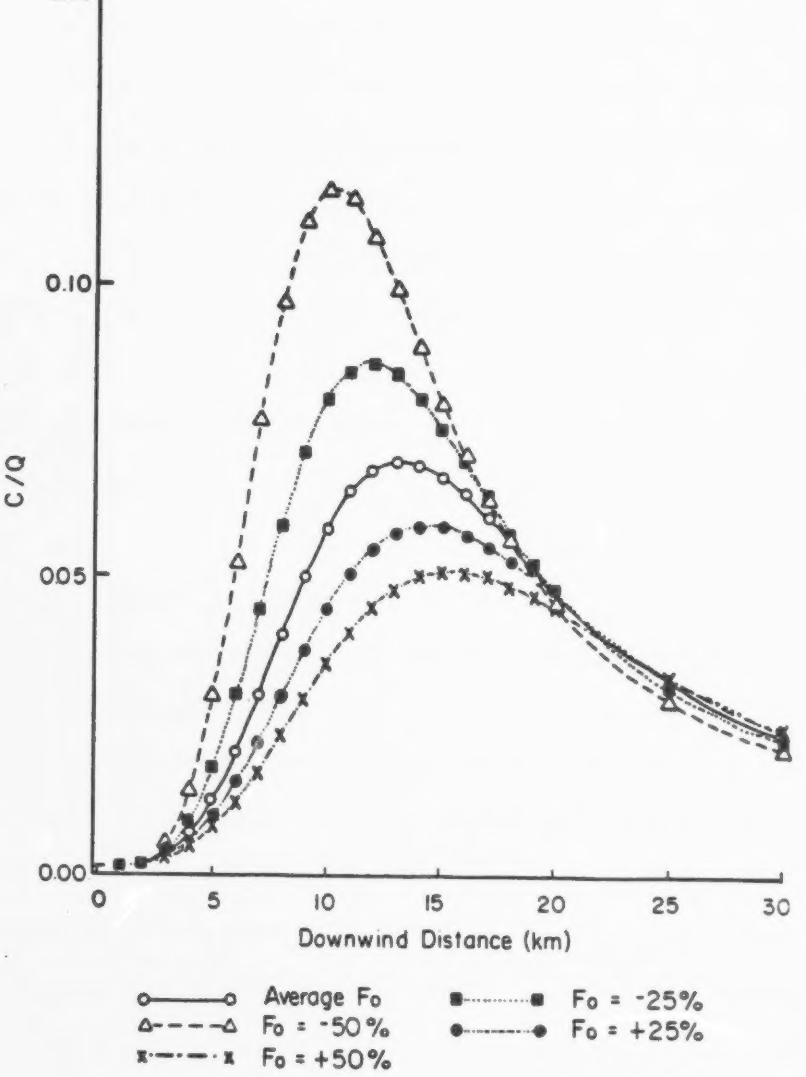

Figure 7.11: F_o sensitivity analysis with normalized concentration. Decreasing F_o increases concentration.

written as:

$$N = [(g/\theta)(d\theta/dZ)]^{0.5} \qquad (7.1)$$

The average Brunt-Vaisalla frequency for the NEMP-I and II experiments was determined to be 0.0195 s^{-1} by Kerman et al. (1982). The maximum N value was 0.0445 s^{-1}. Figure 7.12 illustrates the effect of varying N on the normalized concentration.

The higher N values (i.e., N = 0.0445 and N = 0.0293) result in higher concentrations of fumigant close to the source. The reason for the higher concentration values may stem from plume suppression because of increased marine air stability. This means the plume has even less of a chance to disperse in the stable air and thus becomes more concentrated upon TIBL impaction. Decreasing the value of N aids in the increased (albeit small) dispersion of the plume in the stable air, thus aiding in reducing the ground-level concentrations after plume impaction.

It is important to note that in the sensitivity analysis for N, the TIBL height is kept constant. In reality, however, changing the Brunt-Vaisalla frequency will alter the stability of the marine stable air and thus suppress or increase the TIBL height and affect concentrations. The sensitivity analysis indicates that the A variable used in the TIBL calculation is the most sensitive variable based on the magnitude of the change in concentration and the spatial displacement of the

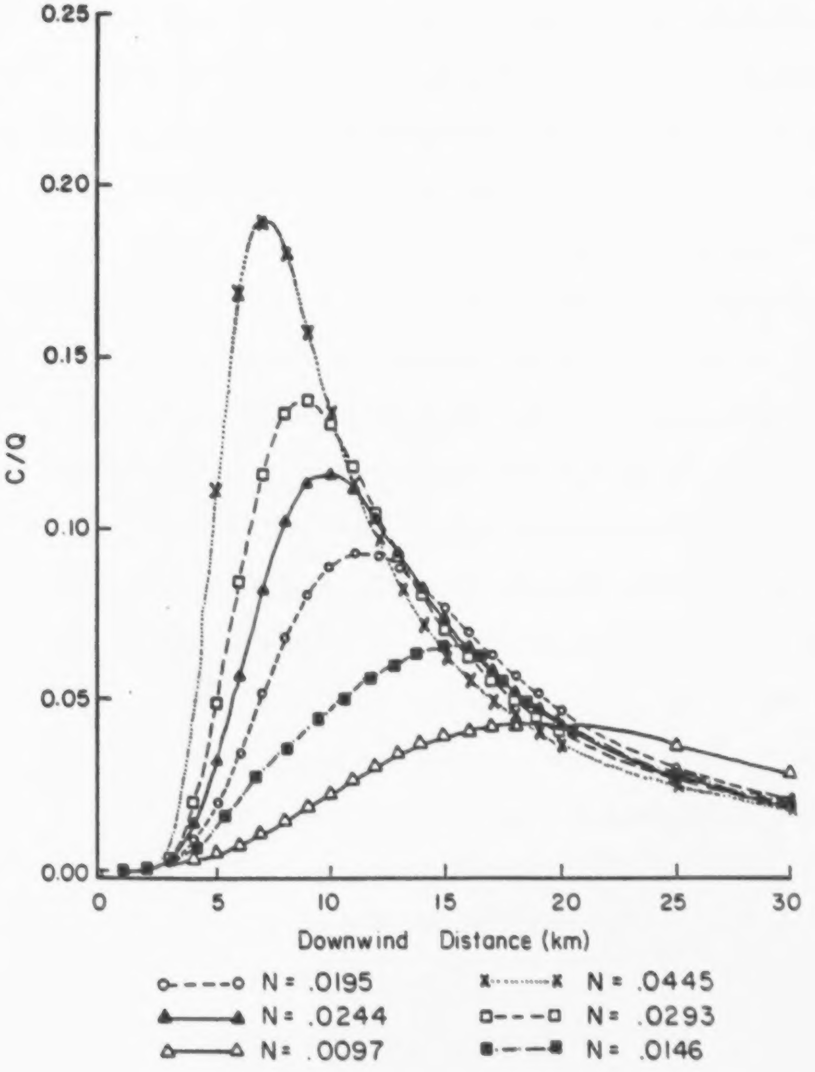

Figure 7.12: Brunt-Vaisalla (N) sensitivity analysis with normalized concentration. High N values imply more stable air above TIBL.

maximum concentration location.

8.0 CONCLUSIONS

In this study two coastal dispersion base models (CSFM and MSFM) and two variations of MSFM (empirical and downdraft) have been evaluated. The study was conducted using a comprehensive coastal dispersion data base. An independent evaluation was also undertaken to determine the best TIBL predictive equation. The conclusions of this study are listed below.

(1) The most significant factor affecting plume dispersion in coastal areas is the shape of the TIBL. A steep TIBL produces high concentrations close to the stack, while a shallower TIBL results in more diffusion farther away from the stack and consequently lesser ground-level concentrations.

(2) Several TIBL prediction models have been identified and evaluated with two independent data bases. From this evaluation it is concluded that the best predictive TIBL equation is the Weisman (1976) formulation. Strong consideration should be given to the use of an initial TIBL height term when using the Weisman (1976) equation with unstable or neutral marine air.

(3) Based on the analysis of dispersion data from the comprehensive NEMP studies it is concluded that the MSFM model of Misra (1980) is the better model for predicting ground-level concentrations from stack releases at the shoreline.

(4) The standard Pasquill-Gifford curves, even with Turner´s correction factor, do not seem appropriate to use in coastal areas. Convective velocity scaling appears to be a better method for characterizing dispersion in the TIBL. Weil and Brower (1984) also arrived at the same conclusion in their study of dispersion coefficients.

The standard air quality models do not include some of the necessary modules (i.e., TIBL, fumigation) required to handle the complexity of dispersion in coastal areas. These models should therefore be modified before being used to simulate shoreline meteorological conditions such as fumigation or trapping. Modifications to the models should be undertaken to incorporate a trapped plume algorithm as in the CSFM model. Caution should also be used in applying the MSFM model to inland coastal releases.

The effects of wind shear on plume dispersion particularly near the TIBL interface need to be determined. The literature survey undertaken for this study indicates that no statistical model takes into account shear. The affect of rotating winds with time because of sea breeze/mesoscale influences has also not been simulated by the models.

The plume data presented by Hoff et al. (1982) and used in the study along with the physically known non-steady state condition of the fumigation zone and variations in TIBL height suggests the need for a strong mobile monitoring component in any coastal dispersion study. Many times during the Nanticoke study mobile monitors were able to track the plume and record high concentrations, while nearby fixed monitors indicated low concentrations.

Finally, it is suggested that a comprehensive study such as the one recommended by the Brookhaven coastal workshop (SethuRaman, 1983) be undertaken to corroborate the results of this study. The coastal dispersion models should be re-run on the new data and cross-comparisons should be made between the two studies.

9.0 RECOMMENDATIONS

The present study using the Nanticoke data set suggests Misra´s model as the best for estimating downwind concentrations of material released from a tall stack at the coastline. Following are the parameters that need to be determined in order to use Misra´s model:

Stack Parameters

Plume buoyancy - F_o ($m^4 s^{-3}$)

Source strength - Q ($g\ s^{-1}$)

Stack height - H_s (m)

Overwater Parameters

Brunt-Vaisalla frequency - N

The Brunt-Vaisalla frequency is given by: $N = [(g/\theta)d\theta/dz]^{1/2}$, where θ is the mean potential temperature (K) in the surface-based inversion layer and $d\theta/dz$ is the mean temperature profile.

The mean temperature profile over water should be measured offshore ideally, but coastal measurements will be acceptable if the temperature difference represents unmodified air and the measurements are made close to the water.

Overland Parameters

Surface heat flux - H_o ($W\ m^{-2}$)

The value of downwind surface heat flux over land is required to estimate the TIBL height and convective velocity scale used in diffusion parameterization. This value is difficult to obtain. Eddy correlation using direct measurements of fluctuations of temperature and vertical velocity is probably the best method, but would require research-grade instrumentation. In the absence of such measurements, indirect methods using temperature gradients (Stunder and Sethu Raman, 1985) or approximations based on solar radiation (Lyons et al., 1983) can be employed, but the errors involved in such usage should be kept in mind while applying the results.

The temperature gradient method involves using values of mean temperatures measured at two different levels from a tower or vertical soundings and an estimation of eddy diffusivity for heat K_H, so that:

$$H_o = \rho c_p K_H \, d\theta/dz$$

where ρ is air density and c_p is the specific heat at constant pressure. One approximation for K_H is to assume it to be equal to the eddy diffusivity for momentum, K_M, which is equal to $u_* kz$ for neutral conditions in the surface layer. Here u_* is the friction velocity, k is von Karman's constant and z is the height above the surface. The friction velocity can be obtained from mean wind profiles in the atmospheric surface layer.

The method based on solar radiation is of the form:

$$H_o = \rho c_p \psi H_c \sin(\pi t_s/D_L)$$

where ψ is the solar insolation factor, H_c is 20% of the solar constant, t_s is the time since sunrise and D_L is the length of day.

Other parameters of interest are:

Mean wind speed at stack height in the stable layer - U_s (m s^{-1})

Mean wind speed in the TIBL - U_m (m s^{-1})
This can be obtained from tower measurements over land, provided the tower is about 100 m high.

Convective velocity scale - w_* (m s^{-1})
This is given by the equation:

$$w_* = (gH_o h/\rho c_p T_A)^{1/3}$$

where g is the acceleration due to gravity, h is the TIBL height and the other terms are as defined.

Average temperature in the TIBL - T_A (C)
This can be obtained from tower measurements or vertical soundings.

Mean values of the constants a_1, a_2 and a_3 may be obtained by experimentally determining values of F_o, U_s, σ_{zs} and σ_{ys} and then solving Equation 3.14:

$$\sigma_{zs} = a_1 (F_o/U_s)^{1/3} t^{2/3} \qquad t \leq 4.5/N$$

$$= a_2 \qquad t > 4.5/N$$

$$\sigma_{ys} = a_3 (F_o/U_s)^{1/3} t^{2/3}$$

where terms are as defined on page 3-17.

Based on Nanticoke data, values of a_1 and a_3 were observed to be 0.4 and 0.67, respectively (Misra, 1980a). With t equal to 4.5/N and a_1 equal to 0.4 (Misra, 1980a), through substitution a_2 may be determined from Equation 3.14 as:

$$a_2 = 1.1(F_o/U_sN^2)^{1/3}$$

Coefficient c, used in the equation for plume rise (refer to the Evaluation Function routine in the MSFM program), may be obtained by experimentally determining values of Δh_s, F_o, U_s and x and then solving the equation:

$$\Delta h_s = c(F_o/U_s)^{1/3}(x/U_s)^{2/3}$$

where Δh_s is plume rise, F_o is plume buoyancy, U_s is the mean wind speed at stack height in the stable layer and x is the downwind distance (Misra and Onlock, 1982). Values of this coefficient were observed to be 1.3 (1978 Nanticoke data) and 0.9 (1979 Nanticoke data). Misra and Onlock (1982) note that these values are quite lower than the recommended value of 1.6 (Briggs, 1975). The discrepancy is considered a result of the higher value (~ 0.8) of entrainment constant obtained for the Nanticoke plume.

10.0 REFERENCES

Anthes, R.A., 1978: The height of the PBL and the production of circulation in a sea breeze model. J. Atmos. Sci., 35, 1231-1239

Ball, R.K., 1960: Control of inversion height by surface heating. Quart. J. Roy. Meteor. Soc., 86, 483-494

Betts, A.K., 1973: Non-precipitating cumulus convection and its parameterization. Quart. J. Roy. Meteor. Soc., 99, 170-196

Bierly, E.W. and E.W. Hewson, 1962: Some restrictive meteorological conditions to be considered in the design of stacks. J. Appl. Meteor., 1, 383-390

Briggs, G.A., 1975: Plume rise predictions. Lectures on Air Pollution and Environmental Impact Analysis. Lecture series, American Meteorological Society, Boston, MA

_____, 1985: Personal Communication.

Caughey, S.J., 1982: Observed characteristics of the atmospheric boundary layer. In: Atmospheric Turbulence and Air Pollution Modeling, F.M. Nieuwstadt and H. Van Dop, pp 107-158

Cole, H. and H. Fowler, 1982: Draft user's manual for the shoreline CRSTER models. United States Environmental Protection Agency, June

_____, and W. Lyons, 1972: The impact of the Great Lakes on the air quality of urban shoreline areas - some practical application with regard to air pollution control policy and environmental decision making. Proceedings: Fifteenth Conference on Great Lakes Research, International Association of Great Lakes Research, Ann Arbor, MI pp 436-463

Cramer, H.E., 1957: A practical method for estimating the dispersion of atmospheric containments. Proceedings: First National Conference on Applied Meteorology, C 33-35, American Meteorological Society, Hartford, CN October

Deardorff, J.W. 1972: Numerical investigations of neutral and unstable boundary layers. J. Atmos. Sci., 29, 91-99

_____ and G.E. Willis, 1983: Response to ground-level concentration due to fumigation into an entraining mixed layer. Atmos. Environ., 17, 1030-1032

_____ and G.E. Willis, 1982: Ground-level concentration due to fumigation into an entraining mixed layer. Atmos. Environ., 16, 1159-1170

_____ and G.E. Willis, 1975: A parameterization of diffusion into the mixed layer. J. Appl. Meteor., 14, 1451-1458

Dooley, J.C., 1976: Fumigation from power plants in the lakeshore environment. U. of Wisconsin-Milwaukee, Air Pollution Analysis Laboratory, Report Number 18, 119 pp

Ellis, H.P., P. Lui, C. Bittle, R. Deland, W. Lyons and K. Parker, 1979: Development and validation of a new prediction model for treating Gaussian dispersion, aerodynamic downwash and fumigation due to lakeshore meteorology. Preprints: Fourth Symposium on Turbulence and Diffusion, American Meteorological Society, Reno NV. 15-18 June pp 576-583

Evelyn, J., 1661: Fumifuguim: The inconvenience of the aer and smoake of London, dissipated. (old English) His Majesty's Command, London England, 41 pp

Fox, D.G., 1981: Judging air quality model performance. A summary of the AMS workshop on dispersion model performance. Bull. Am. Meteor. Soc., 62, 599-609

Freas, W.P. and R.F. Lee, 1977: Sensitivity analysis of the single source (CRSTER) model. EPA-450/2-77-013, E1-E23

Fritts, T.W., F.J. Starheim and B.J. Deihl, 1980: A formulation for defining the development of the TIBL in sea breeze flows. Preprints: Second Conference on Coastal Meteorology, American Meteorological Society, Los Angles, CA 147-150

Gamo, M.S., 1981: A study on the structure of the free convective internal boundary layer during the sea breeze. Report of the National Research Institute for Pollution and Resources (Japan) #19, 89 pp

_____, S. Yamamoto, O. Yokoyama and H. Yashikado, 1983: Structure of the free convective internal boundary layer above the coastal area. J. Meteor. Soc. Japan, 61, 110-124

_____, 1982: Airborne measurements of the free convective internal boundary layer during the sea breeze. J. Meteor. Soc. Japan, 60, 1284-1298

Hanna, S.R., 1983: A simplified scoring system for air quality models. Paper 8336.6. Annual Air Pollution Control Assoc. Meeting, Atlanta, GA June

Hewson, E.W., G.L. Gill and G.J. Walke, 1963: Smoke photography study, Big Rock nuclear power plant, Charlevax, MI. Publication #0415-3P, Department of Oceanography and Meteorology, U of Michigan

_____, 1944: Meteorological investigations in the Columbia River Valley near Trial, BC. Report submitted to the Trail Smelter Arbitral Tribunal, U. S. Bureau of Mines Bulletin #453

Hoff, R.M., N.A. Trivett, M.M. Millan, P. Fellin, K.G. Anlauf, H.A. Wiebe and R. Bell, 1982: The Nanticoke shoreline diffusion experiment, June 1978-III. Ground-based air quality measurements. Atmos. Environ, 16, 439-454

_____ and F.A. Froude, 1979: Lidar observations of plume dispersion in Northern Alberta. Atmos. Environ., 13, 35-43

Holzworth, 1978: Estimated effective chimney heights based on rawinsonde observations at selected sites in the United States. J. Appl. Meteor., 17, 153-160

Johnson, W., 1972: Validation of air quality simulation models. Proceedings, Third Meeting of the Expert Panel on Air Pollution Modeling - Chapter 6, Paris, France, NATO Committee on the Challenges to Modern Society, Publication #14, Brussels, Beligum

Kerman, B.R., 1983: Response to ground-level concentrations due to fumigation into an entraining mixed layer. Atmos. Environ, 17, 1030-1032

_____, 1982: A similarity model of shoreline fumigation. Atmos. Environ., 16, 467-477

_____, R.E. Mickle, R.V. Portelli and N.B. Trivett, 1982: The Nanticoke shoreline diffusion experiment, June 1978-II Internal Boundary Layer Structure. Atmos. Environ., 16, 423-437

Lamb, R.K., 1982: Diffusion in the CBL. In: Atmospheric Turbulence and Air Pollution Modeling by F. Nieuwstadt and H. van Dop, Reidel Company, pp 159-206

_____, 1978: A numerical simulation of dispersion from an elevated point source in the convective PBL. Atmos. Environ., 12, 1297-1304

Lenschow, D.H, 1970: Airplane measurements of planetary boundary layer structure. J. Appl. Meteor., 9, 874-889

_____ and P.L. Stevens, 1980: The role of thermals in the convective boundary layer. Bound. Layer Meteor., 19, 509-532

Lindsey, C. and J. Ramsdell, 1983: Fumigation potential at inland and coastal power plant sites. NUREG/CR-3352 (PNL-4760) United States Nuclear Regulatory Commission, Washington, D. C.

Lui, 1977: A literature review of boundary layer models. Report #79573K Ontario Hydro, Inc., 26 pp

Lyons, W.A., 1977: Mesoscale air pollution transport in southeastern Wisconsin. EPA 600/4-77-010. U. S. Environmental Protection Agency

_____, 1975: Turbulent Diffusion and Pollutant Transport in Shoreline Environments. Lectures on Air Pollution and Environmental Impact Analysis, American Meteorological Society, Boston, MA 136-208

_____, C.S. Keen and J.A. Schuh, 1983: Modeling mesoscale diffusion and transport processes for releases within coastal zones during land/sea breezes. United States Nuclear Regulatory Commission. NUREG/CR - 3542

_____, K. Dooley, L. Keen, J. Schuh and K. Rizzo, 1974: Detailed field measurements and numerical models of SO_2 from power plants in the Lake Michigan shoreline environment. APAL, U. of Wisconsin-Milwaukee, 218 pp

_____, and H.S. Cole, 1973: Fumigation and plume trapping on the shores of Lake Michigan during stable onshore flow. J. Appl. Meteor., 12, 494-510

MacRae, B.L., R.J. Kaleel and D.L. Shearer, 1983: Dispersion coefficients for coastal regions. United States Nuclear Regulatory Commission, NUREG/CR 3149, 45 pp

Maul, P.R., F.R. Barber and A. Martin, 1980: Some observations of the meso-scale transport of sulphur compounds in rural east midlands. Atmos. Environ., 14, 339-354

Misra, P.K., 1982: Dispersion of non-buoyant particles inside a convective boundary layer. Atmos. Environ., 16, 239-243

_____, 1980a: Dispersion from tall stacks into a shoreline environment. Atmos. Environ., 14, 396-400

_____, 1980b: Verification of a shoreline dispersion model for continuous fumigation. Bound. Layer Meteor., 19, 501-507

_____ and R. Onlock, 1982: Modeling continuous fumigation of the Nanticoke generating station plume. Atmos. Environ., 16, 479-489

_____ and P. McMillian, 1980: On the dispersion parameters of plumes from tall stacks in a shoreline environment. Bound. Layer Meteor., 19, 175-185

Moore, G.E., T.E. Stoeckenius and D.A. Stewart, 1982: A survey of statistical measures of model performance and accuracy for several air quality models. EPA-450/4-83-001

Munn, R.E., 1959: The application of air pollution climatology to town planning. Inter. J. Air Poll., 1, 276-278

Ontario Ministry of the Environment, 1979: The Nanticoke May/June 1979 field study: Dispersion and oxidation of SO_2 in the generating station plume and ambient non-methane hydrocarbon concentrations in the Nanticoke area. ARB-TDA Report Number 61-80 August, 314 pp

Pasquill, F. and F.B. Smith, 1983: Atmospheric Diffusion, Third Edition. Ellis Howard Limited, England 437 pp

Peters, L.K., 1975: On the criteria for the occurrence of fumigation inland from a large lake. Atmos. Environ., 9, 809-816

Plate, E.J., 1971: Aerodynamic characteristics of atmospheric boundary layers. United States Atomic Energy Commission, 190 pp

Portelli, R.B., 1982: The Nanticoke shoreline diffusion experiment, June, 1978 - I Experimental design and program overview. Atmos. Environ., 16, 413-421

Prophet, D.T., 1961: Survey of the available information pertaining to transport and diffusion of airborne material over ocean and shoreline complexes. Tech. Report Number 89, Aerosol Laboratory Stanford U., CA

Raynor, G.S., S. SethuRaman and R.M. Brown, 1979: Formation and characteristics of coastal internal boundary layers during onshore flows. Bound. Layer Meteor., 16, 487-514

_____, P. Michael, R.M. Brown and S. SethuRaman, 1975: Studies of atmospheric diffusion from a nearshore oceanic site. J. Appl. Meteor., 14, 1080-1094

Record, F.A, R.N. Swanson, H.E. Cramer, R.K Dumbauld, 1970: Analysis of lower atmospheric data for diffusion studies. GCA Corporation Report Number TR-69-15N, 126 pp

Readings, C.J., E. Galton and K.A. Browmin, 1973: Fine scale structure and mixing within an inversion. Bound. Layer Meteor., 4, 275-287

SethuRaman, S., 1982a: Observations of the boundary-layer wind structure near the land-sea interface. Preprints: First International Conference on Meteorology and Air-Sea Interaction of the Coastal Zone, May 10-14, 1982 The Hague, Netherlands.

_____, 1982b: Proceedings of the Workshop on Coastal Atmospheric Transport Processes. Brookhaven National Laboratory, Upton, NY July 13 - 15, 43 pp

_____, G.S. Raynor and R.M. Brown, 1982: Variation of turbulence in a coastal thermal internal boundary layer. Preprints: Third Joint Conference on the Applications of Air Pollution Meteorology, American Meteorological Society, Boston, MA

_____, A.J. Riordan, T. Holt, M. Stunder, J. Hinman, 1986: Observations of the marine boundary layer thermal structure over the Gulf Stream during a cold air outbreak. J. Clim. and Appl. Meteor., 25, 14-21

Turner, D.B., 1970: Workbook of Atmospheric Dispersion Estimates (revised). United States Environmental Protection Agency, Number 999-AP-26, Research Triangle Park, NC 55 pp

Urbanik, T., P. Cummings and A. Desrosiers, 1981: An analysis of evacuation time estimates around 52 nuclear plant sites. United States Nuclear Regulatory Commission, NUREG/CR - 1856, PNL - 3662 Vol 2 133 pp

United States Environmental Protection Agency, 1981: Interim procedures for evaluating air quality models. Office of Air Quality Planning and Standards, Durham, NC 45 pp

United States Nuclear Regulatory Commission, 1983: Atmospheric dispersion models for potential accident consequence assessment at nuclear power plants. Regulatory Guide 1.145, Washington, DC 24 pp

Van der Hoven, I., 1967: Atmospheric transport and diffusion at coastal sites. Nuc. Safety, 8, 490-499

Van Dop, H., R. Steenkist and F.T.M. Nieuwstadt, 1979: Revised estimates for continuous shoreline fumigation. J. Appl. Meteor. 18, 133-137

Venkatram, A., 1977: A model of internal boundary layer development. Bound. Layer Meteor., 11, 419-437

Venkatram, A. and R. Vet, 1981: Modeling of dispersion from tall stacks. Atmos. Environ., 15, 1531-1538

Weil, 1979: Assessment of plume rise and dispersion models using lidar data, PPSP-MP 24, Environmental Center Martin Marietta Corporation for Maryland, Dept. Natural Resources

_____ and Brower, 1984: An updated Gaussian plume model. J. Air Poll. Control Assoc., 34, 818-827

_____ and Jepson, 1977: Evaluation of the Gaussian plume model at Dickerson Power Plant. Atmos. Environ., 11, 901-911

Weisman, B., 1976: On the criteria for the occurrence of fumigation inland from a large lake -- A reply. Atmos. Environ., 12, 172-173

Willmott, C., 1984: On the evaluation of model performance. Physical Geograpny In Spatial Statistics And Models. G. Gaile and C. Willmott, Editors, Reidel Publishing Company, New York, New York 443-460

_____, 1982a: Some comments on the evaluation of model performance. Bull. Amer. Meteor. Soc., 63, 1309-1313

_____, 1982b: On the climatic optimization of the tilt and azumith of flat plate solar collectors. Solar Energy, 28, 205-216

_____, 1981: On the validation of models. Phys. Geog., 2, 184-194

_____ and D. E. Wicks, 1980: An empirical method for the spatial interpolation of monthly precipitation within California. Phys. Geog., 1, 59-73

Zilitinkevich, R., 1975: Comments on the paper by H. Tennekes. J. Atmos. Sci., 32, 991-992

11.0 APPENDIX

Listed below is the computer code for running the Misra Shoreline Fumigation Model on the UNIVAC computer system.

```
C**********************************************************
C MISRA SHORELINE FUMIGATION MODEL WITH THE TWO VARIATIONS:
C      1. DOWNDRAFT
C      2. EMPIRICAL (DEARDORFF)
C MODIFIED FOR EPA/SRAB IN FINAL FORM - FEBRUARY, 1987
C
C THE PROGRAM CONSISTS OF FOUR PARTS:
C    1. MAIN PROGRAM
C    2. SUBROUTINE CALPK
C    3. FUNCTION EVAL (USED BY CALPK)
C    4. SUBROUTINE SIMP (USED BY CALPK FOR SIMPSON´S RULE
C       CALCULATION)
C
C**********************************************************
C
C********************** MAIN PROGRAM **********************
C  THE FOLLOWING CODE IS THE MAIN PROGRAM WHICH BASICALLY
C  ALLOWS FOR INPUT OF THE DATA FILES (BOTH INTERACTIVE AND
C  FROM INPUT FILES) AND OUTPUT OF THE CONCENTRATION DATA.
C  NOTE:  THE DATA INPUT FILES SHOULD BE INPUT USING
C  @ STATEMENTS.  ALSO, REMEMBER THAT ONE INPUT DATA FILE
C  IS USED FOR MET INFO, WHILE THE OTHER INPUT DATA FILE IS
C  USED FOR RECEPTOR ORIENTATION.  CHANGE DATA FILE INPUT
C  CAREFULLY ------ WATCH THE FORMAT/NAMELIST COMMANDS.
C**********************************************************
C
C  DEFINE VARIABLES:
C
C   A     =  TIBL A factor, given by:
C            ((2*HO)/(RHO*CSUBP*DTHDZ*U))**0.5
C     RHO    =  atmospheric density
C     CSUBP  =  specific heat at constant pressure
C   B     =  w*/U
C   BPARM =  plume buoyancy -- Fo in Misra (1980) (m4s-3)
C   CA    =  coefficient "c" in the equation:
C            DELTAh = c (Fo/U)**1/3(X/U)**2/3
C            (see Misra and Onlock, 1982).
C     DELTAh  =  plume rise
C   DTHDZ =  potential temperature gradient overwater (S)
C   Fo    =  plume buoyancy
C   HO    =  heat flux
C   HSTK  =  stack height
C   N     =  Brunt-Vaisalla frequency
C   NR    =  number of receptors
```

```
C   Q     =  source strength
C   T     =  ambient temperature over land
C   UM    =  mean wind speed in the TIBL
C   US    =  wind speed at stack height in the stable layer
C   X     =  downwind distance
C***********************************************************
      DIMENSION COMENT(20,6),
      TITLE(20),XPP(200),CANS(200),YPP(200)
      COMMON/ONE/ XP,YP,A,B,UM,US,H,HSTK,CN,BPARM,CA
C     SET UP NAMELIST SPECIAL FORTRAN INPUT COMMAND
      NAMELIST /METIN/ A,B,UM,US,BPARM,Q,T,DTHDZ,NR,HSTK
      DATA BLKSS /´    ´/
      DATA JA /´YES´/
      WRITE (6,100)
100   FORMAT ( ´1 MISRA SHORELINE DISPERSION MODEL USING´,
     #´ SIGMA Z GROWTH METHOD...´//´ ORIGINALLY MODIFIED´,
     #´ BY MARK STUNDER - NORTH CAROLINA STATE UNIVERSITY´,
     #´ FOR SRAB -- 10/84´//)
C
C   DETERMINE WHAT VERSION OF THE MODEL WILL BE USED
C
      WRITE (6,90)
90    FORMAT(´1 WHICH VERSION OF THE MODEL WOULD YOU´,
     #´LIKE ?´)
      WRITE (6,91)
91    FORMAT (´ ENTER: 1=BASE 2=DEARDORFF 3=DOWNDRAFT ´)
      READ (5,92) IC
92    FORMAT(I1)
      WRITE(6,110)
110   FORMAT (´ ENTER DESCRIPTIVE TITLE USING UP TO 80´,
     #´CHARACTERS´)
      READ (5,120) (TITLE(I),I=1,20)
120   FORMAT (20A4)
121   CONTINUE
      WRITE(6,130)
130   FORMAT (´ ENTER UP TO 20 COMMENTS.  END COMMENTS´,
     #´WITH A BLANK LINE.´)
      I=0
135   I=I+1
      READ(5,140)(COMENT(J,I),J=1,20)
140   FORMAT(20A4)
      IF (COMENT(1,I) .NE. BLKSS .AND. I .LT. 20) GOTO 135
      NC=I-1
145   CONTINUE
      WRITE(6,150)
150   FORMAT(//´ ENTER METEOROLOGY AND SOURCE VARIABLES: ´)
      WRITE (6,160)
160   FORMAT (´ EXAMPLE: ´/´&METIN A=5.69,B=0.99,CA=1.0´,
     #´UM=7.0,US=7.5,BPARM=614.,Q=5340.,T=300.´,
     #´DTHDZ=-1.31,NR=28,HSTK=198. ´)
```

```
C     READ IN NAMELIST (METIN) DATA
      WRITE(6,165)
165   FORMAT(' NOTE:  YOU CAN USE @ADD FILE.ELEMENT HERE ')
      READ(5,METIN)
C   INPUT SPECIAL METEOROLOGICAL VARIABLES
      WRITE (6,236)
236   FORMAT('1 WHAT IS YOUR VALUE OF N ? ')
      READ (5,237)CNNN
237   FORMAT(1X,F6.4)
      CN=CNNN
      WRITE(6,240) CN
240   FORMAT(/' THE S TO THE 1/2 PARAMETER IS:  ' ,F6.4)
C     CALCULATE DTHETA DZ FROM N VALUE
      DTHDZ=(CN*CN*T)/9.8
C
C      INPUT HEAT FLUX
C
161   WRITE (6,158)
158   FORMAT ('1 WHAT IS THE OVERLAND HO IN W/M2 ? ')
      READ (5,159) HO
159   FORMAT (F4.0)
C
C     DETERMINE A
      A=((2.*HO)/(1004.*1.275*DTHDZ*UM))**0.5
C
169     DO 170 J=1,NC
171   FORMAT(1X,20A4)
170   WRITE(6,171)(COMENT(II,J),II=1,20)
      WRITE(6,175)
175   FORMAT(//)
C
      WRITE(6,180) A
180   FORMAT(/' THE TIBL A FACTOR IS:',F7.2)
C
      WRITE(6,190) B
190   FORMAT(/' B=W*/UM =',F4.2)
C
      WRITE (6,195) UM
195   FORMAT (/' THE MEAN WIND SPEED IN THE TIBL IS:',F5.1)
C
      WRITE (6,197) US
197   FORMAT (/' THE WIND SPEED AT STACK HEIGHT IS:',F5.1)
C
      WRITE(6,200)  BPARM
200   FORMAT(/' THE BUOYANCY PARAMETER IS:',F5.0)
C
      WRITE(6,210) Q
210   FORMAT(/' THE EMISSION RATE IS:',F6.0)
C
      WRITE(6,211) HSTK
211   FORMAT(/' THE STACK HEIGHT IS:',F6.0)
```

```
      WRITE(6,220) T
220   FORMAT(/´ THE AMBIENT TEMPERATURE OVER LAND IS´,
     #´ 1X,F5.1,1X,´DEG. K´)
C
      WRITE(6,230) DTHDZ
230   FORMAT(/´ THE OVERWATER LAPSE RATE IS:´,F5.3)
C
      WRITE (6,231) HO
231   FORMAT(´1 THE HEAT FLUX IS´, 1X,F4.0,1X,´W/M2 ´)
C
C     READ IN RECEPTOR LOCATIONS (USER INPUTTED)
244   WRITE(6,250)
250   FORMAT(1X,´ ENTER RECEPTOR LOCATIONS IN X AND Y´,
     #´ COORDINATES ´)
C
      WRITE(6,260)NR
260   FORMAT(´1 YOU MUST INPUT´,1X,I2,1X,´RECEPTOR PAIRS´)
      WRITE (6,265) NR
265   FORMAT (1X,´INPUT 999 AFTER´,1X,I2,1X,´PAIRS, BUT´,
     #´ MAYNOT BE NES´)
      WRITE(6,270)
270   FORMAT(10X,´ X LOCATION´,10X,´ Y LOCATION´)
      DO 280 I=1,NR
      READ(5,281) XPP(I),YPP(I)
281   FORMAT(2X,F6.0,15X,F6.0)
      F=BPARM
       IF (XPP(I) .EQ. 999 .OR. YPP(I) .EQ. 999) GOTO 330
       XP=XPP(I)
       YP=YPP(I)
C
C                 CALL TO CALPK SUBROUTINE
C   ** BRINGS BACK THE CONCENTRATION VALUES FOR PRINTING **
C
      CALL CALPK(ANS,IFLAG,ERROR,IC)
       CANS(I)=ANS
C      THIS CONVERTS ANSWER TO PPB
      CANS(I)=CANS(I)*Q/(2.6049*1.E-06)
280   CONTINUE
C        PRINT OUT CONCENTRATION VALUES
330   WRITE(6,300)
300   FORMAT(´1 RECEPTOR LOCATIONS AND CONCENTRATIONS IN´,
     #´ PPB ´)
      WRITE(6,310)
310   FORMAT(// 2X,´ X LOCATION´,10X,´ Y LOCATION´,10X´,
     #´ CONCENTRATION´)
      DO 315 I=1,NR
       WRITE(6,320) XPP(I),YPP(I),CANS(I)
320    FORMAT(2X,F6.0,15X,F6.0,16X,F8.3)
315        CONTINUE
C      280 CONTINUE
```

```
      WRITE(6,350)
350   FORMAT(´ DO YOU WANT ANOTHER HOUR?´)
      READ (5,360) IRESP
360   FORMAT (A4)
      IF (IRESP .NE. JA)GOTO 335
      WRITE (6,370)
370   FORMAT(´ WILL THE STACK PARAMETERS BE DIFFERENT?´)
      READ (5,360) JSTK
      JSREAD=0
      IF (JSTK .EQ. JA) JSREAD=1
       GOTO 121
335   WRITE (6,340)
340   FORMAT (´ END OF MODEL RUN´)
      STOP
C   DEBUG UNIT(6),INIT,SUBCHK,SUBTRACE
      END
```

```
CCCCCCCCCCCCCCCCCCCCCCCCCCCCCCCCCCCCCCCCCCCCCCCCCCCCCCCCCCC
C      SUBROUTINE CALPK
C
C      DEFINE VARIABLES:
C
C      A    = A IN H=AX**0.5   (TIBL height "A" factor)
C      ACC  = Desired accuracy of answer
C      BL   = Boundary layer height
C      EVAL = Name of function whose integral is desired
C      H    = Plume height
C      PI   = Constant 3.1415927
C      UM   = Mean wind speed in the TIBL
C      US   = Wind speed at stack height in the stable layer
C      XP   = Distance from source along wind
C      YP   = Distance from source cross wind
C
CCCCCCCCCCCCCCCCCCCCCCCCCCCCCCCCCCCCCCCCCCCCCCCCCCCCCCCCCCC
SUBROUTINE CALPK(ANS,IFLAG,ERROR,IC)
      EXTERNAL EVAL
      COMMON/ONE/XP,YP,A,B,UM,US,H,CN,BPARM,CA,HSTK
      REAL LB
C    THIS LITTLE SECTION INSURES AGAINST ERRORS WITH SMALL
C    NUMBERS
      ACC=10.0E-6
      PI=3.1415927
      IF(XP.GT.0.001)GOTO 1000
      AREA=0.0
      ERROR=0.0
      ANS=0.0
      IFLAG=0.0
      GOTO 100
1000  LB=10.00
      ANS1=0.0
C     NEED TO DETERMINE TRAVEL TIME IN STABLE AIR
C     THIS IS FROM MISRA (1980a) (4.5/N)*US
      XP1=(4.50/CN)*US
C
C     GET TIBL HEIGHT
C
      BL=A*SQRT(XP)
      IF(XP.GE.XP1)GOTO 12
      CALL SIMP(EVAL,LB,XP,ACC,ANS,ERROR,AREA,IFLAG,IC)
C    USE CALL TO SIMP IN VARIOUS WAYS DEPENDING ON WHERE
C    PLUME HITS TIBL DOWNWIND
      GOTO 10
12     CALL SIMP(EVAL,LB,XP1,ACC,ANS,ERROR,AREA,IFLAG,IC)
      CALL SIMP(EVAL,XP1,XP,ACC,ANS1,ERROR,AREA,IFLAG,IC)
10    ANS=ANS+ANS1
100   RETURN
C      DEBUG UNIT (6),SUBCHK,INIT,SUBTRACE
      END
```

```
CCCCCCCCCCCCCCCCCCCCCCCCCCCCCCCCCCCCCCCCCCCCCCCCCCCCCCCCCCC
C      EVALUATION FUNCTION
C      DEFINE VARIABLE:
C      BL  = AX*SQRT(X)
C      CYS = Constant for SIGMA YS (a3 in Misra 1980a)
C      CZS = Constant for SIGMA ZS (a1 or a2 in Misra 1980a)
C      D   = Time = X/US
C      EVAL1, C - Name of function whose integral is desired
C      HSTK = stack height
C      VARZS  = VARZ*VARZ
CCCCCCCCCCCCCCCCCCCCCCCCCCCCCCCCCCCCCCCCCCCCCCCCCCCCCCCCCCC
C
      FUNCTION EVAL(X,IC)
      COMMON/ONE/XP,YP,A,B,UM,US,H,HSTK,CN,BPARM,CA
      REAL MF(2)
      IFLG=0
      ICFLG=1
C   MAKE THINGS SIMPLER BY CALLING LARGE QUANTITIES A
C   SIMPLE VARIABLE
      F=BPARM
      FU=F/US
      FN=4.50/CN
      IF(X.LE.0.001)GOTO 10
      D=X/US
      CZS=0.40
      CYS=0.67
      CH=CA*(FU**(1./3.))
      VARYS=CYS*(D**(2./3.))*(FU**(1./3.))
C   THIS IS THE DISPERSION COEFFICIENT SIGMA Y IN STABLE
C   AIR PER LAMB 1978,1979,1982
      BL=A*SQRT(X)
      BL1=A*SQRT(XP)
C     CLIMIT=3. *BL1/B
C     IF((XP-X).LT.CLIMIT)ICFLG=2
C     ICFLG=1
C
C   FIRST PIECE OF MISRA´S GAUSSIAN DISTRIBUTION FUNCTION
C   EQUATION
C
      MF(1)=1./(2.*3.14159*BL1*UM)
C     MF(2)=1.78/(6.28138*B*UM)
C     SIGMA Z IN STABLE AIR PER LAMB 1979
      VARZ=1.1*(FU/(CN*CN))**(1./3.)
      VAR=B*(XP-X)/3.0
C   IF((XP-X).GT.BL1/B)
C   VAR=(B*(BL1**(1./3.))*((XPX)**(2./3.)))/3.
      IF(D.GT.FN)GOTO 200
C   *D(TIME) LESS THAN AND EQUAL TO LIMITED*
C   CALCULATE PLUME RISE
      H=(CH*(D**(2./3.)))+HSTK
      VARZ=CZS*(D**(2./3.))*(FU**(1./3.))
```

```
C   DERIV=
C         ((UM**(2./3.))/(CZS*(X**(2./3.))))
C        *((132./X)-A/(6*SQRT(X)))
C   CALCULATE THE VALUE OF THE DERIVATIVE.  WHEN LOOKING AT
C   THIS PART, HAVE MISRA (1980) HANDY
      DERIV =(-1./6.)*(A*UM)/(CZS*(F**(1./3.)))
     #*(X**(-7./6.)) +
     #(HSTK * UM)/(CZS*(F**(1./3.)))*(2./3.)*(X**(-5./3.))
C
C   BRANCHING -- DEPENDS ON VALUE OF IC (WHAT VERSION
C   OF THE MODEL YOU WANT).
C       1 = BASE  2 = DEARDORFF  3 = DOWNDRAFT
C       THIS BRANCHES TO VERSION 2 - DEARDORFF
C
       IF (IC .EQ. 1 .OR. IC .EQ. 3)GOTO 950
       TDP=B*(XP/BL1-X/BL)/4.
        IF (TDP .EQ. 0)GOTO 10
        IF (TDP .GE. 1)GOTO 950
         DERIV=DERIV*(3.-2.*TDP)*TDP*TDP
950     VARZS=VARZ*VARZ
        GO TO 300
C
C     *D(TIME) GREATER THAN LIMITED*
C
200   VARZS=VARZ*VARZ
      DERIV=A/(2.*SQRT(X)*VARZ)
        IF(IC .EQ. 1 .OR. IC .EQ. 3)GOTO 300
C       FURTHER BRANCHING FOR DEARDORFF
        TDP=B*(XP/BL1-X/BL)/4.
         IF(TDP .EQ. 0)GOTO 10
         IF(TDP .GE. 1)GOTO 300
         DERIV=DERIV*(3.-2.*TDP)*TDP*TDP
300   SIGS=(VARYS*VARYS+VAR*VAR)
      BLDIFS=(BL-H)*(BL-H)
C
C   TIBL DECISION: DID PLUME HIT TIBL ??
C   NOW WE NEED TO CALCULATE CONCENTRATION
C   THE ALOG IS A FANCY WAY OF TAKING AN EXPONENTIAL IN THE
C   ORIGINAL FORTRAN CODE.  WE HAVE NOT TAMPERED WITH IT.
C
      C1=-.5*(BLDIFS/VARZS+YP*YP/SIGS)
      C=ALOG(DERIV)+C1-(ALOG(SIGS))/2.0
      IF(ABS(C).GT.70.0)GOTO 10
C   TAKE EXP OF WHOLE EXPRESSION .... BEST TO HAVE MISRA
C   1980 HANDY HERE
       EVALL=EXP(C)
C        THIS BRANCHES TO VERSION 3 - DOWNDRAFT
C
       IF(IC .EQ. 1 .OR. IC .EQ. 2)GOTO 666
```

```
C   NOTE:  G(Z) = 0.623*L, WHERE L=A*X**1./2.
C   (TIBL HT. IS L)
C   THIS WAS OBTAINED BY SOLVING THE INTEGRAL USING CRC
C   HANDBOOK
C
        GZ=1.78*A*(X**1./2.)
        GZTEM=(((GZ*0.225*UM)/(XP-X))-.1)**2.
C       DETERMINE SIGMA W
C       B = WSTAR/UM
C       SIGMAW = .37*WSTAR
C
        WSTAR = B*UM
        SIGMAW=.37*WSTAR
C
        GZTEM=(GZTEM/(SIGMAW**2.))*(-.5)
        TEM = EXP(GZTEM)
        XTEM=((A*UM*(X**1./2.))/(.284*SIGMAW*(XP-X)))*0.225
       EVALL=EVALL*TEM*XTEM
C
C     ****** END OF DOWNDRAFT ROUTINE ******
C
C       CFACT=0.
C     IF(ICFLG.NE.2)GOTO 666
C     ARG=-((((1.632*BL1)/((XP-X)*B))-0.198)**2)
C     CFACT=(1./((XP-X)))*EXP(ARG)
C     IF(ABS(ARG).GT.70)CFACT=0.
666   CONTINUE
C       RENAME A PIECE OF THE MISRA GAUSSIAN EQN TO XF
      XF=MF(1)
C     IF(ICFLG.NE.1)XF=MF(2)
C     MUTIPLY THE PIECE BY THE REST OF THE GAUSSIAN EQN
      EVAL=EVALL*XF
C     IF(ICFLG.NE.1)EVAL=EVALL*CFACT*XF
8889  FORMAT(1X,I2,3(2X,E16.5))
8888  FORMAT(1X,I2,7(2X,E12.4))
      GOTO 20
10    EVAL=0
20    CONTINUE
C      DEBUG UNIT(6),SUBCHK,INIT,SUBTRACE
      END
```

```
CCCCCCCCCCCCCCCCCCCCCCCCCCCCCCCCCCCCCCCCCCCCCCCCCCCCCCCCCCCC
C     SUBROUTINE SIMPSON
C   SIMP IS AN ADAPTIVE, ITERATIVE CODE BASED ON SIMPSON´S
C   RULE.  IT IS DESIGNED TO EVALUATE THE DEFINITE INTEGRAL
C   OF A CONTINUOUS FUNCTION WITH FINITE LIMITS OF
C   INTEGRATION
C
C   DEFINE VARIABLE:
C     A,B   = Lower and upper limits of integration
C     ACC   = Desired accuracy of ans.
C     ANS   = Approximate value of the integral of F(X)
C             from A to B
C     AREA  = Approximate value of the integral of
C             ABS (F(X)) from A to B
C     ERROR = Estimated error of ans.
C     F     = Name of function whose integral is desired
C     IFLAG =  1 for normal return
C              2 If it is necessary to go to 30 levels or
C                use length.
C                Error may be unreliable in this case.
C              3 If more than 2000 function evaluations
C                then complete the computations and error
C                is usually unreliable.
C
CCCCCCCCCCCCCCCCCCCCCCCCCCCCCCCCCCCCCCCCCCCCCCCCCCCCCCCCCCCC
C
      SUBROUTINE SIMP(EVAL,A,B,ACC,ANS,ERROR,AREA,IFLAG,IC)
      DIMENSION FV(5),LORR(30),FIT(30),F2T(30),F3T(30),
     #DAT(30),ARESTT(30),ESTT(30),EPST(30),PSUM(30)
C     SET U TO APPROXIMATELY THE UNIT ROUND-OFF
      U=9.0E-7
C
C     INITIALIZE
C
      FOURU=4.0*U
      IFLAG=1
      EPS=ACC
      ERROR=0.0
      LVL=1
      LORR(LVL)=1
      PSUM(LVL)=0.0
      ALPHA=A
      DA=B-A
      AREA=0.0
      AREST=0.0
      FV(1)=EVAL(ALPHA,IC)
      FV(3)=EVAL(ALPHA+0.5*DA,IC)
      FV(5)=EVAL(ALPHA+DA,IC)
      KOUNT=3
      WT=DA/6.0
      EST=WT*(FV(1)+4.0*FV(3)+FV(5))
```

```
1     DX=0.5*DA
      FV(2)=EVAL(ALPHA+0.5*DX,IC)
      FV(4)=EVAL(ALPHA+1.5*DX,IC)
      KOUNT=KOUNT+2
      WT=DX/6.0
      ESTL=WT*(FV(1)+4.0*FV(2)+FV(3))
      ESTR=WT*(FV(3)+4.0*FV(4)+FV(5))
      SUM=ESTL+ESTR
      ARESTL=WT*(ABS(FV(1))+ABS(4.0*FV(2))+ABS(FV(3)))
      ARESTR=WT*(ABS(FV(3))+ABS(4.0*FV(4))+ABS(FV(5)))
      AREA=AREA+((ARESTL+ARESTR)-AREST)
      DIFF=EST-SUM
C
C     IF ERROR IS ACCEPTABLE GO TO 2.  IF INTERVAL IS TOO
C     SMALL OR TOO MANY LEVELS OR TOO MANY FUNCTION
C     EVALUATIONS, SET A FLAG AND GO TO 2 ANYWAY.
C
      IF(ABS(DIFF).LE.EPS*ABS(AREA))GOTO 2
      IF(ABS(DX).LE.FOURU*ABS(ALPHA))GOTO 5
      IF(LVL.GE.30)GOTO 5
      IF(KOUNT.GE.2000)GOTO 6
C
C     HERE TO RAISE LEVEL, STORE INFORMATION TO PROCESS
C     RIGHT HALF INTERVAL LATER.  INITIALIZE FOR ´BASIC
C     STEP´ SO AS TO TREAT LEFT HALF INTERVAL.
C
      LVL=LVL+1
      LORR(LVL)=0
      FIT(LVL)=FV(3)
      F2T(LVL)=FV(4)
      F3T(LVL)=FV(5)
      DA=DX
      DAT(LVL)=DX
      AREST=ARESTL
      ARESTT(LVL)=ARESTR
      EST=ESTL
      ESTT(LVL)=ESTR
      EPS=EPS/1.4
      EPST(LVL)=EPS
      FV(5)=FV(3)
      FV(3)=FV(2)
      GOTO 1
C
C     ACCEPT APPROXIMATE INTEGRAL SUM.  IF IT WAS ON A LEFT
C     INTERVAL GO TO ´MOVE RIGHT´. IF A RIGHT INTERVAL
C     .ADD RESULTS TO FINISH AT THIS LEVEL.  ARRAY
C     LORR(AMNEMONIC FOR LEFT OR RIGHT)  TELLS WHETHER LEFT
C     OR RIGHT INTERVAL AT EACH LEVEL.
2     ERROR=ERROR+DIFF/15.0
3     IF(LORR(LVL).EQ. 0)GOTO 4
      SUM=PSUM(LVL)+SUM
      LVL=LVL-1
      IF(LVL.GT.1)GOTO 3
      ANS=SUM
      RETURN
C
C     ´MOVE RIGHT´.  RESTORE SAVED INFORMATION TO PROCESS
C     RIGHT HALF INTERVAL.
C
4     PSUM(LVL)=SUM
      LORR(LVL)=1
      ALPHA=ALPHA+DA
      DA=DAT(LVL)
      FV(1)=FIT(LVL)
      FV(3)=F2T(LVL)
      FV(5)=F3T(LVL)
      AREST=ARESTT(LVL)
      EST=ESTT(LVL)
      EPS=EPST(LVL)
      GOTO 1
C
C     ACCEPT ´POOR´ VALUE.  SET APPROPRIATE FLAGS.
C
5     IFLAG=2
      GOTO 2
6     IFLAG=3
      GOTO 2
C      DEBUG UNIT (6),SUBCHK,INIT,SUBTRACE
      END
```